

Comparing and contrasting nuclei and cold atomic gases

N.T. Zinner and A.S. Jensen

Department of Physics and Astronomy, University of Aarhus, DK-8000 Aarhus C, Denmark

E-mail: zinner@phys.au.dk

Abstract. The experimental revolution in ultracold atomic gas physics over the past decades have brought tremendous amounts of new insight to the world of degenerate quantum systems. Here we compare and contrast the developments of cold atomic gases with the physics of nuclei since many concepts, techniques, and nomenclatures are common to both fields. However, nuclei are finite systems with interactions that are typically much more complicated than those of ultracold atomic gases. The similarities and differences must therefore be carefully addressed for a meaningful comparison and to facilitate fruitful crossdisciplinary activity. We first consider condensates of bosonic and paired systems of fermionic particles with the mean-field description but take great care to point out potential problems in the limit of small particle numbers. Along the way we review some of the basic results of BEC and BCS theory, as well as the BCS-BEC crossover and the Fermi gas in the unitarity limit, all within the context of ultracold atoms. Subsequently, we consider the specific example of an atomic Fermi gas from a nuclear physics perspective, comparing degrees of freedom, interactions, and relevant length and energy scales of cold atoms and nuclei. Next we address some attempts in nuclear physics to transfer the concepts of condensates in nuclei that can in principle be built from bosonic alpha-particle constituents. We also consider Efimov physics, a prime example of nuclear physics transferred to cold atoms, and consider which systems are more likely to show interesting bound state spectra. Finally, we address some recent studies of the BCS-BEC crossover in light nuclei and compare them to the concepts used in ultracold atomic gases. While many-body concepts such as BEC or BCS states are applicable in both subfields, we find that the interactions and finite particle numbers in nuclei can obscure the clear meaning they have in cold atoms. On the other hand, universal results from atomic physics should have impact in certain limits of the nuclear domain. In particular, with advances in the trapping of few-body atomic systems we expect a more direct exchange of ideas and results.

PACS numbers: 03.75.Hh, 74.20.Fg, 21.60.-n,

Contents

1	Introduction	2
2	Condensates	5
2.1	Structure of Bose condensates	6
2.2	Center-of-mass motion	8
2.3	Mean-field description	9
2.4	Condensates of Pairs of Fermions	11
3	Pair correlations	12
3.1	The BCS-approximation	13
3.2	Pertinent properties of the BCS solution	17
3.3	The BCS-BEC crossover	19
4	The Atom Gas from a Nuclear Perspective	22
4.1	Two-component Atomic Fermi Gases	22
4.2	Interaction in a Shell Model Picture	27
4.3	Mapping atomic and nuclear degrees of freedom	29
4.4	Fermionic few-body systems	31
5	Bosonic structures in few-body systems	34
5.1	Mean-field versus Localization	34
5.2	Symmetries, Localization versus Delocalization	37
5.3	Trapped Few-Boson Systems	38
5.4	Nuclear α -particle condensates	40
6	Efimov Physics	43
6.1	Basic derivation and occurrence conditions	43
6.2	Scaling properties and examples of Efimov physics	47
6.3	Measurable consequences in physics systems	50
6.4	New directions	52
7	BCS-BEC in Nuclear Physics	54
7.1	From infinite matter to neutron halo nuclei	54
7.2	Crossover in Finite Halo Nuclei	56
8	Conclusions and perspective	59

1. Introduction

The last two decades have witnessed dramatic developments in terms of realizing Bose-Einstein condensates and degenerate Fermi gases which has been driven by the experimental advanced in trapping and cooling dilute atomic gases (Pethick & Smith 2008, Pitaevskii & Stringari 2003, Leggett 2006, Bloch et al. 2008, Giorgini et al. 2008). Typically, these system contain thousands or even millions of particles, but very recently samples with very small particle numbers have been realized (Serwane et al. 2011, Zürn et al. 2012, Bakr et al. 2010, Sherson et al. 2010, Weitenberg et al. 2011). This regime is particularly interesting since the physics that can be learned here might aid our understanding of mesoscopic and microscopic systems in

other subfields. One such venue is nuclear physics, where particle numbers are finite. This raises an interesting question of how concepts from the large system limit, such as condensation or superfluidity, transfer to small systems. In the current presentation we will address similarities and differences between the physics of nuclei and ultracold atomic gases.

There are a number of immediate contrasts that must be highlighted in a comparison of nuclear and cold atoms. First, the notion of scattering length and effective range expansion (Landau & Lifshitz 1981) is very efficient for cold gases since they are valid for very low energy and the typical collision energies approach the zero-energy limit. In more traditional atomic collision physics and in charged Fermi liquids in metals the long-range Coulomb interaction complicates this simple description of the two-body interaction. Secondly, nuclei are self-bound system implying that repulsive and attractive parts of the nuclear interaction must balance. In the atomic gas with external confinement there is no such requirement and the system can be studied in a wider range of regimes in principle. The relatively small particle numbers and the self-bound structure can have important consequences to the conceptual transfer between the subfields and will be a prime concern in this presentation. Furthermore, nuclear methods deal with structures resembling those of present interest in cold atomic gas investigations, i.e. (i) two inherently different but similar components, spin-up and down of neutrons and protons, as in mixed condensates, (ii) “unbound” boson pairs of nucleons in the superfluid BCS low-energy regime, (iii) boson expansions in terms of pairs of fermionic nucleon as molecular condensates, (iv) bosonic α -particle cluster structure as in one-component Bose condensates, (v) α -clusters and nucleons in mixed boson-fermion structures.

In broad terms, nuclear and atomic-molecular physics have a lot of concepts, phenomena, and techniques in common. The reasons are to be found in the short-range character of the different interactions and the finite spatial extension of systems with a finite number of particles. Specifically characteristic units of length L_0 (interparticle spacing) and mass m can be used to construct a unit of energy $E_0 = \hbar^2/(mL_0^2)$. Using L_0 and E_0 as length and energy units provide dimensionless quantities which remove superficial large differences, emphasize similarities and allow focus on the interesting principal scale-independent differences (Amorim et al. 1997, Riisager et al. 2000). We will carefully compare relevant dimensionless parameters for both fields. An important dimensionless quantity is the density n multiplied by the third power of the scattering length a , i.e. na^3 , which is related to the classical mean free path λ by $na^3 \sim a/4\pi\lambda$. In general the size of λ indicates which structure is preferred, e.g. mean field structure when $\lambda \gg L_0$ and strong correlations when $\lambda \simeq L_0$ (Bohr & Mottelson 1975, Siemens & Jensen 1987). This corresponds roughly respectively to $na^3 \ll 1$ and $na^3 \simeq 0.1 - 10$ for atoms where $a/L_0 \sim 10 - 100$ and nuclei where $a/L_0 \sim 1$ (away from resonance).

The nucleon-nucleon interaction range in finite nuclei is comparable to the nuclear radius and the mean free path at low excitation energy (Bohr & Mottelson 1975, Siemens & Jensen 1987). These nucleon-nucleon properties are not (necessarily) the same as in free space. The nuclear system is dense, and more than s -waves contribute. Both mean-field (single-particle or quasi-particle motion) and collective (rotational and vibrational motion of spatial, spin, and pairing) degrees of freedom are important in realistic descriptions (Bohr & Mottelson 1975). For atoms and molecules it is intuitively clear that the important degrees of freedom must be those related to the spatial orientation, the intrinsic excitations and the relative motion of the individual atoms (Haken & Wolf 1995). For both nuclei and atoms or molecules macroscopic as

well as microscopic properties are therefore necessary ingredients in the descriptions.

The self-bound, leptodermous (thin skin) nuclear systems (Myers & Swiatecki 1969) emphasize the importance of surface properties as for mesoscopic condensed matter systems (Reimann & Manninen 2002). Similar deviations from homogeneous bulk properties appear as correlations in trap- or optical lattice confined atomic systems (Bloch et al. 2008, Giorgini et al. 2008). The common theoretical quantitative techniques include the mean-field and BCS pairing approximations, linear response (including random phase approximations), ab initio variational minimization, shell model diagonalization in restricted Hilbert spaces, and density functional methods.

The present paper is devoted to a comparison of common concepts and structures in nuclei and cold atomic gases. Striking similarities are seen in many discussions that employ the notion of condensation and paired states in both subfields. However, a careful comparison is demanded when concepts that traditionally refer to infinite systems are applied to finite systems such as nuclei or trapped atomic gases containing only very few atoms. Our aim is to facilitate and clarify exchange of important ideas, basic concepts and essential techniques between the two broad fields of physics. For a comprehensive review of experimental and theoretical developments in cold atomic gases we refer to (Bloch et al. 2008, Giorgini et al. 2008).

Our starting point will be mean-field theory and we define the concepts of condensate and paired state in this context. Particular care is taken to address the problems with finite particle number and we therefore discuss at length the notion of condensate and condensate fraction. Paired states of fermionic particles in both nuclear and cold atomic gases are discussed mainly within the BCS theory which is widely used in both arenas. We also discuss the interesting physics of the transition from weakly-coupled paired states to a condensate of strongly bound two-body molecules as it is described within the BCS formulation (BCS-BEC crossover), and we address strongly-interacting Fermi gases in the unitarity limit. Along the way we take care to distinguish between generic features and model-dependent details that originate from certain convenient choices of model-space, effective interactions, etc.

An important topic is the comparison of different scales in cold atomic gases and in nuclei. In particular, the isolation of relevant dimensionless quantities is essential. We undertake such a discussion next, explaining the degrees of freedom of both fields, and pointing out similarities and differences. An extended discussion of the cold atomic two-component fermionic gas is given from a nuclear physics perspective within the traditional shell model picture that should be helpful for applying nuclear physics techniques and concepts directly to cold atomic gases. As an example, we discuss few-body fermionic trapped atomic gases and compare them to light nuclei.

We then turn to some specific examples of bosonic structures and condensates in few-body nuclear systems and also in trapped few-body atomic gases that have been studied theoretically in recent years. We employ a concept of quantum localization which can predict zero-temperature phases of quantum matter, and show how it is connected to more common measures of quantum degeneracy. The case of finite systems of bosons is subsequently discussed with emphasis on the competition between localization of particles and mean-field states. For finite systems localization is unfavourable to the formation of a condensate. In nuclear physics, we apply these concepts to light nuclei that are believed to have cluster structures, and for which condensation of α -particles have been proposed as a potential structure of the system.

Efimov physics is discussed next. Originating in nuclear physics, the concepts of an infinite number of bound three-body states around the threshold for two-body

binding which has recently been experimentally studied with cold atomic gases. This constitutes a beautiful example of crossdisciplinary fertilization. We discuss the concept of universal three-body bound states and give criterions for which systems are best suited for its observation. Finally, we discuss neutron-rich matter within the context of the BCS-BEC crossover. Again, we focus on few-body aspects and consider light halo nuclei that have a low-density surface occupied mostly by neutrons. Here we address which features related to the crossover can be described as universal and which are model-dependent.

The current presentation is organized in sections with slightly different aims. The discussion of condensates in Section 2 is directed from atomic towards nuclear physics, implying that the content is well known in atomic and has to be defined properly in nuclear physics. The properties of pair correlations in Section 3 are common to nuclear and atomic physics but there are subtle issues with choices of model-space and residual pairing interactions in nuclear physics that we point out. Section 4 contains a description of atomic gas properties such as length and energy scales, degrees of freedom, etc., translated into nuclear physics language. Section 5 discusses few-body applications of the concepts of atomic boson gases in nuclear physics and in Section 6 we specialize to the topical Efimov effect in both nuclei and atomic gases. Section 7 is devoted to a discussion of BCS-BEC crossover physics in neutron-rich matter with particular emphasis on light nuclei and particular choices in the models that describe the nuclear interactions. Finally, section 8 contain a brief summary and conclusions.

2. Condensates

Bose-Einstein condensates were initially predicted as the result of a phase transition of non-interacting bosons below a critical temperature. This was at first considered a pathology of no interaction, but after the discovery of superfluidity in bosonic ^4He in 1938 by Kapitza (Kapitza 1938), Allen and Misener (Allen & Misener 1938), Fritz London had the insight that superfluidity might in fact be a sign of condensation (London 1938). A few years later Landau explained superfluidity in terms of the linear spectrum of the low-energy excitations in the system (Landau 1941). He also introduced a two-fluid model with a superfluid and a normal component, the former of which is related to the condensed particles. Superfluidity is connected with the excitation spectrum, whereas condensation is a property of the 'natural' stationary state of the system as given by the one- or two-body density matrix introduced below. From the point of view of atomic and nuclear physics, the latter concept is the more important and hence our focus in the following.

As a large number of identical bosons are allowed simultaneously in the same single-particle quantum state it can be macroscopically occupied. An important aspect of condensed matter physics and the theory of phase transitions in three-dimensional space is that of long-range order. As we will discuss below, this concept is also useful in the case of finite systems where it is connected to the coherent state that a Bose system can condense into. The properties of boson condensates are extensively investigated in laboratories under a variety of conditions defined by ingenious combinations of external electromagnetic fields (Pethick & Smith 2008, Bloch et al. 2008, Grynberg & Robilliard 1999). In contrast, for fermions only one particle is allowed in a given quantum state. However, an entity consisting of an even number of fermions exhibits boson symmetry properties, and in particular these composite particles can occupy the same quantum state. The Cooper pairs of fermions in the BCS theory are

examples arising due to an attractive two-body interaction (Cooper 1956, Bardeen et al. 1957, Leggett 2006). Superconductivity and superfluidity are in this sense the same phenomena which can be seen in Landau's theory of phase transitions for these systems (Landau & Lifshitz 1958, Pitaevskii & Lifshitz 1980). For a summary of the concepts and historical development in superfluidity we refer to Leggett (Leggett 1999).

In nuclei, prominent examples of bosonic substructures are α -particles which from the early days were suggested as building blocks of nuclei (Wigner 1937, Wheeler 1937, Wefelmeier 1937, Brink 1966), and pairs of nucleons within the BCS theory (Bohr et al. 1958, Bohr & Mottelson 1975). Numerous examples exist of both fundamentally bosonic atoms and molecules and also of binary bound fermionic molecules (Haken & Wolf 1995). When composite boson structures begin to get close to each other and interact, the ideal boson structure is no longer maintained. The intrinsic degrees of freedom become important and true microscopic fermionic nature is revealed. We shall here first discuss the definition and structure of boson condensates and in the next subsection the connection to bosons formed by two fermions via BCS-pairing.

2.1. Structure of Bose condensates

The ideal Bose condensate (BEC) is defined through quantum statistics for bosonic particles (Fetter & Walecka 1971, Pethick & Smith 2008, Pitaevskii & Stringari 2003). The prediction is that below a certain temperature these systems will have a macroscopic number of particles, N_0 , in the lowest energy state. Here macroscopic occupation refers to the thermodynamic limit where $\lim_{N \rightarrow \infty} (N_0/N)$ has to be finite when N is the total number of particles. The ideal Bose condensate with $N = N_0$ is then by definition non-interacting since the inevitable correlations otherwise would prevent some particles from being in the same quantum state. This depletion of the condensate due to interactions depends on na^3 where $a > 0$ is the scattering length characterizing the two-body interaction at low energy and n is the particle density. When $a < 0$, the bosons attract and only a limited number of particle can condense without collapsing as we will discuss below. However, to achieve condensation in an experiment the particles must be confined inside a trap. The presence of such an outer one-body trapping potential alters the particle spectrum but BEC can still occur for dilute gases in spatially extended traps (Pethick & Smith 2008, Pitaevskii & Stringari 2003).

To be accurate in discussions of BEC we need to decide on an appropriate and robust definition. The most widely accepted basic definition, revolving around the density matrix for the system in question, was given early on in (Penrose 1951, Landau & Lifshitz 1958, Penrose & Onsager 1956, Yang 1962). We shall follow (Yang 1962) and specify properties of the N -body density matrix arising from the wave function Ψ for the many-body system of N particles. We first define the one-body density matrix, ρ_1 , by

$$\begin{aligned} \rho_1(\vec{r}, \vec{r}') &\equiv Tr |\Psi(\vec{r})\rangle \langle \Psi(\vec{r}')| \\ &= \int d\vec{r}_2 d\vec{r}_3 \dots d\vec{r}_N \Psi^*(\vec{r}, \vec{r}_2, \dots, \vec{r}_N) \Psi(\vec{r}', \vec{r}_2, \dots, \vec{r}_N), \end{aligned} \quad (1)$$

where $\vec{r}_i, i = 1, \dots, N$, are the particle coordinates. The choice of integration omitting $i = 1$ is arbitrary as Ψ is symmetric under any particle interchange. We assume that Ψ is normalized to N after integration over all coordinates of $|\Psi|^2$.

The positive definite matrix ρ_1 with two continuous indices is hermitian and can thus be diagonalized by a unitary transformation, i.e. we can decompose this density matrix as

$$\rho_1(\vec{r}, \vec{r}') = \sum_i \lambda_i \phi_i^*(\vec{r}) \phi_i(\vec{r}'), \quad (2)$$

where λ_i are the eigenvalues (which are positive) and ϕ_i the corresponding single-particle eigenfunctions each normalized to unity. We order the eigenvalues to decrease in size with i . Integrating the diagonal part of the density matrix we get N , i.e.

$$\int d\vec{r} \rho_1(\vec{r}, \vec{r}) = \sum_i \lambda_i = N. \quad (3)$$

We define the system as a simple BEC when one and only one of the eigenvalues λ_1 remains of the order of magnitude N for increasing N , i.e. one large eigenvalue in the thermodynamic limit. Thus the wave functions for a BEC is dominated by a wave function that is a simple (symmetric) product of the same single-particle wave function ϕ_1 , i.e. $\Psi \approx \Pi_i \phi_1(\vec{r}_i)$. Notice that this holds for condensates that are close to the ideal non-interacting case. A counterexample is atomic ^4He which has very strong correlations and thus only 10% of a given sample will be in the condensed state. This definition inherently compares structures for different (large) numbers of particles. More than one eigenvalue may be large even in the limit of large N . Such states are called fragmented BEC and they have recently received increasing attention, particularly in connection with gases of more than one species of atoms and also with respect to condensation of asymmetric (different number of particles) two-component systems (Pethick & Smith 2008, Pitaevskii & Stringari 2003, Mueller et al. 2006).

The concept of off-diagonal long-range order is closely related to the behavior of the one-body density matrix in the limit where $|\vec{r} - \vec{r}'|$ becomes large compared to the system size (Yang 1962). Let us then consider a possible limiting form of ρ_1 , i.e.

$$\lim_{|\vec{r} - \vec{r}'| \rightarrow \infty} \rho_1(\vec{r}, \vec{r}') = F^*(\vec{r})F(\vec{r}') + \rho'_1(\vec{r}, \vec{r}'), \quad (4)$$

where the first term has the product form obtained by diagonalization. If the function ρ'_1 tends to zero in this limit one would say that the system is a BEC with order parameter F which depends on the coordinate. Then F is interpreted as the condensate wave function, $F \rightarrow \phi_0 \sqrt{N}$, containing N particles and obtained in the mean-field approximation. Thus Eq. (4) separates ρ_1 into the product part related to the largest eigenvalue and the rest of the sum in Eq. (2) denoted by ρ'_1 . One can show under rather general conditions that ρ'_1 vanishes for homogeneous 3-dimensional Bose systems (Leggett 2006) and also in the case of trapped condensates (Naraschewski & Glauber 2001). Thus this alternative definition of BEC is equivalent to that of one large eigenvalue in the expansion in Eq. (2).

The one-body density matrix for a BEC in a trap was experimentally measured about a decade ago (Bloch et al. 2000) and the expected coherence was confirmed. This corresponds to what is known as first-order coherence (Naraschewski & Glauber 2001). Second-order coherence (related to the two-body density matrix) is connected to the famous Hanbury-Brown and Twiss effect (Hanbury-Brown & Twiss 1956, Baym 1969, Baym 1998). The corresponding bunching effect has been observed in optics (Bachor & Ralph 2004) and in cold bosonic atoms (Yasuda & Shimizu 1996, Fölling et al. 2005, Schellekens et al. 2005). The analogous anti-bunching in electronic systems (Henny et al. 1999, Oliver et al. 1999, Kiesel et al. 2002), for neutrons (Iannuzzi

et al. 2006), and in fermionic cold atoms (Rom et al. 2006). Recent experiments have even begun to study third-order coherence (large eigenvalues in the third-order correlation function) and the nucleation of a ^4He BEC (Hodgman et al. 2012).

2.2. Center-of-mass motion

There is one possible flaw in this equivalence between the two definitions of BEC above. Unfortunately that is related to trapping in external one-body potentials which is employed in all laboratory experiments. The problem is that the center-of-mass motion is not decoupled as for a self-supported system. The center-of-mass of the N particles do not coincide with the center of origin for the external field. Then the particles can for example move coherently in rotational states without changing their relative motion. This would show up as simultaneously existing BEC-like structures with eigenvalues of comparable magnitude even when the number of particles increases. This was pointed out in (Pethick & Pitaevskii 2000) and an alternative definition of BEC was suggested to remove the effect of the center-of-mass motion, i.e. using the internal one-body density matrix where only relative coordinates enter. Then different rotational motion build on the same intrinsic BEC would all lead to one large eigenvalue of the internal one-body density matrix.

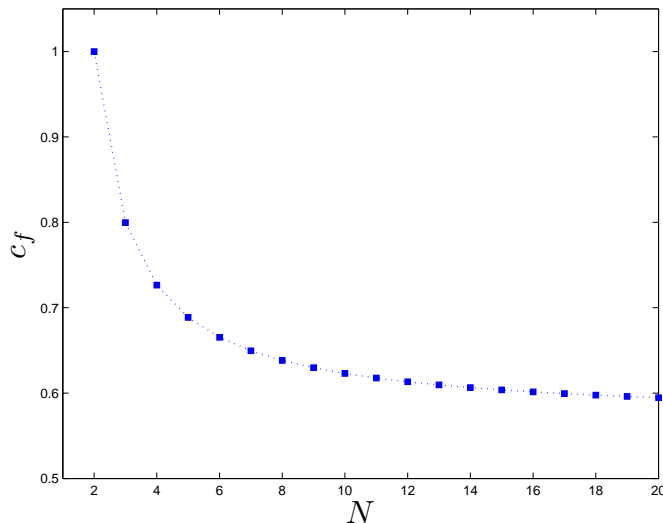


Figure 1. Condensate fraction, c_f , as function of the number of particles, N , for a gaussian mean-field wave function when the center-of-mass has been separated out as discussed in the text.

We can illustrate by a gaussian mean-field wave function of range b where the center-of-mass coordinate separates out leaving only relative coordinates in the internal wave function, i.e.

$$\Psi_{int}(\{\mathbf{r}_i\}) = (b\sqrt{\pi})^{-3(N-1)/2} \exp(-\rho^2/(2b^2)), \quad (5)$$

$$\rho^2 \equiv \sum_{i=1}^N q_i^2, \quad \mathbf{q}_i \equiv \mathbf{r}_i - \mathbf{R}, \quad \mathbf{R} \equiv \frac{1}{N} \sum_{i=1}^N \mathbf{r}_i, \quad (6)$$

where the coordinates \mathbf{q}_i are measured from the common center-of-mass \mathbf{R} . This wave function is invariant under rotations around \mathbf{R} . Following (Pethick & Pitaevskii 2000)

the internal one-body density matrix $\rho(\mathbf{q}_1, \mathbf{q}'_1)$ is now found by inserting $\mathbf{q}_N = -\sum_{i=1}^{N-1} \mathbf{q}_i$ in Eq. (5), i.e.

$$\begin{aligned} \rho(\mathbf{q}_1, \mathbf{q}'_1) &\propto \int d^3\mathbf{q}_2 d^3\mathbf{q}_3 \dots d^3\mathbf{q}_{N-1} |\Psi_{int}|^2 \\ &\propto \exp\left(-\frac{\mathbf{q}^2 + \mathbf{q}'^2}{b^2} + \frac{(N-2)(\mathbf{q}' + \mathbf{q})^2}{(N-1)4b^2}\right). \end{aligned} \quad (7)$$

The condensate fraction obtained through the largest eigenvalue is then (Gajda 2006) $c_f = 8/(1 + \sqrt{2 - 2/N})^3$ which decreases with N from 1 for $N = 2$ towards about 0.57 for large N . This is illustrated in figure 1. However, the choice of relative coordinates is arbitrary (Gajda 2006) and we could as well choose \mathbf{q}_1 supplemented by a set of $N - 1$ independent Jacobi coordinates. Then the density matrix corresponding to Eq. (5) would factorize and give $c_f = 1$. This fact has also been addressed in (Yamada et al. 2008, Yamada et al. 2009). Clearly these discussions are only relevant for finite systems where the center-of-mass can move. Thus the distinctions become less and less important with increasing particle number, but at the same time interesting for a smaller number of particles in BEC-like states.

2.3. Mean-field description

The initial definition of BEC as a number of particles in the same single-particle state immediately points to a mean-field approximation or independent particle model. The only assumption is that the many-body wave function is a symmetric product of single-particle wave functions. With this restriction the variational principle gives the lowest energy solution for any Hamiltonian. This implies that the average effect of the interactions between the particles are included in this approximation. Obviously any interaction would prefer to correlate the particles either to avoid or to exploit the interaction. This cannot be expressed in the mean-field product wave function which is the ideal BEC structure. Thus any deviations beyond the mean-field must reduce the BEC content. In other words interactions introduce correlations which attempt to destroy the BEC structure.

For cold atoms the zero-range approximation for bosons has been used successfully in the form of the self-consistent mean-field Gross-Pitaevskii equation (Gross 1961, Pitaevskii 1961, Pethick & Smith 2008, Pitaevskii & Stringari 2003). It is demonstrated for dilute systems to be very efficient in reproducing data for interacting condensates with inter particle repulsion. For attractive interactions ($a < 0$), the system collapses unless some measures are taken to avoid this part of the Hilbert space. However, quasi-stable solutions exist of finite size and energy if $N|a|/b < 0.65$ where b is the trap length of the external harmonic potential (Ruprecht et al. 1995, Kagan et al. 1998, Pitaevskii & Stringari 2003, Pethick & Smith 2008, Bohn et al. 1998, Sørensen et al. 2004). Figure 2 shows the effective potential barrier of an attractively interacting condensate based on a gaussian variational calculation including also higher-order effective range corrections (Zinner & Thøgersen 2009). The variational wave function is

$$\Psi(r) = \frac{\sqrt{N}}{\pi^{3/4} \sqrt{(qb)^3}} \exp\left(-\frac{r^2}{(qb)^2}\right), \quad (8)$$

where $b = \sqrt{\hbar/m\omega}$ is the oscillator length, N is the particle number, and q is the dimensionless variational parameter. The quasi-stable solution are located in the local

minimum around $q \sim 1$. These solutions decay into deeper lying (collapsed) states of the many-body system, e.g. non-condensate like states where a number of binary or many-body bound states are present perhaps in some mixture with dilute atomic states confined by the external field. When $N|a|/b$ is much lower than the critical value the lifetimes of the condensate is much longer than the experimental time.

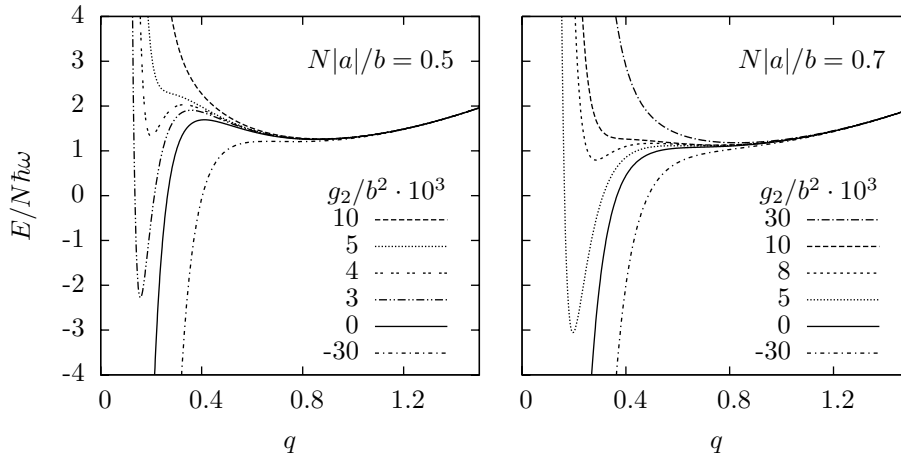


Figure 2. Energy of a BEC with fixed $N|a|/b$ as function of the variational parameter q , i.e. the size of the condensate (proportional to b). The higher-order interaction term $g_2 = a^3/3 - ar_e/2$ includes the effective-range correction through r_e . It modifies the height and shape of the barrier through which macroscopic quantum tunneling occurs. The left panel has $N|a|/b = 0.5 < 0.65$ and the right panel shows results for $N|a|/b = 0.7 > 0.65$, i.e. on both sides of the stable regime when g_2 can be neglected. The right panel demonstrates that higher-order corrections can stabilize an attractively interacting condensate. Taken from (Zinner & Thøgersen 2009).

The mean-field treatment provides the optimal solution where the BEC product wave function is maintained. The most sensible definition of correlations in many-body physics is in terms of deviations from the simple mean-field product wave function. Therefore when we define BEC through the one-body density and its eigenvalues we have an intuitive access to understand the effects of correlations on a BEC. Expanding the full correlated many-body wave function on a basis of different mean-field product wave functions, a number of non-zero eigenvalues (λ_i) would appear with corresponding single-particle wave functions. The condensate fraction is then given by the largest eigenvalue, λ^* , as λ^*/N . Imagine that we turn on interactions slowly in an ideal BEC. The condensate fraction then decreases from unity and many eigenvalues of order 1 would appear. Approaching the thermodynamic limit by increasing N while maintaining the same interactions would again increase the largest eigenvalue and the condensate fraction towards unity. Even rather strong two-body interactions would not destroy the BEC structure reached for large N (Mueller et al. 2006, Thøgersen et al. 2007). This does not necessarily mean that the BEC structure is unaltered by the interactions and the additional particles. It means that the best approximation by a product wave function, depending on interactions and N , is approached (Lieb et al. 2002).

2.4. Condensates of Pairs of Fermions

Combining two fermions into a, possibly bound, entity produces a system with boson characteristics. Redefining the degrees of freedom from single-particle to two-particle center-of-mass and relative coordinates, and integration over the relative coordinates in the density matrix, allow use of the general definition of boson condensates. However, if the intrinsic two-body structure cannot be frozen, we need a generalization of the BEC concept to systems of fermions. Due to the Pauli exclusion principle any one-body density matrix will always have eigenvalues that are less than or equal to one, so using this to look for coherence makes little sense. However, as Yang (Yang 1962) shows, the two-body density matrix, ρ_2 , for fermions should be used instead of the one-body density matrix ρ_1 . The definition of ρ_2 is

$$\begin{aligned} & \rho_2(\vec{r}_1, \vec{r}_2, \vec{r}'_1, \vec{r}'_2) \\ &= \int d\vec{r}_3 \dots d\vec{r}_N \Psi^\dagger(\vec{r}_1, \vec{r}_2, \dots, \vec{r}_N) \Psi(\vec{r}'_1, \vec{r}'_2, \dots, \vec{r}_N), \end{aligned} \quad (9)$$

which may have eigenvalues, λ_i , of order N , i.e.

$$\rho_2(\vec{r}_1, \vec{r}_2, \vec{r}'_1, \vec{r}'_2) = \sum \lambda_i \phi_i^*(\vec{r}_1, \vec{r}_2) \phi_i(\vec{r}'_1, \vec{r}'_2). \quad (10)$$

It is then natural to find these eigenvalues and define a fermion condensate as the structure where one of these eigenvalues is large as for BEC. The connection to a boson condensate of composite particles is then readily seen by change to relative and center-of-mass coordinates $\vec{r} = \vec{r}_1 - \vec{r}_2$, $\vec{R} = (\vec{r}_1 + \vec{r}_2)/2$, and subsequent integration over the ‘‘intrinsic’’ \vec{r} -coordinates, i.e.

$$\rho_1(\vec{R}, \vec{R}') = \int \rho_2(\vec{r}_1, \vec{r}_2, \vec{r}'_1, \vec{r}'_2) d\vec{r} d\vec{r}'. \quad (11)$$

If $\phi_i(\vec{r}_1, \vec{r}_2)$ factorizes in the (\vec{R}, \vec{r}) coordinates the fermion condensate reduces to a boson condensate of pairs of fermions. This two-body density matrix determines the second-order coherence of the system for both fermions and bosons as was mentioned above.

In many cold atomic gas experiments with fermions the system has two internal states, similar to electrons in condensed-matter systems. The fermions carry an effective half integer quantum number (the physical origin of this will be discussed in later sections). We have suppressed this index here. When internal states are present, one can think of the coordinates in Eq. 9 as containing both spatial coordinate and internal state information.

Some very simple, although pathological, limits of very few particles have been discussed in nuclei. For two identical bosons the one-body density matrix is automatically of the form in Eq. (2) with only one term in the summation which means maximum eigenvalue and ideal Bose condensate. Thus when the center-of-mass wave function is controlled by an external field or included as in (Pethick & Pitaevskii 2000) this definition implies that two bosons always form a condensate. Two fermions with identical orbital wave function and antisymmetric relative spin wave function automatically factorize as in Eq. (10) with one term. This implies that two identical fermions in a state of lowest energy are in a fermion condensate. Furthermore, the composite system of two fermions is by definition in a boson condensate consisting of one particle. These rather pathological limits demonstrate that composites of few particles with properly chosen definitions can fulfil the criteria for a condensate. Of course one must still determine whether this has any additional physical significance

in the relevant system at hand. We will discuss these questions in a few simple cases in the second part of the review.

3. Pair correlations

Before we discuss pairing correlations in two-component Fermi systems, we first address an important question related to the choice of model space and interactions. This is necessary since there are several choices involved before one arrives at some properly defined model to which pair correlations and a particular method of solving pairing Hamiltonians can be applied. This is the case for both finite and infinite systems, and it is important to keep track of the effective interactions and model spaces that are applied when addressing generic features or universal behavior.

In the spirit of density functional computations, a sufficiently well chosen density functional would provide any desired accuracy of the true energy (Kohn & Sham 1965, Dreizler & Gross 1995). However, correlations are entirely missing in the one-body structures of the wave functions. To investigate effects of correlations it is therefore necessary to use a Hilbert space that goes beyond one-body product states. As correlations are driven by interactions it is also necessary to know precisely which interaction to use in the extended space. These connections and the practical implementations in nuclear and atomic physics are completely different.

A natural starting point in both subfields is some form of self-consistent mean-field model. For fermions the most common choice is the Hartree-Fock approximation (Fetter & Walecka 1971, Negele 1982, Siemens & Jensen 1987, Pethick & Smith 2008). For identical bosons (fermions) the Hilbert space is (anti)symmetrized products of single-particle wave functions. Several extensions of the Hartree-Fock method are in use. In nuclear physics, a prominent example is the Hartree-Fock-Brueckner scheme (Fetter & Walecka 1971, Siemens & Jensen 1987) which takes medium effects of Pauli blocking into account in a self-consistent manner. For cold atomic gases similar medium effects have been taken into account in various other ways (Heiselberg et al. 2000, Stoof et al. 2009). For the present discussion we keep things simple and stay at first within the framework of the standard Hartree-Fock approximation. Later on we comment on some important features of going beyond this approximation in connection with polarization effects, induced interactions and the renormalized zero-range BCS model.

A mean-field Hartree-Fock calculation requires suitable two-body interactions as input. In atomic gases the diluteness of the system makes the zero-range approximation extremely accurate even around broad Feshbach resonances where the effective range remains small (Köhler et al. 2006) (a more detailed discussion of Feshbach resonances is given in Section 4.1). However, it is remarkable that nuclear physics mean-field calculations employ zero-range interactions since nuclei are not dilute as the range of the nucleon-nucleon potential is comparable to the interparticle distance in the nucleus. Cold atomic gases are usually dilute in this sense and zero-range interactions are more appropriate (at least away from interaction resonances as we will discuss below). An interesting comparison can be made to fermionic liquid ^3He which is a dense system.

In general, it is crucial to relate the chosen interaction with the allocated Hilbert space (Barrett 1980, Suzuki & Lee 1980, Suzuki 1982, Brandow 1967, Poves & Zuker 1981). This must be done whether one uses zero-range or some other form as the model interaction, although using a finite-range potential can often help avoid

divergences. The physical interaction must be transformed to apply in a restricted Hilbert space, and the operators for other observables than the energy must be correspondingly transformed. Properly done all physics is then correctly maintained. The connection between basic and effective (transformed) interactions can easily be complicated or downright impossible to trace. It is for example rigorously necessary to work with up to N -body interactions, not only the simple initial two-body interactions (Suzuki & Lee 1980, Suzuki 1982). In any case, nuclear and atomic physics differ tremendously in both effective interactions and Hilbert space even when identical techniques are employed (Barrett 1980).

The nuclear force is at low energy expanded in terms of the relative momentum between the nucleons, and only terms up to second order is maintained (Siemens & Jensen 1987). This Skyrme interaction corresponds to zero-range in coordinate space (Skyrme 1956). The inevitable collapse for attractive potentials in Hartree-Fock applications is avoided by a completely phenomenological (still zero-range) density dependence, or alternatively multi-body forces (Negele & Vautherin 1972, Negele & Vautherin 1975). The strengths of the different terms are then adjusted to reproduce observables like energies and sizes of a series of nuclei. The connection to the basic nucleon-nucleon interaction is lost.

In atomic physics the zero-range interaction in mean-field calculations leads for identical bosons to the Gross-Pitaevskii equation (Gross 1961, Pitaevskii 1961, Pethick & Smith 2008, Pitaevskii & Stringari 2003). The total wavefunction for N bosons in factorized form, $\Psi = \prod_{i=1}^N \phi(\vec{r}_i)$, leads to the stationary Gross-Pitaevskii equation for ϕ which reads

$$-\frac{\hbar^2}{2m} \nabla^2 \phi(\vec{r}) + V_{ext}(\vec{r})\phi(\vec{r}) + \frac{4\pi\hbar^2 a}{m} |\phi(\vec{r})|^2 \phi(\vec{r}) = E\phi(\vec{r}), \quad (12)$$

where m is the boson mass and E the energy per particle. The non-linear interaction term, which gives rise to many interesting physical effects in condensates, are well-described by this equation (Pitaevskii & Stringari 2003). The strength of the interaction is chosen to reproduce large distance, or equivalently low-energy scattering properties within a confining external field. This amounts to reproduce the physical atom-atom scattering length by the Born approximation of the potential (Pethick & Smith 2008, Pitaevskii & Stringari 2003). The intuitive explanation is that Hartree-Fock product wave functions in the one-body external potential corresponds to free uncorrelated solutions for which the Born approximation is sufficient. For repulsion the solution can then immediately be obtained. The collapse for attraction is avoided by restriction of the Hilbert space to larger distances or, equivalently to, lower energies. The connection to low-energy two-body scattering properties is maintained, and the strength related to the scattering length in this limit.

3.1. The BCS-approximation

Correlations in general and pair correlations in particular arise only by going beyond the Hartree-Fock or Gross-Pitaevskii approximation. The neglected residual interaction must be defined relative to the main part accounted for in the mean-field approximation. In atoms the residual interaction is rather well-determined as connected to the basic physical interaction. However, for nuclei this immediately presents the problem that the procedure is not unique since the starting point is phenomenological. The residual and mean-field interactions for nuclei must then be related through the same phenomenology. Conclusions about physics beyond the

region where the parameters are adjusted can be very uncertain. Recent advances in deriving low-momentum interactions for use in few- and many-body nuclei promise to improve on this situation by decoupling the troublesome high-momentum parts of the typical nucleon-nucleon interaction while preserving the correct scattering phase shifts (Epelbaum et al. 2009, Bogner et al. 2010). These developments may be relevant for the interchange between nuclei and cold atoms. However, as these technical issues are not necessary for the purpose of discussing pairing correlations in the BCS approximation, we focus here on the more phenomenological approach traditionally employed for nuclei.

Pair correlations can be incorporated on an equal foot with the single-particle degrees of freedom by extension of the Hartree-Fock to the Hartree-Fock-Bogoliubov (or Bogoliubov-de Gennes in the atomic literature) approximation (de Gennes 1999, Bohr & Mottelson 1975, Ring & Schuck 1980, Dobaczewski & Nazarewicz 2012). To grasp the main idea, the simplest extension is sufficient which is to supplement the mean-field treatment by the BCS approximation. For simplicity we assume identical energy spectra, ϵ , for the different internal states of the fermions we have in mind. In traditional superconductivity, the two internal states of the electrons are of course the spin degrees of freedom, whereas in a two-component ultracold atomic Fermi gas the internal states are typically two states with different hyperfine projections (this will be discussed in greater detail below). We will also assume that the same number of particles occupy each internal state forming pairs. The latter condition means that we consider here only such balanced systems where the original implementation of the BCS theory applies. When the system is imbalanced, a number of exotic states like the FFLO pairing state (characterized by a oscillating pairing gap parameter) have been predicted (see (Casalbuoni & Nardulli 2004) for a recent review). In nuclei, the different internal states are given by time-reversal symmetry (Bohr et al. 1958, Bohr & Mottelson 1975, Ring & Schuck 1980, Siemens & Jensen 1987), and in cold atomic gases by the two decoupled hyperfine states with controlled frozen occupation (see Section 4). The role of time-reversal symmetry was already discussed in the context of superconductors by Anderson (Anderson 1959). The Hamiltonian, after subtraction of the Lagrange multiplier term μN , is

$$\begin{aligned} H_\mu &= H_{mf} - \mu N + H_R \\ &\equiv \sum_i (\epsilon_i - \mu) (a_i^\dagger a_i + a_{\bar{i}}^\dagger a_{\bar{i}}) - \sum_{i,j} G_{ij} a_i^\dagger a_{\bar{i}}^\dagger a_{\bar{j}} a_j, \end{aligned} \quad (13)$$

where the single-particle energies ϵ_i , the creation a_i^\dagger , and annihilation a_i operators refer to the single-particle mean-field states $|i\rangle$. The internal states, time-reversed or hyperfine, are denoted by a bar and we assume $\epsilon_i = \epsilon_{\bar{i}}$. The single-particle energies are measured with respect to the chemical potential μ multiplying the number operator N . If the spectra of each component are not the same, we need a sum of two terms each related to the two types of internal states. The matrix elements G_{ij} of the residual interaction H_R , beyond the mean-field H_{mf} then denotes the two-body interaction between pairs of particles in time-reversed (hyperfine) mean-field states. This piece of the interaction is called the pairing interaction, and it should not be confused with neither the full two-body interaction employed in the mean-field potential nor any other residual contribution to the matrix elements, e.g. related to other correlations like vibrational or rotational excitations in the RPA treatment.

The BCS approximation then consists in

$$H_\mu \approx H_{mf} - \mu N - \sum_i \Delta_i (a_i^\dagger a_i^\dagger + a_i a_i) , \quad (14)$$

which is diagonalized exactly by the Bogoliubov transformation

$$a_i^\dagger = u_i \alpha_i^\dagger - v_i \alpha_i , \quad a_i = u_i \alpha_i + v_i \alpha_i^\dagger , \quad (15)$$

where the new quasi-particle creation α_i^\dagger and annihilation α_i operators also obey fermion anti commutation rules. The result is

$$H_\mu \approx U_0 + \sum_i E_i (\alpha_i^\dagger \alpha_i + \alpha_i \alpha_i^\dagger) , \quad (16)$$

$$U_0 = 2 \sum_i \epsilon_i v_i^2 - 2 \sum_i \Delta_i u_i v_i , \quad (17)$$

The occupation numbers v_i^2 and quasi-particle excitation energies E_i are

$$v_i^2 = 1 - u_i^2 = \frac{1}{2} \left(1 - \frac{\epsilon_i - \mu}{E_i} \right) , \quad (18)$$

$$E_i = \sqrt{(\epsilon_i - \mu)^2 + \Delta_i^2} . \quad (19)$$

The chemical potential μ and the gaps Δ_i are determined for a given average number of particles $N_0 = \langle N \rangle$ from the equations

$$N_0 = 2 \sum_i v_i^2 , \quad 2\Delta_j = \sum_i G_{ij} \frac{\Delta_i}{E_i} . \quad (20)$$

The new BCS ground state wave function related to the α_i^\dagger quasi-particle operators is expressed by

$$|BCS \rangle = \prod_i (u_i + v_i a_i^\dagger a_i^\dagger) |0 \rangle , \quad (21)$$

where $|0 \rangle$ is the “vacuum” related to the a_i operators. It is also possible to write an analogue of the BCS theory presented here that conserves particle number by using projection (Dietrich et al. 1964, Adornes & Kyotoku 1992, Leggett 2006) although these can become considerably more complicated. Schematic and exactly solvable pairing models have also been studied in great detail (Dukelsky et al. 2004, Pan & Draayer 1999).

The pair correlations obtained in the BCS-approximation are derived from the residual interaction expressed in terms of the two-body matrix elements, G_{ij} , of the interaction between pairs in time-reversed states, see Eq. (13) An approximation of constant pairing matrix-elements, G , independent of i and j is very instructive and often also reflects correct average pairing properties. This is an approximation when the single-particle states are different from plane waves even for a zero-range interaction. Then the gap $\Delta_i = \Delta$ also becomes state-independent and the occupation numbers v_i^2 in Eq. (18) are seen only to deviate from zero or unity around the Fermi surface where the least bound particles reside. This indicates a tendency of pairing as a surface phenomenon for finite systems (Bohr et al. 1958, Bohr & Mottelson 1975).

A zero-range residual interaction leads to constant matrix-elements for plane wave single-particle states. However, the summations for constant G , e.g. in Eq. (20), produce an unphysical divergence which is removed by a cut-off in the sums at a finite value of i . The price is an adjustment, depending on the cut-off, of the value of G to a physical observable (Huang 1987, Pethick & Smith 2008). The mean-field solutions

usually deviate from plane waves arising in free space with no external confinement. However, the gap equation can in fact be solved for arbitrary mean-field states with constant matrix-elements, as discovered early on by Richardson (Richardson 1963). Any residual pairing interaction, including zero-range, will have state-dependent matrix-elements in general. It is then as convenient to use a realistic residual interaction of finite range which automatically removes the divergence. Numerical treatment is then necessary but nowadays only marginally more difficult.

The new ground state in Eq. (21) describes a system of (Cooper) pairs of particles with opposite momenta and zero total angular momentum. This result applies to continuous mean-field spectra for any attractive short-range residual interaction, and for discrete (finite) systems above a critical strength, G_c (Bohr et al. 1958, Fetter & Walecka 1971, Siemens & Jensen 1987). This ground state is sometimes called the pair condensate to emphasize the analogy with boson condensates. The first excited state is, for constant matrix elements, at 2Δ corresponding to the energy required to break one pair. The gain in energy from the normal state with a Slater determinant wave function (a filled Fermi sea) to the superfluid state is $g(\mu)\Delta^2/2$ where $g(\mu)$ is the single-particle level density at the Fermi energy μ (Fetter & Walecka 1971). Here we ignore low-energy collective modes which appear at zero excitation energy in the infinite system limit but which are pushed up to finite energy (i.e. they have an excitation gap) in finite systems as well (Landau & Lifshitz 1958).

These conclusions are quite remarkable when considering that in three dimensions it takes a finite attraction to even produce a bound state. Here (almost) any small attraction produces a qualitatively different solution. In the original treatment of the effect by Cooper (Cooper 1956) this occurs since the pairing is assumed to occur only near the Fermi surface. The problem then becomes effectively two-dimensional or, equivalently, a one-dimensional problem with a linear spectrum around the Fermi energy. Here it is well-known that an arbitrarily weak attraction leads to a bound state (Landau & Lifshitz 1981, Simon 1976, Volosniev, Fedorov, Jensen & Zinner 2011). The presence of the Fermi sea, however, implies that we are dealing with a true many-body effect. In the cold atomic gases the zero-range approximation is accurate and should be used also in the Cooper pair problem. However, the pairing interaction is now constant everywhere in the Fermi sea and this introduces the need for renormalization of the divergent bound-state equation. The bound-state remains but its energy changes. In nuclear physics, the problem is usually treated by employing a cut-off either by hand or by using a finite-range interaction that gives vanishing matrix elements above some energy scale. Thus, we see that different methods are in fact needed to extract the same physics in different fields. We also caution that one should be careful to distinguish between the Cooper pair energy and the BCS gap parameter which have similar expressions as function of the pair interaction strength (or scattering length) but different exponents (de Gennes 1999, Leggett 2006). All this should serve as a warning of the trouble that one faces when extending these concepts to small systems with few particles both in nuclear and cold atomic systems.

To summarize for nuclei, both mean-field and residual interactions are often chosen phenomenologically. It is then of less importance whether parameterizations are for a pairing residual potential, for the matrix elements themselves, or if less details are required, for the constant matrix elements combined with a cut-off. For atoms the mean-field potential is to a large extent determined by the external one-body potential although the physical two-body interaction also may contribute. The contributing matrix elements in mean-field and residual pairing interaction are not the

same although for atoms both are obtained directly from the low-energy scattering properties of the physical two-body interaction. It should be emphasized once again that the two distinct states that have the paired structure are time-reversed orbits in nuclei but they are states of different hyperfine projection in the case of cold atoms (we give more details in Section 4.3).

For atoms the procedure for the BCS-calculations could be to choose a potential of for example gaussian shape and adjust range and strength to reproduce the desired scattering length for particles in paired states. The range is very small compared to the dimension of the systems and the simplifications of a zero-range interaction is therefore tempting. However, this immediately introduces a divergence in the gap equations (Eq. (20) with $G_{ij} = G$), and a renormalization procedure becomes necessary. The method usually adopted is based on the observation that the scattering length expression from the Lippmann-Schwinger equation formally resembles the gap-equation, Eq. (20), with the same type of divergence (similar to the procedures used for Fermi gases with repulsive hardcore interaction (Fetter & Walecka 1971, Pitaevskii & Stringari 2003)). Subtraction of these two divergent equations replaces the pairing matrix element by the physical scattering length for particles in paired states, i.e.

$$\frac{m}{2\pi\hbar^2 a} = \sum_{\mathbf{k}} \frac{1}{\epsilon_{\mathbf{k}}} - \sum_{\mathbf{k}} \frac{1}{E_{\mathbf{k}}}, \quad (22)$$

which combined with the number equation in Eq. (20) provide gap, Δ , and chemical potential, μ (Eagles 1969, Leggett 1980, Engelbrecht et al. 1997, Papenbrock & Bertsch 1999, Chen et al. 2005a). This derivation is based on the assumption that the mean-field wave functions are plane waves leading to constant pairing matrix elements for the zero-range residual interaction. Thus the approximation is exact for a non-interacting system in an infinite volume. To be valid the system must therefore be dilute and spatially extended. If we start with a finite-range potential then the limit of zero-range must be approached after the infinite volume limit.

In the discussion above we have ignored the effect on pairing from polarization of the background Fermi gas. This effect was considered shortly after the introduction of BCS theory by Gorkov and Melik-Barkhudarov (Gorkov & Melik-Barkhudarov 1961) (often referred to as the GMB correction) who calculated a reduction by a factor of $(4e)^{-1/3} \sim 0.4514$ on the transition temperature from paired to normal phases in a dilute Fermi gas. The zero-temperature value of the gap discussed above is reduced by the same factor. This effect was later discussed in the specific context of ultracold atomic Fermi gases (Heiselberg et al. 2000) and similar effects have been pointed out for Bose-Fermi and Bose-Bose mixtures (Pethick & Smith 2008). Such medium effects are relevant for many condensed-matter systems such as for instance liquid ^3He where the equilibrium ground-state is determined from a manifold of degenerate possibilities by medium effects (Vollhardt & Wölfle 1990). In the context of nuclear physics, this discussion also has a long history which is intimately connected with Hartree-Fock-Bruckner theory and the independent pair approximation (Fetter & Walecka 1971, Siemens & Jensen 1987, Dickhoff & Neck 2005). For nuclear matter, the inclusion of medium polarization reduces the gap similar to the GMB corrections (Chen et al. 1993, Wambach et al. 1993, Schulze et al. 1996).

3.2. Pertinent properties of the BCS solution

The BCS solution reveals two-particle correlations through the so-called pair wave function Ψ_{pair} , i.e. the amplitude for finding one particle in \vec{r}_1 and another in \vec{r}_2 . We

have

$$\Psi_{pair}(\vec{r}_1, \vec{r}_2) \propto \langle BCS | \psi^\dagger(\vec{r}_1) \psi^\dagger(\vec{r}_2) | BCS \rangle, \quad (23)$$

where ψ^\dagger is the spatial creation operator which is expressed by the mean-field wave functions ϕ_i in the external field as

$$\psi^\dagger(\vec{r}) = \sum_i (\phi_i(\vec{r}) a_i^\dagger + \phi_{\bar{i}}(\vec{r}) a_{\bar{i}}^\dagger). \quad (24)$$

In terms of the u and v coefficients of Eq.(15) (Leggett 2006), one obtains

$$\Psi_{pair}(\vec{r}_1, \vec{r}_2) \propto \sum_i u_i v_i (\phi_i(\vec{r}_1) \phi_{\bar{i}}(\vec{r}_2) + \phi_i(\vec{r}_2) \phi_{\bar{i}}(\vec{r}_1)), \quad (25)$$

which is a symmetrized product wave function of the spatially identical wave functions ϕ_i and $\phi_{\bar{i}}$. We have omitted the antisymmetric internal wave function, spin singlet for nuclei and antisymmetrized product of hyperfine states for atoms.

The uv -factor, $u_i v_i = \Delta_i / 2E_i$, implies that the states within an energy interval of Δ around the Fermi level are the main contributors to Ψ_{pair} . When the mean-field wave functions are plane waves as for a homogeneous system the pair wave function in Eq. (23) becomes the Fourier transform of the uv -product with respect to the relative coordinate, and as such it depends only on the difference between \vec{r}_1 and \vec{r}_2 . For finite systems like nuclei the center-of-mass motion of the two particles are equally important in Ψ_{pair} as suggested by the relation $2(\vec{r}_1^2 + \vec{r}_2^2) = (\vec{r}_1 - \vec{r}_2)^2 + (\vec{r}_1 + \vec{r}_2)^2$. The wave function separates exactly into an independent center-of-mass factor for a harmonic oscillator potential, and approximately for other potentials.

The pair wave function, Ψ_{pair} , carries information about the two-body correlation for particles around the Fermi level. It can be used to compute properties related to the pairs as if it is an ordinary wave function. For instance, the relative mean square radius is obtained by

$$\langle r^2 \rangle = \int d^3 \vec{r}_1 d^3 \vec{r}_2 (\vec{r}_1 - \vec{r}_2)^2 |\Psi_{pair}(\vec{r}_1, \vec{r}_2)|^2, \quad (26)$$

where the center-of-mass coordinate in Ψ_{pair} can be removed completely for a homogeneous system and decoupled for a harmonic oscillator external mean-field. The expectation value in Eq. (26) is often called the mean square radius of a Cooper pair (Leggett 2006).

For a homogeneous system of fermions with two internal states and a zero-range two-body pairing potential, $\Psi_{pair}(\vec{r})$ is for large values of $r = |\vec{r}_1 - \vec{r}_2|$ given by (Leggett 2006)

$$\Psi_{pair}(r) \propto \frac{\sin(k_F r)}{k_F r} e^{-\sqrt{2}r/\xi'}, \quad (27)$$

where k_F is the wavenumber at the Fermi energy and $\xi' = \hbar^2 k_F / (m\Delta)$ with Δ as the pairing gap at the Fermi surface. Thus ξ' is seen as the characteristic length of the pair correlation (historically one considers $\xi = \xi'/\pi$ which is the so-called Pippard coherence length (Fetter & Walecka 1971)). The constant of proportionality in Eq. (27) depends on Δ and the density of state at k_F . The generic form of the pair wave function is shown in figure 3. From Eq.(27) we clearly see that the value of k_F determines the density of nodes of the pair wave function. These oscillations are often used as a signature of BCS behavior. However, in finite systems they can arise from other mechanism as we shall see in the nuclear case in Section 7. Except for the

exponential factor, the expression in Eq. (27) is exactly that of a free particle (or pair in relative coordinates) having an energy corresponding to k_F (also shown in figure 3). It is therefore apparent that the true many-body character of the BCS solution is found in the exponential decay of the pair correlation. However, in nuclei ξ' is large and therefore the exponential region is not entered before finite-size effects set in. We will return to this point when we consider BCS in finite nuclei in Section 7.

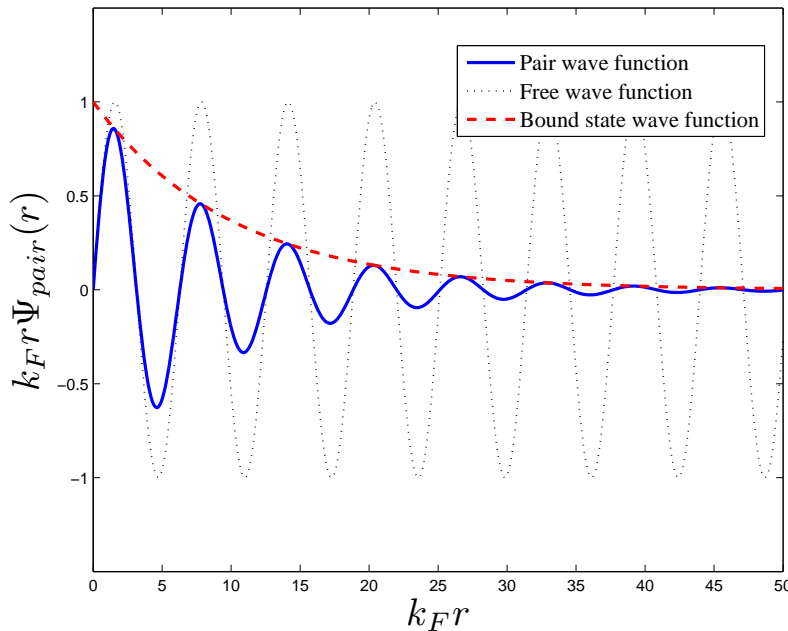


Figure 3. Plot of the pair wave function, Eq. (27), multiplied by $k_F r$ as function of $k_F r$ (solid (blue) line) for $k_F \xi' = \sqrt{200}$ (weak-coupling BCS limit). For comparison, we also show the non-interacting wave function with momentum k_F (dotted (black) line) and the bound state wavefunction corresponding to the exponential damping in Eq. (27) (dashed (red) line).

For finite systems large ξ' complicates the signature of BCS from the pair-wave function since there will always be an exponential suppression of the wave function for radii that are outside the potential range. Reduction of the BCS many-body wave function to a two-body pair wave function yields Eq. (25) which has the largest amplitude when the uv -factor is maximum, i.e. around the Fermi level where $u^2 = v^2 = 1/2$. This largest component ($k = k_F$) is responsible for the oscillating term in the approximation of Ψ_{pair} in Eq. (27). The exponential damping on the other hand becomes pronounced at large distances and grows with $\xi^{-1} \propto \Delta$. Since the condensate fraction (of Cooper pairs) is also proportional to Δ (Leggett 2006), we conclude that this damping is caused by the presence of the condensate at low energy (corresponding to large distance).

3.3. The BCS-BEC crossover

The physics of the BCS-BEC crossover originates from considerations of strongly coupled superconductors by Eagles (Eagles 1969) and atomic Fermi gases by Leggett

(Leggett 1980). The central observation is that by varying the two-particle interactions between the electrons/alkali atoms from weak to strong, one should observe a transition from the BCS paired state to a molecular BEC state where the relative two-body bound state is the relevant degree of freedom, hence the name BCS-BEC crossover. Intermediate stages would presumably have both pairs, molecules, and single fermions. It is important to emphasize that this is not a phase transition in the usual sense of Landau's theory of symmetry breaking transition but rather a smooth transition. The BCS-BEC crossover is the focus of intensive studies currently, both in condensed-matter, atomic, and nuclear physics. In particular, the use of optical lattices in ultracold atomic gas physics hold great promise for achieving insights into models that are typically applied in condensed-matter systems and are likely a key to a better understanding of high- T_c superconductivity (Chen et al. 2005a, Leggett 2006, Bloch et al. 2008, Giorgini et al. 2008).

The physics associated with crossover, i.e. the transition from extended pairs to tightly-bound molecules, is found already in the relatively simple Leggett model (Leggett 2006), which is expressed in the homogeneous version of the gap and number equations in Eqs. (20) and (22). These equations yield gap, Δ , and chemical potential, μ , for any given density $n = k_F^3/(3\pi^2)$, where k_F is the Fermi momentum related to the Fermi energy $\epsilon_F = \hbar^2 k_F^2/(2m)$. By dimensional analysis, $\Delta = \epsilon_F f(k_F a)$ and $\mu = \epsilon_F g(k_F a)$, where f and g can be determined numerically. We also have $(k_F a)^3 \propto n a^3$ (typical values are given in Table (1)). In the ultracold gases one fixes the density and then vary a through a Feshbach resonance (Bloch et al. 2008). Then we can move from the BCS regime ($k_F a \rightarrow 0^-$), where $\Delta \propto \exp(-1/k_F |a|)$ and $\mu \propto \epsilon_F$ (Leggett 2006), through unitarity at the threshold for two-body binding, where $|a|^{-1} \rightarrow 0$, and into the deep BEC regime ($k_F a \rightarrow 0^+$), where $\mu \propto -\hbar^2/2ma^2$. The latter shows that the energy per particle is half the binding energy of the molecules in the deep BEC limit as it should be. Also, one can show that in the BEC limit, $\Delta \propto \epsilon_F/(na^3)^{1/3}$. For the pair wave function of (27), this implies that $\xi' \propto a$. The bound state wave function in figure 3 is then exactly of the expected form, $e^{-r/a}/r$, and becomes a delta function for very tightly bound pairs ($a \rightarrow 0$). Importantly, keeping a constant and varying n is another way that one can explore the crossover. This can be seen by realizing that in the simple Leggett model, the dimensionless control parameter is $k_F a \propto n^{1/3}$. This observation will be important for the application discussed in Section 7.

The crossover is then the sequence of structures occurring as the interaction is varied from weak attraction describable in BCS-theory, via stronger attraction barely binding pairs, to strong attraction with substantial binding energy of pairs. When pairs can bind it is energetically advantageous to place all bound pairs in the same lowest mean-field level for pairs, thus forming a BEC of these bosons made of two fermions that exists only in the confinement of the external field. The transitions in this sequence is driven by adiabatic or sudden changes of the interaction or equivalently of a , resulting in corresponding dynamic evolution of the structure. This can either be evolution towards an equilibrium or by establishing quasi-stationary coherent oscillations between the initial state of paired atoms to the structure of a molecular BEC (Pethick & Smith 2008, Bloch et al. 2008, Giorgini et al. 2008).

The unitary region is of considerable interest since $|a| \rightarrow \infty$ means that the system effectively loses a scale, and the divergent scattering length can thus not be used as expansion parameter when calculating the energy of the system (Bertsch 1998, Giorgini et al. 2008). In this situation, the structure has to be independent of a , and hence

is referred to as the universal limit. For a Fermi system, we thus expect the energy to be proportional to the only scale in the problem: $E/N = \frac{3}{5}(1 + \beta) \frac{\hbar^2 k_F^2}{m}$, where β (sometimes given as $\eta = 1 + \beta$) is a parameter that must be determined numerically. Monte Carlo approaches (Carlson et al. 2003, Astrakharchik et al. 2004, Chang et al. 2004) give a value of $\beta = -0.58 \pm 0.01$, which indicates considerable more binding than the BCS mean-field result of $\beta = -0.41$. Analogous universal relations can be defined also in the imbalanced case (Giorgini et al. 2008) where the two internal states of the fermions are unequally occupied. The bottom line is that any Fermi system is expected to exhibit similar universal behavior provided a is large compared to other length scales.

In atomic physics, the simple homogeneous version of the gap equation in Eq. (22) is most commonly used. The assumptions are low density, negligible effects from the trap, and consequently plane wave states. In this dilute limit distances are large, momenta small, and only binary encounters are expected to contribute to the physics. These conditions are met in a typical atomic physics setup, where the density, n , is fixed and the scattering length, a , is varied.

Low density and plane waves are usually not applicable in finite nuclear systems, where the basic interaction in principle is fixed by the nucleon-nucleon potential. The bare (physical) neutron-neutron scattering length (~ -18 fm) is an order of magnitude larger than the range of the nuclear force (~ 1.4 fm), see Tab. (1). Thus, there is hope that a system of low density neutrons would show universal behavior and be described by something resembling a BCS-BEC crossover model. The approximately infinite neutron matter that one might expect to find in a neutron star therefore seems like an obvious candidate for applying crossover theory to nuclear systems (Lattimer & Prakash 2004).

However, the need for effective nucleon-nucleon potentials complicates the problem. This leads us back to the problem of separating mean-field and residual interactions for nuclei. To illustrate, we note that if one uses BCS theory in infinite nuclear matter with a realistic bare neutron-neutron potential, then one finds a value that is much smaller than both the measured gap and the value from the otherwise successful semi-empirical mass formula (Fetter & Walecka 1971). Of course, finite systems yield different results, but for large nuclei one should expect fair agreement with this limit. An effective neutron-neutron interaction can be used to give a better gap, but this is then only applicable in a strictly defined limited context in a local area of the nuclear chart and within a particular approximation scheme (such as BCS theory).

The unitary Fermi gas and the BCS-BEC crossover dynamics that can be studied with cold atomic Fermi gases also plays an important role in elucidating the nature of the so-called 'pseudogap' regime which has been proposed in connection with high-temperature superconductivity (Chen et al. 2005*b*, Chen et al. 2009). Theoretical studies find a pseudogap phase above the critical temperature for superfluidity due to preformed pairs (Randeria 1998, Janko et al. 1997, Yanase & Yamada 1999, Perali et al. 2002, Bruun & Baym 2006, Barnea 2008). However, these preformed pairs are not condensed due to large fluctuations and the underlying Fermi statistics of the particles. These predictions have been confirmed by ab-initio Monte Carlo calculations (Magierski et al. 2009, Magierski et al. 2011) and can also be obtained using quantum cluster expansions (Hu et al. 2010). A number of recent experiments (Stewart et al. 2008, Gaebler et al. 2010, Perali et al. 2011) provide strong support for

performed pairs and for the pseudogap theory (Randeria 2010).

4. The Atom Gas from a Nuclear Perspective

In order to meaningfully discuss the similarities and differences between the atomic and nuclear physics systems it is imperative to understand the relevant quantum states involved in the two situations. Therefore we will now discuss the much studied two-component Fermi gas from atomic gas physics. Bosonic states in nuclei will be addressed later in relation to α -particles. Then we will compare and contrast the interaction in the atomic physics systems with that typically employed in nuclear physics in the framework of the (nuclear) shell model. We shall continue to emphasize corresponding degrees of freedom in nuclei and cold atomic gases. Also for convenience we have collected in Table (1) a number of typical values for characteristic key quantities in the two systems.

4.1. Two-component Atomic Fermi Gases

By now the production of degenerate Fermi gases has been achieved by many experimental groups around the world (Bloch et al. 2008, Giorgini et al. 2008). However, this was initially a considerable challenge since the evaporative cooling of a single species of fermions is hindered by the Pauli exclusion principle since they are basically non-interacting. This means that the gas cannot equilibrate and lower its temperature by expelling the fastest moving atoms. If one instead prepares a gas with a population of two different species of fermions, then low-energy s -wave interactions are no longer forbidden and degeneracy can be reached (Ketterle & Zwierlein 2008). Typically the Fermi temperature, $T_F = \hbar^2 k_F^2 / 2mk_B$, is around $T_F \sim 1\mu\text{K}$, whereas experiments can cool the gas to $T \lesssim 200\text{nK}$, thus $T/T_F \lesssim 0.2$ so the degenerate regime is truly reached. The typical density of atoms in the trap is around 10^{13} cm^{-3} . This translates to an average interatomic distance of about 500 nm, which is much bigger than atomic sizes (of order 0.1 nm) and inter-atomic potential ranges of order 1-10 nm. In contrast, nucleons in nuclei have average interparticle distances of the order $\sim 1 \text{ fm}$ which is the same order as the nucleon size (see Table (1)) (Bohr & Mottelson 1975), and nuclei are never dilute in the sense of atoms in an ultracold trapped gas. The criterion for diluteness in the atomic case is usually $na^3 \ll 1$ (away from Feshbach resonances). In nuclei, na^3 is of order one or larger. This is one reason to be careful in comparing the two systems.

The atoms must be confined by an external field, a trap, and two distinctly different degrees of freedom are present, i.e. internal ones related to the atom itself and external ones related to the atoms in the trap. Correspondingly, two different energy scales emerge, i.e. the spacing of (external) trap eigenstates and the energy difference of the (internal) atomic states. We will now discuss these in detail for the relevant experimental setup.

The internal atomic quantum numbers are those of the standard hyperfine interaction, obtained from the coupling of the angular momentum (orbital, \mathbf{L} , and spin, \mathbf{S}) of the electrons and the nuclear spin, \mathbf{I} , into total spin \mathbf{F} and projection m_F . The complete set of quantum numbers is $(\mathbf{J}, \mathbf{I}, \mathbf{F}, m_F)$. In a magnetic field only m_F is conserved. In the limits of high and low field strengths there are good asymptotic quantum numbers (Pethick & Smith 2008). Systems with two components corresponding to population of the lowest two hyperfine states (of two different given

projections m_F) have been extensively studied (Ketterle & Zwierlein 2008), and recently also three-component systems (three different m_F values) have been realized in experiments (Ottenstein et al. 2008, Huckans et al. 2009, Nakajima et al. 2010). The hyperfine energy splitting for different m_F due to the magnetic field is of order 10^{-6} eV for the alkali atoms typically used in experiment (Pethick & Smith 2008). This is much smaller than any electronic transition in the atoms.

The external quantum numbers depend on the trap which often is harmonic and we shall use those of the harmonic oscillator, which for the isotropic case is (nlm) . Typically, the oscillator (trap) length $b = \sqrt{\hbar/Am_N\omega}$ (where m_N is the nucleon mass, ω the trap angular frequency, and A the mass number of the trapped species) is of the order of $1\mu\text{m}$ in a large trap. This can be translated into an energy $\hbar\omega = 4.18 \cdot 10^{-11} A^{-1} (1\mu\text{m}/b)^2$ eV. We immediately see that the trap level spacing $\hbar\omega$ is much smaller than the hyperfine splitting of order μeV . In total, the two-component Fermi gas in a trap therefore has two different internal states, m_F and m'_F , and each atomic state is in addition to the m_F -value associated with external quantum numbers, (nlm) .

If we assume a distribution of identical fermions occupying the (lowest two) hyperfine states, the lowest oscillator levels would be occupied for each m_F depending somewhat on the temperature. Inelastic collisions can in principle change the hyperfine projections of a pair of atoms. These processes are, however, suppressed and the two-component Fermi gas is therefore in practice stable with a fixed number of atoms in each hyperfine state (Ketterle & Zwierlein 2008). The hyperfine states can be considered as frozen degrees of freedom when we describe the system. The internal and external degrees of freedom are uncoupled, and no spontaneous process exist that changes the internal quantum numbers on the timescale of up to seconds of a typical experiment (Ketterle & Zwierlein 2008). This decoupling is what allows one to treat separately these two sets of degrees of freedom and use product wave functions.

Beside the one-body external field also two-body interactions between the atoms are present, thereby introducing another energy and length scale into the problem. The central part of the two-body interactions between the atoms is of the van der Waals type with characteristic length scale of 10-100 Bohr radii (0.5-5 nm) and typical low-energy s -wave scattering lengths can be 100-1000 Bohr radii and of both signs (ignoring for now the interesting case of Feshbach resonances). The average distance (500 nm) in the cloud estimated above is larger than these interaction lengths. This would imply that two-body interactions are weak. The ratio of the interaction energy, E_I to the energy of the trap, E_{HO} can be estimated for N atoms in a harmonic oscillator mean-field potential of length b and a δ -interaction of strength given by the scattering length a , i.e. $E_I/E_{HO} \sim N^{1/6} a/b$ (Pethick & Smith 2008). If we take typical numbers, $a \sim 10 - 100\text{nm}$ and $b \sim 1 - 10\mu\text{m}$, we therefore see that with $a/b \sim 0.1 - 0.001$ the ratio will be small even for millions of particles. The effect of interactions on the ground state away from resonance is therefore usually small.

The two-body interaction may, however, be varied experimentally by utilizing Feshbach resonances resulting in anything from attraction to repulsion corresponding to scattering lengths in the interval $[-\infty; \infty]$ (Chin et al. 2010). The Feshbach resonance technique exploits two internal atomic two-body states of different magnetic moments, which means that the relative energy of the two states can be controlled by an externally applied magnetic field. We illustrate the situation in figure 4. When the scattering energy in the in-coming (open) channel is resonant with a bound state in a closed channel of different magnetic moment, the scattering length blows up and passes

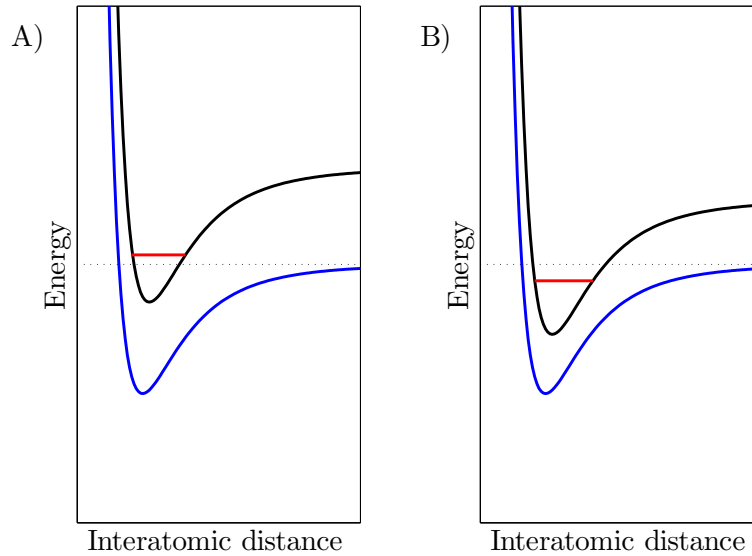


Figure 4. Illustrative plot of the physics of a Feshbach resonance. The lower (blue) potential curve indicates the open (in-coming) channel of two atoms in a given spin state, while the upper (black) curve is the closed channel that is in a different spin state from the open channel. The dotted horizontal line indicates the relative energy of the incoming atoms. The horizontal (red) line in the closed channel indicates the presence of a bound state. By tuning an externally applied magnetic field the open and closed channel potential curves can be moved relative to each other. In A) the bound state is above the relative energy, while it is goes below in B). The characteristic divergence of the scattering length, a , happens when the bound state energy coincides with the relative energy of the incoming atoms, and a changes sign when going from situation A) to B).

through infinity as the magnetic field is varied. One thus has laboratory control of the effective interaction of the atoms in the (open) scattering channel. This situation is connected with the number of bound states of the two-body interaction. The point at which the scattering length diverges is where another bound state appears (or disappears) in the potential. Note that Feshbach resonances which are properties of the two-body potentials occur for all atomic systems, irrespective of whether they are bosonic or fermionic species. However, the s -wave interaction can of course only occur between two bosons, a boson and a fermion, or two different internal states of fermions. For a single-component Fermi gas (fully polarized) the dominant interactions are usually in the p -wave channel. We also note here that there is a slight abuse of common language in scattering theory where the word 'resonance' usually denotes a feature (typically a peak) in the scattering cross section. In the realm of ultracold atomic gases, a Feshbach 'resonance' most often refers to the divergence in the scattering length as a certain external (usually magnetic) field is varied. The cause of this behavior of the scattering length is of course associated with a resonance in the traditional sense between an open and a closed channel as explained above.

A common parametrisation of the s -wave scattering length variation as the

magnetic field is tuned around a Feshbach resonance takes the form

$$a(B) = a_{bg} \left(1 - \frac{\Delta B}{B - B_0} \right), \quad (28)$$

where B_0 is the magnetic field position corresponding to a resonance at zero energy, ΔB is called the resonance width, and a_{bg} is the background value of the scattering length away from the resonance. ΔB and a_{bg} can be of both signs in general. Values and parameters for Feshbach resonances in different atomic systems can be found in (Chin et al. 2010). Correlations may increase tremendously when the scattering length diverges as the resonance is approached. Different features like BCS-BEC crossover and universality as in Efimov physics (Section 6) then arise with a demand to describe the correlations. This can be compared with the nuclear physics case where the predetermined strong nuclear interactions causes a highly correlated ground state configuration. Mean-field effects are still prominent but correlations often contribute significantly.

We now estimate the ratio of interaction energy to mean-field energy in a nucleus in order to compare to the atomic physics ratio found above. We use a crude harmonic oscillator value for the mean-field part and a phenomenological estimate for the residual pairing interaction. The mean-field energy is $N\epsilon_F \sim N\hbar\omega(6N)^{1/3}$, where ϵ_F is the Fermi energy, and we have $\hbar\omega = 41/\sqrt{N}$ MeV (see Table. (1)). The energy gain from the pairing interaction is proportional to the single-particle level density $g_F \approx N/10$ MeV⁻¹ at the Fermi energy times the square of the pairing gap $\Delta \approx 12/\sqrt{N}$ MeV (Bohr & Mottelson 1975). Thus the ratio is about $1/(5N^{5/6})$ which is small and further decreases with the number of nucleons. In terms of this estimate, the nuclear and atomic system are only comparable in the weak-coupling limit where $|a| \rightarrow 0$. When the atomic scattering lengths are large, the nuclear and atomic systems are basically incomparable, i.e. the fundamental interactions are completely different implying that the physics also is different. We note that the weak-coupling limit is not very interesting in nuclei since there is a critical interaction strength for superfluidity in finite Fermi systems. However, this does not imply that the methods and techniques cannot be carried from nuclei to atomic gases. Advanced nuclear models can deal with correlations in both fields.

In studies of trapped (two-component) atomic Fermi gases one can often replace the discrete one-body oscillator levels by the homogeneous spectrum, essentially switching to continuous momentum space. This is because the oscillator level spacing is very small and the spectrum can be well approximated as a continuum. This also holds for strong interactions, where local density or Thomas-Fermi approximations often are applied (Pethick & Smith 2008, Pitaevskii & Stringari 2003, Giorgini et al. 2008).

The temperature scale of ultracold atomic gas experiments is in the range $T \sim 10 - 100$ nK which is extremely small but nevertheless non-zero. The corresponding energy $k_B T \sim 10^{-12} - 10^{-11}$ eV is larger than the typical atomic trap spacing. Thus, the spectrum is approximately continuous and sums can be converted to appropriately weighted integrals in thermodynamic considerations. If the trap becomes tighter (small b) this approximation is no longer expected to be accurate as the level spacing of the trap states goes as $\hbar\omega \propto b^{-2}$. Then one must explicitly use the discrete spectrum and the quantum numbers of the harmonic trap. In this respect, tight traps with very few particles is the case most closely related to nuclei (Serwane et al. 2011, Zürn et al. 2012). Alternatively, a very deep periodic optical lattice potential can have

single sites that are approximately harmonic and contain only a few particles (Bloch et al. 2008), again closer to the situation in small nuclei. The notion of temperature is, however, somewhat ill-defined for isolated systems like self-bound nuclei where the energy is conserved. The temperature is only useful in connection with average quantities in sufficiently excited nuclei where the level spacing is relatively small (Bohr & Mottelson 1975, Siemens & Jensen 1987).

The tunability of atomic interactions through Feshbach resonances is an important feature of experiments that enable studies of physical system over broad regions of parameter space. In particular, one is forced to think more in terms of generally applicable theories. In nuclear physics a number of scales are intrinsic to the problem and do not change, even when considering stellar environments such as neutron stars. Typical values are listed in Tab. (1). A prominent example is the neutron-neutron scattering length which is $a \sim -18$ fm. This is an order of magnitude larger than the typical interaction range in nuclei of $r_0 \sim 1.4$ fm. This would suggest that neutron matter is in a universal regime, i.e. that the physics does not depend on the specific details of the inter-neutron potential only on the scattering length and the density of the neutron matter. The dimensionless measure of the strength of the interaction in this situation is $k_F a$ with $k_F \propto n^{1/3}$ the Fermi wave vector for a homogeneous system. This is similar to a two-component atomic Fermi gas close to a Feshbach resonance where a diverges. However, the correction to the scattering length description which is given by the effective range is intrinsically large in nuclei, $r_e \sim 2.7$ fm (Siemens & Jensen 1987). So when $k_F a$ is large so is $k_F r_e$. A theory that takes the effective range correction into account was discussed in (Schwenk & Pethick 2005) while a recent numerical study can be found in (Gezerlis & Carlson 2010). Problems with non-universal corrections also arise in connection with bosonic few-body systems, when the range of the potential, r_0 , is neglected and only the scattering length is kept, i.e. r_0/a or r_e/a are small, as is often done in effective field theory calculations of few-body properties (Deltuva & Lazauskas 2010).

In the cold atomic gases there is, however, a handle also on the relation between a and r_e near a Feshbach resonance. This stems from the fact that the effective range can be related to the width of the Feshbach resonance, ΔB (Chin et al. 2010). In fact, in zero-range models, $r_e(B)$ on resonance ($|a| = \infty$) is given by

$$r_{e0} = -\frac{2\hbar^2}{ma_{bg}\Delta B\Delta\mu}, \quad (29)$$

with m the atomic mass and $\Delta\mu$ the difference in magnetic moment between the coupled channels that cause the resonance (Petrov 2004, Jonsell 2004). The effective range can thus be reduced by working with broad resonances. Many cold atomic Fermi gas experiments have aimed for the universal physics as a diverges and have worked with broad resonances where background scales are small (Bloch et al. 2008, Ketterle & Zwierlein 2008). Also the wide resonances are easier to work with from an experimental point of view as they require less resolution on the applied magnetic field. However, very recent experiments have now started utilizing narrow resonances (Gross et al. 2010).

An aspect of recent interest for experiments is the ability to tune the scattering length to zero at $B = B_0 + \Delta B$ in the parametrisation of Eq. (28) (Roati et al. 2007, Pollack, Dries, Junker, Chen, Corcovilos & Hulet 2009). This was used to reduce interactions in atom interferometry (Fattori, D'Errico, Roati, Zaccanti, Jona-Lasinio, Modugno, Inguscio, & Modugno 2008) and to probe magnetic dipolar

interactions (Fattori, Roati, Deissler, DErrico, Zaccanti, Jona-Lasinio, Santos, Inguscio & Modugno 2008). In zero-range models of Feshbach resonances, the effective range is a function of the magnetic field, $r_e(B)$, and in fact diverges when $a \rightarrow 0$ (Zinner 2009), a fact that also holds for a model potential like the attractive $1/r^6$ potential which is the outer part of the atomic van der Waals interaction (Gao 1998). The only remaining scales are then a_{bg} and r_{e0} from Eq. (29). For a bosonic system this can lead to strong modification of the stability properties around the resonance (Zinner & Thøgersen 2009, Thøgersen, Zinner & Jensen 2009, Zinner 2011). For atomic Fermi gases the regime where $a \rightarrow 0$ remains largely unexplored which is due to the fact that the experimental use of broad resonances dominates the field and makes this non-interacting limit less interesting at the moment. As experiments become more sophisticated it is, however, clear that one should include the non-universal corrections from a non-zero effective range in the description of experimental findings.

4.2. Interaction in a Shell Model Picture

We now consider the interaction in the atomic gases and compare the language to the treatment of interactions in the standard nuclear shell model through two-body matrix elements. This will also lead us to a discussion of how to map the two-component Fermi gas with and without trap into the nuclear system of a single nucleon species. We also comment on the possibility of using the isospin formalism to describe multi-species Fermi systems.

As mentioned, the interactions of typical two-body terms in atomic gases and in nuclei are vastly different (see Tab. (1)). The atomic interactions are of ranges that are several orders of magnitude smaller than the average distance in dilute gases. For nuclei it is quite the opposite. Here the range is a few Fermis which is similar to the radius of the nucleus. The observation of pairing gaps and superfluidity in atomic gases demonstrates that interactions are very important, so in this respect atomic gases are similar to nuclei. However, we will now address a very fundamental difference that can cause confusion.

In the atomic gases, the two-body interaction originates from the van der Waals force and is a real physical interaction (Weiner et al. 1999, Köhler et al. 2006). The Hamiltonian is divided into an external one-body piece given by the trap and the two-body interaction from the atom-atom collisions governed by the van der Waals interaction. In the nuclear case, this kind of splitting is not provided a priori as the nucleon-nucleon interaction is all there is. However, in practice most methods find it convenient to split the interaction into a mean-field and a residual two-body interaction. The mean-field is chosen to reproduce average bulk properties such as energies and shell closures, whereas the residual interaction should reproduce features beyond mean-field such as collective states, superfluid properties, etc.

In practice, this splitting for nuclei is rather arbitrary and context dependent, because the basic as well as the effective nucleon-nucleon interaction is phenomenologically adjusted to selected observables. With a chosen interaction the split is seemingly optimized with the self-consistent mean-field (Ring & Schuck 1980). However, the very choice of effective interaction depends on both the selected observables and the chosen method of computation e.g. resulting in a limited Hilbert space (Siemens & Jensen 1987). The residual interaction is then whatever is left over from any given mean-field computation. These are essential problems of nuclear physics that have plagued the field.

Table 1. Estimates of typical parameters and ratios of interest in nuclear and cold atomic gas systems in natural units of MeV and fm for nuclei, and eV and nm for atoms. The bosons in the table under nuclear physics are effective constituents. For cold atomic gases we merely cite a few alkali species of recent interest. n is the particle density. r_0 is the characteristic distance of the interparticle force, which is the van der Waals length for cold atomic gases. The scattering length is given for both neutron-neutron (nn) and neutron-proton (np) for nuclei. N is the number of atoms (with two spin states for the two-component gas considered in the table) and A is the number of nucleons. b is the harmonic trap size for atoms and the system size for nuclei. $\hbar\omega$ is the trap level spacing of the outer confinement for atomic gases, whereas for nuclei it is the level spacing in a mean-field oscillator model (Fetter & Walecka 1971). $E_{HO} \sim N\hbar\omega(6N)^{1/3}$ is the total mean-field energy for atoms and $E_{HO} \sim N\hbar\omega(3A/2)^{1/3}$ for nuclei. $\epsilon_K = \hbar^2/mr_0^2$ is the characteristic kinetic energy of the interparticle potential and ϵ_{int} is the energy difference between the internal degrees of freedom. For atoms this is the hyperfine scale ΔE_{hf} , whereas for a single nucleon system with equal spin up and down components it is roughly the mean-field splitting $\hbar\omega$. E_I is the average value of a typical residual interaction for nuclei and for atoms we use $E_I/E_{HO} \sim N^{1/6}a/b$ as in the text. Δ is the typical BCS pairing gap. The numbers for atoms given in the latter part of the table are for $N = 10^6$, expect for the Fermi energy, E_F , which is given by $E_F = (3\pi^2)^{2/3}\hbar^2n^{2/3}/2m$ where m has been taken as the ${}^6\text{Li}$ mass for atoms and the nucleon mass for nuclei.

Quantity	Nuclear Physics	Cold Atomic Gases
Fermions	neutron, proton	${}^6\text{Li}$, ${}^{40}\text{K}$, etc.
Bosons	deuteron (np), α	${}^7\text{Li}$, ${}^{85}\text{Rb}$, etc.
n	0.10-0.15 fm $^{-3}$	$10^{10} - 10^{13}$ cm $^{-3}$
$d = n^{-1/3}$	~ 2 fm	500-5000 nm
r_0	~ 1.4 fm	0.5-5 nm
a (non-resonant)	-18 fm (nn) 5 fm (np)	(\pm)10-100 nm
$n a ^3$	$10^1 - 10^3$	$10^{-6} - 10^{-2}$
A/N	10-100	$10^3 - 10^6$
b	$1.2A^{1/3}$ fm	1-10 μm
$\hbar\omega$	$41/\sqrt{A}$ MeV	$\lesssim 10^{-11}$ eV
E_{HO}	$47A^{5/6}$ MeV	$\lesssim 10^{-3}$ eV
ϵ_K	10 MeV	$10^{-7} - 10^{-5}$ eV
ϵ_{int}	$\sim \hbar\omega$	$\Delta E_{hf} \sim 10^{-6}$ eV
E_I	5-15 MeV	$\lesssim 10^{-4}$ eV
E_F	$\sim 43 - 56$ MeV	$10^{-12} - 10^{-10}$ eV
Δ	0.5-2 MeV	$\lesssim 0.5\epsilon_F$
$E_I/N\epsilon_K$	0.02-0.2	0.01-1
E_I/E_{HO}	0.006-0.04	0.1-0.001
Δ/ϵ_F	< 0.05	≤ 0.5

In the following we will point out some of the problems that different choices of mean-field and residual interactions can cause. In the atomic case the choice is in this sense much more pure. At most it can be debated where to put mean-field contributions from the two-body interaction. Great care must be exercised to provide a useful and meaningful comparison which can be used to transfer techniques and concepts.

Let us now discuss the atomic interactions from a nuclear physics perspective. First we argue that s -waves of the relative motion of two scattering atoms are the dominant two-body term for the two-component gas. To distinguish from the external trap quantum number l we name the two-body relative orbital angular momentum l_r . Recall that the gas is extremely dilute with average atom-atom distance much larger than the interaction range. The two-body wave function approaches zero as r^{2l_r} ,

where r is the relative distance. For $l_r \neq 0$ there is a very small probability of finding the particles at small r -values, whereas for $l_r = 0$ the probability is non-zero. For very short-range interactions, it is therefore a good approximation to restrict interactions to the s -wave channel.

The $l_r = 0$ two-body states are symmetric, and the Pauli principle can only be satisfied by using an antisymmetric combination of the other parts of the wave function. If the system is fully polarized with all atoms in a single hyperfine state, then s -waves would be Pauli forbidden. The atoms therefore essentially do not interact, only very weakly through odd parity Pauli allowed relative states, i.e. dominantly by p -waves. On the other hand, two atoms in different hyperfine states can interact much stronger through the allowed relative s -wave interaction.

In nuclei the situation is quite different as the nucleon-nucleon interaction has a hard-core part which generates terms of all multiplicities where the strength diminishes slowly for increasing l_r (Bohr & Mottelson 1975, Siemens & Jensen 1987). Furthermore the spin-dependence is quite complicated and spin-dependent terms are strong in nuclei. This is why a full analogue with dilute gases of atoms is only appropriate for low density nuclear matter (ideally low-density neutron matter to avoid Coulomb interaction) or perhaps in very neutron-rich or halo nuclei. We will discuss some examples in the following sections.

4.3. Mapping atomic and nuclear degrees of freedom

The shell model has been extremely successful in nuclear (structure) physics. First a mean-field is generated, self-consistently and often phenomenologically adjusted, as a basis for a more detailed description. The preferred non-self-consistent phenomenological choice is the so-called Woods-Saxon potential (Bohr & Mottelson 1975), which provides bound state single-particle properties similar to that of a harmonic oscillator. For nucleons in the mean-field, a sizable spin-orbit coupling is present with opposite sign compared to the spin-orbit term for electrons in atoms. Due to the strong spin-orbit coupling in nuclear physics, it is customary to work in the coupled representation where orbital angular momentum l and nucleon spin $s = 1/2$ is coupled to $j = l \pm 1/2$ (Fetter & Walecka 1971).

For atomic physics applications of nuclear methods this coupled basis is not the most convenient choice. To spell out the precise analogies for a two-component atomic system we relate the external atomic trap degrees of freedom with the nuclear orbital motion, and the internal atomic hyperfine states with the two spin projections of the nucleon. Since the external and internal atomic degrees of freedom are effectively decoupled, an uncoupled product basis of nuclear orbital and spin motion is the closest analogy. This essentially corresponds to a harmonic oscillator without spin-orbit coupling.

To be specific we consider a two-body matrix element in the interacting nuclear shell-model with the interaction relevant for the two-component atomic gas. First we have to specify the mapping of atomic states to nuclear states. For this we choose to work with a *single* species of a spin $1/2$ nucleon. The obvious thing is to map the two hyperfine states of the two-component atomic gas to the two spin projections of the nucleon. The nuclear two-body spin wave functions can be either singlet or triplet (total spin of 0 or 1) which corresponds to atomic antisymmetric or symmetric (internal) hyperfine combinations, respectively.

The atomic two-body interaction acts in the s -wave (external) channel on opposite

hyperfine (internal) states only. This maps to s -wave nuclear interactions between opposite nucleon spin projections only. Therefore, the s -wave atomic interaction in nuclear physics notation should be expressed as $V_{atom}(r) = P_{S=0}V_2(r)P_{S=0}$, where $V_2(r)$ is the spatial part of the interaction in terms of the relative coordinate r and $P_{S=0} = (1 - \vec{\sigma}_1 \cdot \vec{\sigma}_2)/4$ is the projection onto the spin singlet (antisymmetric) component of the two-body state. One can now use the standard methods of angular momentum coupling to transform between coupled and uncoupled representations and thus calculate any matrix element needed. An explicit calculation and transformation for the zero-range interaction can be found in (Özen & Zinner 2009).

An important point in the mapping above is that the two hyperfine atomic states in a two-component Fermi gas are mapped to a single species of nucleon with each nucleon spin direction mapped to one of the two hyperfine states. Of course there are both protons and neutrons in nuclei and one could ask whether this has interesting analogies in atomic physics. The first obvious system to look for is that of trapped gases with two species of fermionic atoms, each with two internal hyperfine states. In this case the s -wave interactions between identical atoms in different hyperfine states would remain but between unlike atoms all combinations of hyperfine states would have finite interactions. This could resemble the situation in nuclear physics where neutron-neutron, neutron-proton, and proton-proton s -wave interactions are all allowed including extensively studied pairing interactions of different types (Dean & Hjorth-Jensen 2003). However, the neutron and proton interactions should then not be related as in nuclear physics but translated into independent atomic interactions each connected to their own individual hyperfine states. Recently such systems have been seriously explored in alkaline-earth gases with the purpose of use for quantum computation (Daley et al. 2008, Gorshkov et al. 2009), and for testing $SU(N)$ -models for large N (Gorshkov et al. 2010, Xu 2010). Experiments are also on-going (Fukuhara et al. 2009, De et al. 2009). Nuclear physicists often use isospin as a quantum number representing the similarity of neutrons and protons in strong interactions (Siemens & Jensen 1987). Isospin is a measure of the symmetry of the wave function resulting from the permutation symmetry of neutrons and protons in the Hamiltonian. Therefore, it is not obvious that isospin has an analogue in the atomic systems. This is because the scattering properties of atoms depend sensitively on species and hyperfine states and would therefore most likely strongly break this symmetry. The alkaline-earth gases above are, however, an example where the spin of the atomic nucleus can be mapped onto isospin (Gorshkov et al. 2010).

Another possibility is a two-component system of bosons where particles in the same hyperfine state are allowed. The three interactions between pairs in the same and in different hyperfine states should then be similar to an isospin 1 system. Also a three-component fermionic atomic system has three possible s -wave interactions (Ottenstein et al. 2008, Wenz et al. 2009) and could resemble an isospin 1 system. However, it must be kept in mind that generally the scattering lengths are different between different hyperfine components. Treating them as equal can be a good approximation at times and may help understand the symmetries of the system. Of course, a full quantitative analogy requires that one takes the different scattering lengths into account directly.

A concrete example of a fruitful interaction between nuclear physics methods and the physics of cold atomic gases is the pairing gap (Bohr & Mottelson 1975). This can be defined independently of any particular theory, as

$$\Delta(N) = \frac{E(N+1) - 2E(N) + E(N-1)}{2} \quad (30)$$

with $E(N)$ the ground-state energy of the N -body system. Extrapolation of the pairing gap in nuclear physics from binding energy differences as in (30) presupposes that the underlying structure is unchanged by adding or subtracting one nucleon. This assumption is not always well fulfilled as for example deformation may change rapidly when closed shell configurations are approached. A way to remove this problem to second order in such smoothly varying effects (such as deformation) is to use instead the double difference (Jensen & Hansen 1984)

$$\frac{1}{4} [E(N-2) - 3E(N-1) + 3E(N) - E(N+1)] \quad (31)$$

This is usually an improvement although a slightly larger range of nuclei are employed. For cold atomic gases such a procedure is typically not necessary as the expression in (30) is sufficiently accurate.

The gap is a measurable quantity, both for nuclei and for ultracold Fermi systems. In the nuclear setup, there are many advanced many-body methods that go considerably beyond BCS theory to calculate the gap. As ultracold gases become smaller and finite size and small particle numbers begin to be important, these methods can be directly transferred from nuclear physics by simple re-ordering and re-interpretation of models and interactions as we have discussed above.

4.4. Fermionic few-body systems

A particular promising venue where nuclear physics and ultracold atoms can have large overlap is in the study of fermionic systems with a limited number of particles. This is a natural condition for the physics of light nuclei with intrinsically fermionic nucleon constituent. Usually the number of atoms in a cold atomic gas experiment has been of order $10^3 - 10^6$ and a theoretical approach based on few-body methods is obviously doomed. However, recently microtraps have been built that are capable of trapping very few atoms ($1 - 10$) at very low temperatures (Serwane et al. 2011, Zürn et al. 2012). Furthermore, it is now possible to address single lattice sites in an optical lattice and produce and probe only a few atoms on such a site (Bakr et al. 2010, Sherson et al. 2010, Weitenberg et al. 2011). These developments provide hope that aspects of nuclear physics can be simulated with cold atomic gas setups in a very direct manner.

In the meantime, a question of immense theoretical interest for fermionic two-component systems was posed back in 1999 by George Bertsch and concerns the nature of the ground-state of a system of fermions with two internal states when the interaction between fermions in different internal states have a large scattering length (going to infinity, i.e. the unitarity limit). The relevance of this question for atomic gases has been outlined above, whereas for nuclear physics it is relevant for instance in neutron matter where the scattering length in the singlet channel (opposite spin direction) is large compared to the range of the nucleon-nucleon interaction. This question has sparked immense activity both for large and for small systems (a recent review can be found in (Giorgini et al. 2008)). Here we are interested in the connection to nuclei and to cold atom experiments with a limited number of particles. We will therefore focus almost exclusively on small particle number.

Early studies of this interesting question in the homogeneous case have already been discussed in Section 3.3 and here we focus on the case where the particles are confined by an external harmonic potential. An analogy to nuclei can be made by considering a mean-field potential where nucleons are confined to interact through the residual interaction.

Table 2. Energies (in units of $\hbar\omega$) calculated with the SMMC method for a trapped fermion gas with scattering lengths $a/b = 11$ (BEC) and $a/b = -1.0$ (BCS) for different particle numbers N . The statistical uncertainty is given in parenthesis. HOSD denotes the non-interacting energies. From (Zinner et al. 2009).

N	HOSD	BEC	BCS	N	HOSD	BEC	BCS
2	3	1.72(3)	2.49(3)	12	32	20.7(2)	27.23(2)
3	5.5	3.9(2)	4.84(2)	13	35.5	24.0(2)	30.21(2)
4	8	4.96(3)	6.84(4)	14	39	26.0(1)	33.16(2)
5	10.5	7.1(3)	9.14(2)	15	42.5	29.1(1)	36.08(5)
6	13	8.11(7)	11.08(5)	16	46	30.9(1)	39.03(2)
7	15.5	10.6(2)	13.28(5)	17	49.5	33.6(2)	41.98(2)
8	18	11.58(5)	15.21(4)	18	53	35.7(1)	44.89(2)
9	21.5	14.8(2)	18.30(4)	19	56.5	39.0(1)	47.85(2)
10	25	16.34(6)	21.27(3)	20	60	40.8(1)	50.75(2)
11	28.5	19.3(2)	24.28(2)	21	65.4	44.5(2)	54.50(2)

The early seminal study of Busch *et al.* (Busch et al. 1997) demonstrates that for two trapped fermions in opposite internal states the ground-state energy is $2\hbar\omega$ (see (Zinner 2012) a discussion of this model in both two- and three-dimensional traps and for a review of the relevant theoretical work and experimental support). An important benchmark for the two-component fermionic few-body problem in a harmonic trap is the exact solution for three particles at unitarity where the ground-state energy is $4.27\hbar\omega$ (Werner & Castin 2006*a*, Werner & Castin 2006*b*). These results was followed by several numerical studies of three and four trapped fermions (Stetcu et al. 2007, Alhassid et al. 2008, von Stecher & Greene 2007), and for up to 30 fermions (Chang & Bertsch 2007, Blume et al. 2007). All these studies found agreement with the exact result for three particles and furthermore established that five fermions have an energy of $5\hbar\omega$ to within a few percent at unitarity. We note that these nice universal results at unitarity break down if the two kinds of fermions have different masses at which point finite-range corrections must be taken into account (Blume & Daily 2010).

A number of studies have pursued the energy and structural properties of fermionic systems as the scattering length is varied across the Feshbach resonance using various numerical methods for three and four fermions (Stetcu et al. 2007, von Stecher & Greene 2007, Blume & Daily 2009, Daily & Blume 2010) and for larger systems as well (von Stecher et al. 2008, Zinner 2009). This can be viewed as an attempt to address the physics of the BCS-BEC crossover from the few-body side. In particular, methods rooted in exact diagonalization that have been used abundantly in nuclear physics can be directly applied to the study of fermionic systems as the scattering length is varied (Stetcu et al. 2007, Alhassid et al. 2008).

The shell model Monte Carlo approach (Koonin et al. 1997) is a traditional nuclear physics method that has been recently applied to study trapped few-body systems with fermions as the interaction is varied (Zinner 2009). In Table 2 we show results for up to 21 fermions in a harmonic trap for a positive and a negative scattering length that is close to unitarity. Notice how the results for two, three, and four particles lie on each side of the energies at unitarity quoted above. The three-dimensional harmonic oscillator trap comes with its well-known shell structure. This is illustrated in figure 5 where the upper panel shows the energy divided by the scaling expected in a Thomas-Fermi approximation. One clearly see an odd-even effect which is most pronounced on

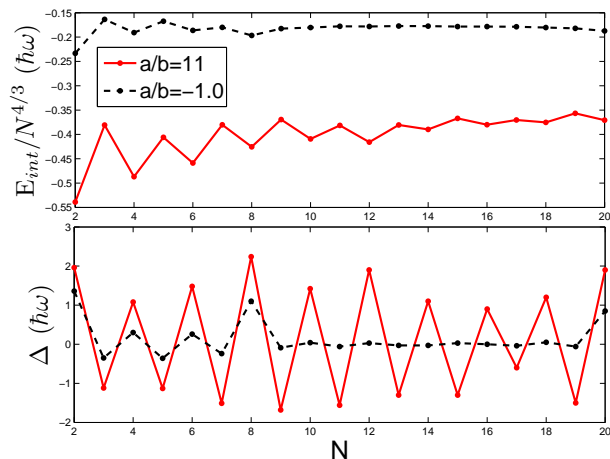


Figure 5. Scaled energies $E_{int}/N^{4/3}$, where $E_{int} = E - E_{g=0}$ (upper panel), and $\Delta(N) = E(N+1) - 2E(N) + E(N-1)$ (lower panel) as a function of particle number N for $a/b = 11$ (solid) and $a/b = -1.0$ (dashed). From (Zinner et al. 2009)

the BEC side of the resonance. A useful observable for such effects is the pairing gap discussed at the end of Section 3.2. In the lower panel of figure 5 the gap is depicted as function of particle number. The shells are seen to matter most on the weaker BCS side of the resonance. This is consistent with the finding using other methods such as fixed-node diffusion (Blume et al. 2007) and Green’s function Monte Carlo (Chang & Bertsch 2007), and with density functional theory using the local density approximation (Bulgac 2007). Similar gaps are also found in two-dimensional systems (Rontani et al. 2009).

We now consider some analogous systems from few-body nuclear physics. Nucleons are fermionic spin one-half particles and one could imagine having a two-neutron or two-proton state, the former would be more desirable due to its lack of Coulomb repulsion. However, it is well-known that only the neutron-proton system is bound (naturally occurring as the atomic deuteron, ${}^2\text{D}$). Considering then three-nucleon structures the possibilities are three neutrons, ${}^3\text{H}$ or ${}^3\text{He}$. We are interested in a comparison to the few-body cold atom systems discussed above, and will focus on neutrons for the moment since the scattering length for neutrons is large.

Since the neutron-neutron scattering length is so large it indicates that the system is close to the resonance ($|a| \rightarrow \infty$) where a bound state appears. It is then reasonable to explore whether the additional neutrons in three and four neutron clusters could provide an overall bound system. Early experimental studies provide no evidence for either system (Fairman & Meyerhof 1973). A claim of a tetra-neutron signal appeared in 2002 (Marqu es et al. 2002), which could, however, not be reproduced (Aleksandrov et al. 2005). From a theoretical point of view, it was realized much earlier that tri- and tetra-neutron cluster are unbound when using nuclear forces that give reasonable predictions for nearby bound nuclei such as ${}^3\text{H}$, ${}^3\text{He}$ and ${}^4\text{He}$ (Bevelacqua 1980). Recent calculations using state-of-the-art modern nucleon-nucleon potentials support this conclusion for both the tri- (Hemmdan et al. 2002, Lazauskas & Carbonell 2005) and tetra-neutron system (Pieper 2003).

The situation is somewhat different if one starts to consider neutron-rich few-

body nuclei that have one or a couple of protons. A nice example is ${}^5\text{H}$. It could be the structure of a deuteron (neutron-proton) and a tri-neutron but in fact has the structure of triton, ${}^3\text{H}$, plus two neutrons (de Diego et al. 2007). The latter implies that it could have an interesting three-body spectrum related to Efimov states to be discussed in Section 6. Adding one or two more neutrons would give hope of realizing a tri- or tetra-neutron plus ${}^3\text{H}$ system. However, these attempts have also been futile. In the case of two protons, i.e. in the Helium isotopic chain, one can play the same game and this has been continued all the way up to ${}^{10}\text{He}$. A review concerning the limits of stability for different isotopic chains can be found in (Thoennessen 2004).

The nuclear studies of such exotic few-body states with large imbalance of neutrons over protons are difficult due to the complicated structure of the nuclear interaction. As the interactions are well under control in cold atoms in general and also in experiments with only a few fermionic atoms, one can hope to gain insights into the general issue of small interacting Fermi systems that can be transferred into the nuclear physics domain.

5. Bosonic structures in few-body systems

The BEC structure is defined by mean-field properties. The mean-field approximation for self-bound finite systems violates translational invariance and includes a spurious center-of-mass motion. This approximation easily obscures all finite number effects, as e.g. shell effects. Conversely, a proper N -body wave function Φ only depends on $N - 1$ independent relative coordinates in conflict with the mean-field product structure. Suitable coordinates in the one-body density matrix have to be specified to allow computation of the eigenvalues which in turn decide whether a given structure can be classified as a BEC. We believe that only one combination of coordinates and wave functions is reasonable, i.e. use of initial single-particle coordinates and a total wave function where the relative wave function Ψ is multiplied by a center-of-mass function adjusted to maximize the largest eigenvalue of the resulting one-body density matrix.

Before application of BEC definitions it is desirable to know whether a given system is strongly or weakly correlated as in solids or liquids, crystal or mean-field structures, localized or delocalized structures. Second, constraints from basic symmetry requirements related to conserved quantum numbers are crucial for finite systems. After discussions of these general questions we turn to applications of α -clustering and condensation in nuclei.

5.1. Mean-field versus Localization

A system of N particles prefer crystallization at low temperature (T) if the two-body interaction has a sufficiently deep minimum to localize the relative wave function around the corresponding distance. Alternatively, the zero point motion in a weaker attraction could be larger than the range of the potential and the particles would move across the potential wells created by neighboring particles. Then each particle would rather be subject to the average potential from all particles and the mean-field approximation would be appropriate.

To classify the potentials Mottelson, following earlier work by de Boer on the solid state of noble gases (Ashcroft & Mermin 1976), introduced in (Mottelson 1999) the quantity parameter Λ_{Mot} as the ratio between the kinetic and potential energy

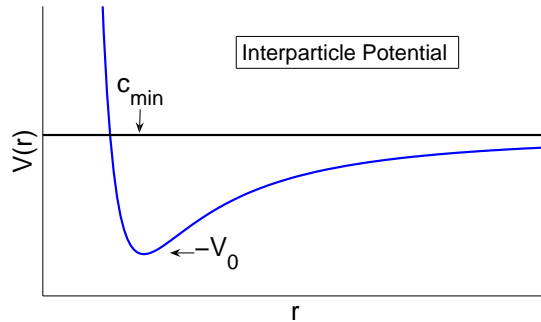


Figure 6. Illustrative plot of the inter-particle potential as a function of relative distance.

of particles located in a relative two-body potential (see Fig. 6). Using the notation of the figure, this parameter can be written

$$\Lambda_{Mot} = \frac{K}{|V|} = \frac{\hbar^2}{mc_{min}^2|V_0|}, \quad (32)$$

where m is the mass of the particles, with V_0 the depth and c_{min} the position of the assumed potential minimum. The kinetic energy K is estimated as $K = \hbar^2/mc_{min}^2$ with the momentum $p \sim \hbar/c_{min}$ and the reduced mass $m/2$. The potential energy is estimated as the value V_0 at the equilibrium position. The quantity parameter does not distinguish between bosons and fermions, implying that the criterion is a truly profound way to classify physical systems.

Mottelson noticed (Mottelson 1999) that $\Lambda_{Mot} \sim 0.1$ marks a transition between solid and liquid (mean-field) behavior. At $T = 0$ both atomic ${}^4\text{He}$ and ${}^3\text{He}$ are liquids with $\Lambda_{Mot} > 0.1$ whereas Ne and molecular H_2 are solids with $\Lambda_{Mot} < 0.1$. For nucleons $\Lambda_{Mot} \sim 0.4$ and therefore nuclei are expected to be described rather well by mean-field models. The physical interpretation is straightforward. When Λ_{Mot} is small, the kinetic energy is small compared to the potential which keeps the particles in their equilibrium positions and produces a solid. When Λ_{Mot} is large, the kinetic energy (zero point energy in the well) is larger than the depth and the particles move to distances greater than c_{min} . We note that the usual characteristic of a solid in condensed-matter physics which is the breaking of translational symmetry in the crystal lattice is not obviously applicable to the finite systems we consider here. The total wavefunction must of course be rotationally invariant, but by looking at the wavefunction as a function of the spatial coordinate for fixed center-of-mass position the localized 'solid' structure will emerge as concentrations of the probability density. Fig. (7) illustrates this for the $N = 3$ case.

When we say that the system exhibits mean-field behavior the statement is that there are single-particle wave functions extending over the whole volume occupied by the particles. However, since we are addressing interacting systems these mean-field wave functions include effects from all the other particles. The corresponding particles are "effective" in contrast to physical and the wave functions are often called quasi-particle orbits. The statement that $\Lambda_{Mot} > 0.1$ can then be reformulated by saying the low-energy quasi-particle excitations have large (compared to the systems spatial extension) mean-free path (Mottelson 1999), which is the same as total delocalization.

The quantality condition can be related to other criteria from quantum and statistical mechanics. We first distinguish between systems at a given temperature determined by an external reservoir and finite (nuclear) systems where an unambiguous way to assign a temperature does not exist. For a specified T the thermal de Broglie wavelength for ideal gases is given by (Fetter & Walecka 1971, Huang 1987)

$$\lambda_{dB}(T) = \frac{2\pi\hbar}{\sqrt{2\pi mk_B T}}, \quad (33)$$

which may be obtained from $\lambda = 2\pi\hbar/p$ and $p^2 = 2\pi mk_B T$, where p is the momentum, m is the particle mass and k_B is Boltzmann's constant. This wavelength can be used to characterize when a quantum gas of either fermions or bosons will display strong quantum behavior as the temperature is lowered. For a Bose gas the condition is $1 \ll [\lambda_{dB}(T)]^3 n$, where n is the particle density. We have $d \sim n^{-1/3}$ (with d the inter-particle distance), and this criterion can thus be written $1 \ll \lambda_{dB}(T)/d$. For a Fermi gas one has similarly $\lambda_{dB}/d \propto \sqrt{\epsilon_F/k_B T}$, where ϵ_F is the Fermi energy. We thus see that for $k_B T \ll \epsilon_F$, the de Broglie wavelength will be much greater than the average inter-particle spacing.

We used that the kinetic energy of each particle on average is $\pi k_B T$ up to factors of order unity. We assume that the total energy E of the two-body system is close to zero, implying that an estimate of the kinetic energy is $|V_0|$, see Fig. (6). Then the criterion for quantum degenerate behavior is

$$1 \ll \Lambda_{deg} \equiv \frac{\lambda_{dB}(T)}{d} = \frac{2\pi\hbar}{d\sqrt{2\pi m|V_0|}} = \sqrt{2\pi\Lambda_{Mot}}, \quad (34)$$

where we used $d \sim c_{min}$ and $V = V_0$ (see Fig. (6)). We therefore see how one can relate the quantality condition to the relation for the breakdown of the classical gas regime in statistical mechanics. Again there is no distinction between bosons and fermions, explaining the universality of Mottelson's criterion for such seemingly different systems.

Alternatively, in a finite isolated system where temperature is not assigned the de Broglie wavelength can instead be defined for the motion of the constituents as $\lambda_{dB} = 2\pi\hbar/\sqrt{2m(E-V)}$. If we now use $E \sim 0$ and $V = -V_0$, we get the same relation as in Eq. (34) except for an unimportant factor of $\sqrt{\pi}$. Thus the quantality parameter Λ_{Mot} is again related to the de Broglie wavelength of motion, λ_{dB} , and the typical inter-particle distance.

The physics interpretation is that the wavelength, both with and without temperature, compared to the inter-particle distance determines the character of the structure, i.e. small wavelengths prefer solids and large wavelengths prefer mean-field structures. More quantitatively if the wavelength reaches the order of the inter-particle distance, coherent quantum structure is preferred. The critical value is $\Lambda_{deg} \simeq 1$ or equivalently $\Lambda_{Mot} \simeq 1/(2\pi) = 0.16$ in nice agreement with the observation that $\Lambda_{Mot} \simeq 0.1$ is the critical value (Mottelson 1999). The competition of mean-field and cluster states in nuclei has recently been addressed using state-of-the-art nuclear energy density functionals (Ebran et al. 2012a, Ebran et al. 2012b) using both relativistic and non-relativistic functionals. The results obtained are consistent with the simpler models discussed above.

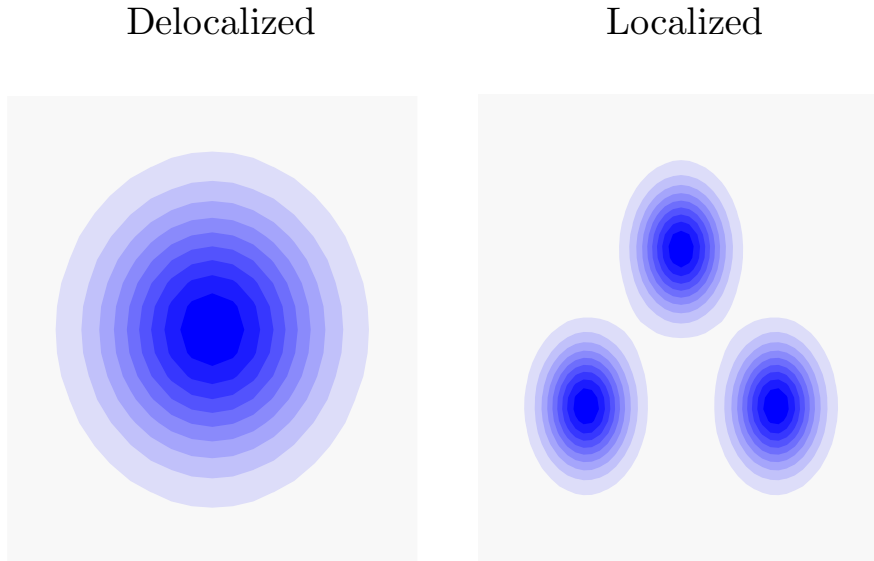


Figure 7. Illustrative plot of the delocalized wave function in Eq. (35) and the localized one in Eq. (36) for $N = 3$.

5.2. Symmetries, Localization versus Delocalization

Precise condensate criteria are derived from the one-body density matrix, $\rho_1(\vec{r}, \vec{r}')$, defined in Eq. (1). To illustrate effects of symmetry and localization we use gaussian wave functions. This allows analytic derivations yet containing the generic features of interest. A perfect mean-field product N -body wave function is given by

$$\Psi(\{\mathbf{r}_i\}) = (b\sqrt{\pi})^{-3N/2} \exp\left(-\sum_{i=1}^N r_i^2/(2b^2)\right), \quad (35)$$

where \mathbf{r}_i is the i th coordinate. This wave function, illustrated in Fig. (7), as well as all other mean-field wave functions violate translation invariance, or equivalently momentum conservation, which is restored by integrating $\Psi(\{\mathbf{r}_i - \mathbf{R}'\}) \exp(i\mathbf{P} \cdot \mathbf{R}')$ over all \mathbf{R}' (Siemens & Jensen 1987). The result, Ψ_{int} , of lowest energy has $\mathbf{P} = 0$ which for Eq. (35) results in Eq. (5) which also is invariant under rotations around the center-of-mass \mathbf{R} .

In contrast to the mean-field solution in Eq. (35), the particles can be correlated and the wave function Ψ_{loc} in a body-fixed coordinate system localized in distributions around preferred points \mathbf{R}_k , i.e.

$$\Psi_{loc}(\{\mathbf{r}_i\}) \propto \sum_{\{p\}} \exp\left(-\sum_{i=1}^N (\mathbf{r}_i - \mathbf{R}_{p(i)})^2/(2B^2)\right), \quad (36)$$

where the normalization is omitted and full symmetry is achieved by the summation over all permutations p of the set of numbers $\{1, 2, \dots, N\}$. This is illustrated in Fig. (7) for $N = 3$. The translational invariance is restored precisely as for Eq. (35), i.e. the invariant wave function is obtained from Eq. (36) by the substitution $\mathbf{r}_i \rightarrow \mathbf{q}_i = \mathbf{r}_i - \mathbf{R}$

with a corresponding change of normalization constant. The rotational invariance is broken for Ψ_{loc} in Eq. (36) but recovered for states of zero angular momentum by equally weighted linear combinations of all spatial rotations of Ψ_{loc} .

The condensate fraction depends strongly on the degree of localization as we can see explicitly by computing the one-body density matrix for Eq. (36). We assume very narrow non-overlapping gaussians and obtain

$$\begin{aligned} \rho_1(\mathbf{r}, \mathbf{r}') &= (B\sqrt{\pi})^{-3/2} \\ &\times \sum_{k=1}^N \exp(-((\mathbf{r} - \mathbf{R}_k)^2 + (\mathbf{r}' - \mathbf{R}_k)^2)/(2B^2)), \end{aligned} \quad (37)$$

which has N equally large eigenvalues while all others are zero. This is a condensate fraction of $1/N$ corresponding to one single-particle state for each of the N particles. However, after restoration of rotational symmetry only eigenvalues zero remain. If the widths, B , of the gaussians increase and they begin to overlap with each other one eigenvalue separates out and becomes finite. Increasing the width leads to increasing overlap with a product wave function like Eq. (35).

We can quantify by computing the overlap between the factorized and localized wave functions in Eqs. (35) and (36), i.e.

$$\langle \Psi | \Psi_{loc} \rangle = \left(\frac{2bB}{b^2 + B^2} \right)^{3N/2} \exp\left(-\frac{\sum_{k=1}^N R_k^2}{2b^2 + 2B^2}\right), \quad (38)$$

which only is close to unity when $b \sim B$ and either $R_i/B \ll 1$ or $R_i/b \ll 1$. Eq. (38) is also obtained if one averages Ψ_{loc} over all possible angles to obtain a rotationally invariant wave function. Thus a substantial condensate fraction requires that the overlap of Ψ_{loc} with Eq. (35) is large.

The discussion above is very simple to relate to the Mottelson quantity. The widths of the gaussians increase with the zero-point energy in the two-body potentials, which corresponds to increasing kinetic energy in Eq. (32). The states then overlap and one eigenvalue of the density matrix will grow in magnitude. On the other hand, the depth of the potential tends to localize the particles with decreasing widths for increasingly attractive potentials. The density matrix will thus have N eigenvalues of order one.

5.3. Trapped Few-Boson Systems

As discussed in Section 2.1, the characterization of cold atomic Bose gases from the one-body density matrix has been explored in great detail for large samples of atoms. To compare nuclei with relatively few particles to atomic gases we now discuss the case of a small number of bosons in a trap. Monte Carlo studies exist for the homogeneous (Giorgini et al. 1999) and the trapped case (duBois & Glyde 2001) that consider the total energy per particle. However, these results are for large systems of more than a hundred bosons. Diffusion Monte Carlo was performed for systems of $N = 2 - 50$ particles (Blume & Greene 2001), and also variational Monte Carlo has been used (Hanna & Bluhme 2006). The energy per particle obtained in the smaller systems are in good agreement with that obtained from larger systems. However, they also show considerable depletion of the condensate fraction at large scattering lengths. Common to these studies is the use of repulsive two-body potentials. This has the drawback that the range of the potential increases essentially linearly with the scattering length, i.e.

at large scattering length the range of the potential can become as large as the inter-particle spacing and the details of the potential can no longer be neglected. In this non-universal limit, where the range of the potential is comparable to the scattering length, the energy cannot be expressed in terms of only the scattering length, and an effective one-channel model for the effective interaction is no longer sufficient.

A solution to this problem is to use an attractive finite-range interaction as a model potential. This would also seem more realistic in terms of providing an effective one-channel model for the Feshbach resonances of experiments. It is well-known that potentials like the attractive gaussian or square well can attain any value for the scattering length as one increases the strength around the threshold for the appearance of a two-body bound state. This brings in the complication that the many-body problem will have many self-bound negative-energy states when bound states are allowed for a pair of bosons. However, if one uses direct numerical diagonalization, then all states are determined and it turns out that states with the properties expected of condensates appear as excited states in a quasi-continuum that are orthogonal to all the bound negative-energy states (Thøgersen et al. 2007). An example of this is shown in Fig. 8.

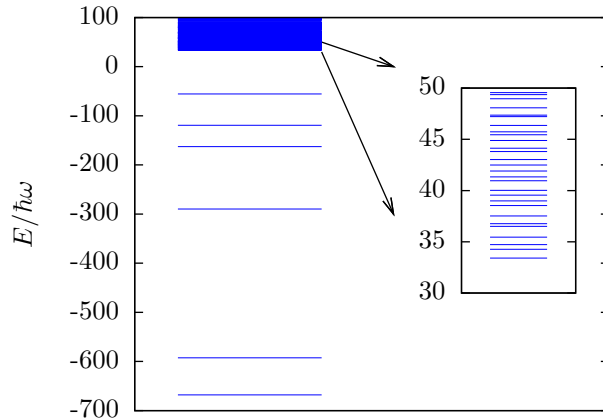


Figure 8. A typical spectrum (in the vicinity of zero energy) of a system of $N = 20$ bosons in an isotropic harmonic oscillator trap, interacting via an attractive gaussian two-body potential with one bound state and a positive scattering length. The inset shows the beginning of the so-called quasi-continuum spectrum. From (Thøgersen et al. 2007).

The condensate nature of the lowest state in the quasi-continuum can be verified by calculating the central density of the cloud. For a completely delocalized mean-field condensate state one would expect the bosons to occupy the entire trap. Indeed, as shown in Fig. 9, one finds that the first state of positive energy fulfills this conditions, whereas the negative-energy self-bound states have a much larger density and thus smaller volume per particle. This is also reflected in the condensate fraction which is small for the negative-energy states, is unity for the lowest state in the quasi-continuum, and then decreases slowly for higher-lying states (Thøgersen et al. 2007).

Another very important question is the behavior of the condensate fraction as a function of particle number. In Fig. 10 the condensate fraction is shown as the (positive) scattering length is increased for 10, 20, and 30 bosons in a trap. We clearly see the depletion of the condensate as the interaction is increased, and that this effect

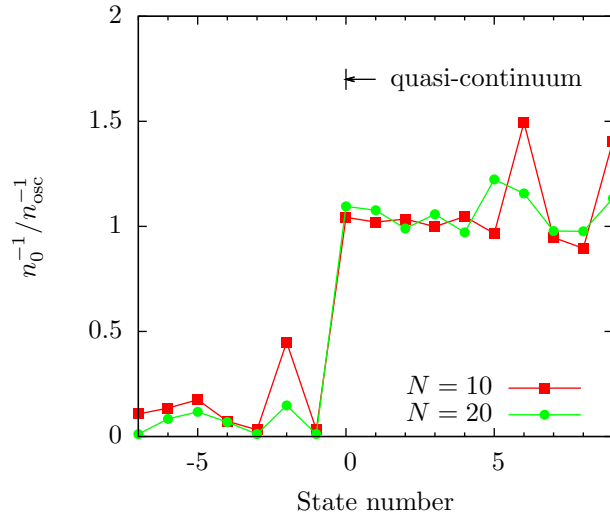


Figure 9. The inverse central density n_0^{-1} (in oscillator units $n_{osc} = \pi^{-3/2}Nb^{-3}$, where b is the oscillator length) for a system of N bosons in an isotropic harmonic oscillator trap, interacting via an attractive gaussian two-body potential, with scattering length $a = 119\text{au}$ as function of the state number. The lowest state with positive energy is numbered zero. From (Thøgersen et al. 2007).

is more severe as the particle number decreases. This demonstrates the general trend that small condensates are very fragile when interactions, and in turn correlations, are strong. Similar results can be obtained using harmonic approximation methods to the N -body problem in one, two and three dimensions at the Hamiltonian level (Załoska-Kotur et al. 2000, Yan 2003, Gajda 2006, Armstrong et al. 2011, Armstrong et al. 2012a, Armstrong et al. 2012b, Armstrong et al. 2012c, Volosniev et al. 2013) and via path integrals (Brosens et al. 1997a, Brosens et al. 1997b, Brosens et al. 1997c, Brosens et al. 1998a, Brosens et al. 1998b, Tempere et al. 1998, Tempere et al. 2000, Lemmens et al. 1999). These facts should serve as a warning that systems with very low particle numbers are hard to meaningfully describe in the same terms as condensates. Below we will look at an example from nuclear physics and the use of α -particles as a degree of freedom in the nucleus.

5.4. Nuclear α -particle condensates

The idea of α -particles as essential entities in the structure of nuclei arises from the small α -radius, the relatively large binding and the spin saturation of both neutrons and protons. Attempts were made in the early days of nuclear physics to construct nuclear structure from α -particles and valence nucleons (Wigner 1937, Wheeler 1937, Wefelmeier 1937). When more information became available these cluster structures turned out to be less than robust as indicated by the overlapping densities of the different α -particles. Thus there are no compelling reasons for clusterization of nucleons into α -particles in the bulk at nuclear densities. A review on clustering in general and α -clusters in particular can be found in (Freer 2007).

On the other hand, α -cluster models are able to explain many properties of specific light nuclei (Brink 1966). The most prominent examples are the ground

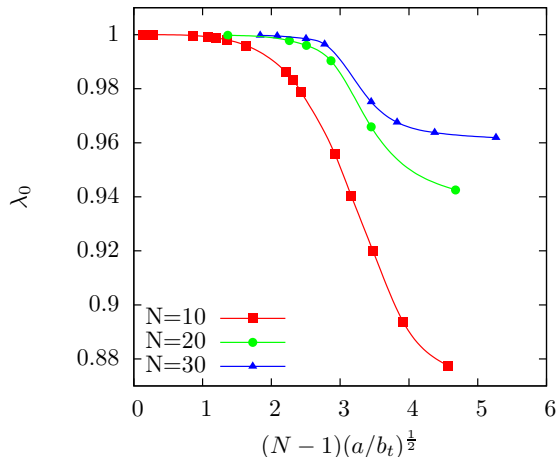


Figure 10. The condensate fraction of a BEC-state of a system of N identical bosons in an isotropic harmonic oscillator trap with attractive gaussian two-body potential as function of $(N-1)(a/b)^{1/2}$ where b is the oscillator length. From (Thøgersen et al. 2007).

state of ${}^8\text{Be}$ and the so-called Hoyle-state in ${}^{12}\text{C}$, both α -unstable 0^+ -states below all other particle emission thresholds (Hoyle 1954, Cook 1957). These structures were accurately described many years ago (Horiuchi 1970, Harvey & Jensen 1972, Uegaki et al. 1977) and later on confirmed in numerous theoretical works, see e.g. (Kanada-En'yo 1998, Descouvemont 2002, Neff & Feldmeier 2004). Based on calculations that are approximations to earlier results these states were recently interpreted as a condensate of respectively two and three α -particles (Tohsaki et al. 2001, Tohsaki et al. 2004, Funaki et al. 2002, Funaki et al. 2008, Funaki et al. 2009, Funaki et al. 2010).

Since the α -particles have spatial extension and internal structure, the general condensate condition must be supplemented by the further requirements (i) that inert α -particle constituents must be present, and (ii) that the α -cluster wave function must be orthogonal to all other many-body excited states or equivalently that the internal α -particle degrees of freedom decouple from relative degrees of freedom.

The quantity condition for an effective α - α potential can be estimated through a common parametrization in terms of an attractive and a repulsive gaussian (Ali & Bodmer 1966). The minimum value is $V_0 \approx 5-8$ MeV (including the Coulomb energy of ≈ 2 MeV) for $c_{min} \approx 2.5-3.0$ fm and $\Lambda_{Mot} \approx 0.1-0.2$. Thus the mean-field model is first choice for point-like α -particles but they have a strong tendency to localize. Thus a substantial condensate fraction can be expected for such idealized point-like particles.

However, α -particles have internal structure, finite extension, and interact via both attractive short-range and repulsive long-range forces. They have essentially to touch each other to form a resonance or bound state because the Coulomb repulsion otherwise would blow the pieces apart. At such relatively small distances the intrinsic nucleonic many-body degrees of freedom easily get excited. The restricted Hilbert space describing condensates, i.e. mean-field for α -particles and all nucleonic structures frozen, gets increasingly inadequate with increasing excitation energy, E^* , simply because the many-body density of states increases exponentially. The α -cluster

structure is most likely to be prominent at the α -disintegration thresholds which increase with nuclear excitation energy as $E^* \approx 7(N_\alpha - 2)$ MeV, where N_α is the number of α -particles in the cluster. Thus only small N_α is possible. Quantitative estimates can be found in (Zinner & Jensen 2008*a*).

To be specific we illustrate with details from the most well-known candidate, i.e. the Hoyle state of three α -particles in ^{12}C which has about 90% overlap with α -particles in relative s -waves around the center-of-mass (Matsumura & Suzuki 2004, Suzuki & Takahashi 2002, Funaki et al. 2003, Chernykh et al. 2007). This corresponds to a one-body density eigenvalue of about 0.7, computed by assuming the optimum center-of-mass wave function (Matsumura & Suzuki 2004, Suzuki & Takahashi 2002). At the same time α -cluster models show α -particle density distributions localized around specific points in space (Chernykh et al. 2007). Reconciling these results, where apparently both localization and large condensate fraction are present in the same wave function, is only possible with large widths of the localized wave in Eq. (36). This effectively recovers (most of) the independent particle wave function in Eq. (35). Since the width is large the particles are sufficiently separated to remove the need for nucleon antisymmetrization and the α -particles are present.

Thus, condition (i) is rather easily fulfilled provided the wave functions are constrained to describe essentially non-overlapping α -clusters. However, this structure is rarely an accurate approximation as conditions (ii) only is expected to hold for $N_\alpha \leq 4$ for the condensate candidates. For low excitation energy, the α -particles would overlap and the nucleon degrees of freedom wash out the α -clusterization. At higher excitation energy, the condensate wave function constructed in the limited Hilbert space, would be smeared out over numerous other close-lying states. Collective states are also very unlikely to display features of a condensate as the Coulomb interaction will mix these with other states. The realization of condensates of α particles in nuclei therefore face severe and likely insurmountable obstacles.

In relation to our discussion of trapped few-body Bose systems in Section 5.3, we note that for three or four bosons the depletion for strong interaction is severe. The α -particle studies use an effective α - α interaction that is typically a parametrisation as in (Ali & Bodmer 1966). Small changes in this interaction can thus cause large deviations in the condensate fraction. Describing these α -cluster states in terms of properties applied to condensates can therefore quickly be very model-dependent, leaving the interpretation less useful.

The linear chain structures of α -particles (Zinner & Jensen 2008*a*) at the break-up threshold (which can be organized in so-called Ikeda diagrams (Ikeda et al. 1968)) are conceptually similar to the one-dimensional atomic condensates called Tonks-Girardeau structures (Paredes et al. 2004, Kinoshita et al. 2004). Such nuclear states have been searched for and for many years the Hoyle state in ^{12}C was the favorite candidate. However, the linear chain suffers from precisely the same difficulties as the α -condensate discussed above (Zinner & Jensen 2008*a*).

Discussions about possible condensate structure are not constructive without an experimentally observable distinction from other structures. First, all one-body properties are excluded as signals. Condensates are diagnosed through coherence properties of the wave function, not by density distributions. This immediately implies that one-body observables like elastic scattering cross sections used in (Chernykh et al. 2007) cannot be used to distinguish between condensates and other structures. Second, the experiments almost inevitably at some point detect large-distance properties which in the context of coherence is related to the long-range order

parameter. For α -particles no product structure at large distance is possible due to the Coulomb repulsion. To see the short-distance bulk structure responsible for the large one-body density eigenvalue require detection of properties of structures differing by one or more particles (Gajda 2006). The results should remain unchanged except for the normalization proportional to particle number. Based on these observations, it is unclear what new physical consequences arise from approximating the fully correlated cluster states (as in (Uegaki et al. 1977)) with less accurate α -particle condensate states as no observable are available that can distinguish between the two. In any case one must also remember that all cluster states are approximations to the real nuclear states.

6. Efimov Physics

About forty years ago the Efimov effect was suggested as an anomaly appearing in a three-body system when at least two of the two-body subsystems simultaneously have short-ranged bound states at zero energy (Efimov 1970, Efimov 1971). The three-body system then has infinitely many bound states with exponentially decreasing binding energies and correspondingly increasing mean square radii. In figure 11 we present an example of the three-body spectrum considered by Efimov. The properties of these states are independent of the potentials supporting the two-body states at zero binding energy. The only requirements are that three dimensions are available, the potentials are of short-range and sufficiently attractive to provide borderline binding. We shall in this section give the simple arguments with corresponding derivations, and generalize the concept of model independence to a broader class of phenomena called Efimov physics. We shall discuss possible occurrence in nuclear, molecular or atomic systems, and the recent experimental verification in cold atoms using the technique of Feshbach resonances.

6.1. Basic derivation and occurrence conditions

Convenient coordinates for three particles are the hyperradius ρ and the five hyperangles Ω . It suffice here to define ρ by

$$m\rho^2 = \frac{1}{m_i + m_k + m_j} \sum_{i < j} m_i m_j (\mathbf{r}_i - \mathbf{r}_j)^2 \quad (39)$$

in terms of an arbitrary normalization mass m , the three masses m_k , $k = 1, 2, 3$, and the three particle coordinates \mathbf{r}_k . The pertinent properties of the Schrödinger or Faddeev equations in the present context can be extracted from the lowest effective (hyper)radial equation (Nielsen et al. 2001)

$$\left[-\frac{d^2}{d\rho^2} - \frac{\xi^2 + 1/4}{\rho^2} + \kappa^2 \right] f(\rho) = 0, \quad (40)$$

where $\kappa^2 = -2mE/\hbar^2$, and ξ is a dimensionless function of ρ determined from the interactions and the angular equations. Outside the ranges of the interactions the function ξ turns out to be independent of ρ , strongly mass (m_k) dependent (Jensen & Fedorov 2003), and ξ is a real number provided two or all three subsystems have bound states at zero energy.

The solution for the radial wavefunction is then $f \propto \sqrt{\rho} K_{i\xi}(\kappa\rho)$ where $K_{i\xi}$ is the modified Bessel function of the second kind. For small κ we get $f \propto \sqrt{\rho} \sin(\xi \ln(\rho/\rho_0))$

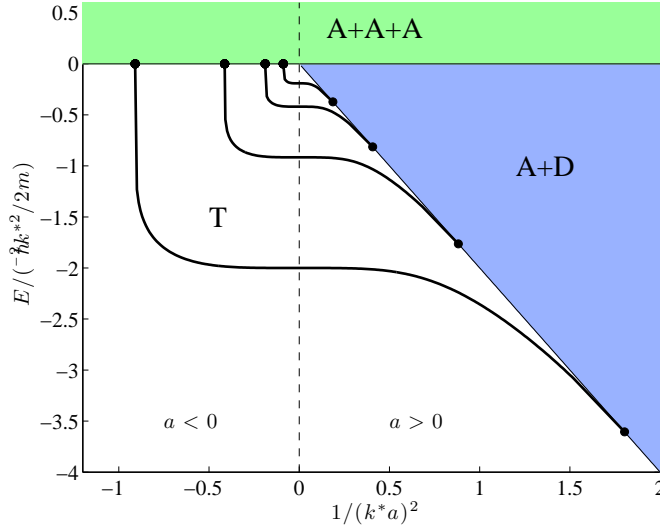


Figure 11. Energy of Efimov States as function of the scattering length. k^* is the background scale fixing the Efimov spectrum as explained in the text. On the $a < 0$ side there are no bound dimers and the trimer states (T) terminate in the three-particle continuum ($A + A + A$), whereas on the $a > 0$ side the states terminate at the atom-dimer continuum ($A + D$). Both axis have been scaled by a power of $1/8$ in order to make the similarities in the spectrum clear.

where ρ_0 is a constant defining the arbitrary length scale chosen from eq.(40) when $E \rightarrow 0$. Then ρ_0 is the first node of the wavefunction. This approximation for f could be found directly by testing the solution $f \propto \rho^{1/2 \pm i\xi}$ in eq.(40) for small κ . For large ρ the wavefunction must fall off exponentially for a bound state, i.e. $f \propto \exp(-\kappa\rho)$. The bound state energies are found by the condition $K_{i\xi}(\kappa\rho_0) = 0$, that is from the nodes of the Bessel function $K_{i\xi}(z_n) = 0$ with $\kappa_n = z_n/\rho_0$. For small κ this implies $z_n = z_0 \exp(-n\pi/\xi)$ or

$$E_n = E_0 \exp(-2n\pi/\xi) \quad , \quad \langle \rho^2 \rangle_n = \frac{\hbar^2(1 + \xi^2)}{3m|E_n|} . \quad (41)$$

These scaling relations clearly only depend on the value of ξ and an energy or length scale E_0 or ρ_0 which are determined by the finite-range potentials and the boundary conditions at small distance. If the potentials are strongly attractive a number of bound three-body states may appear at energies lower than the scaled sequence in eq.(41).

This scaling limit is reached when the scattering lengths diverges to infinity (bound state at zero energy) in comparison with the ranges of the potential. The sequence is terminated when the spatial extension of the state becomes comparable to an average of the scattering lengths. Thus we find the Efimov sequence for large scattering length, as well as for potential ranges approaching zero which is the Thomas collapse (Thomas 1935). Both effects are therefore described by these expressions.

The crucial property is the inverse square behavior of the effective potential in eq.(40) in (at least) a region of space. This form arises at distances between the effective range R_e of the two-body potentials and their scattering length a . All Efimov states are located in this region of space. By counting the number of nodes of f in this

interval we find the number of bound states to be $N_E \approx \xi/\pi \ln(a_e/R_e)$. If the strength of the $1/\rho^2$ potential is $-1/4$ only an infinitesimal negative or positive addition would produce either infinitely many bound states or none at all.

The decisive parameter is then the strength ξ which determines the character of the potential, that is infinitely many for real ξ or no bound state for imaginary ξ . The eigenvalue of the hyper-angular equation determines ξ . For identical bosons the equation is (Jensen & Fedorov 2003)

$$8 \sinh(\xi\pi/6) = \xi\sqrt{3} \cosh(\xi\pi/2) . \quad (42)$$

with the solution $\xi = 1.00624$. For non-identical bosons where all scattering lengths still are large the equation is (Jensen et al. 1997)

$$\left(\frac{\xi \cosh(\xi\pi/2)}{2F} \right)^3 - \left(\frac{\xi \cosh(\xi\pi/2)}{2F} \right) \frac{(f_1^2 + f_2^2 + f_3^2)}{F^2} = 2 , \quad (43)$$

where $F = (f_1 f_2 f_3)^{1/3}$ and

$$f_k = \frac{\sinh(\xi(\pi/2 - \varphi_k))}{\sin(2\varphi_k)} \quad (44)$$

$$\varphi_k = \arctan \left(\sqrt{m_k(m_i + m_j + m_k)/(m_i m_j)} \right) . \quad (45)$$

The limit of identical bosons is obtained from eq.(43) for $\varphi_k = \pi/3$. When only the two scattering lengths between particle pairs (j, k) and (i, k) are large the ξ equation becomes (Jensen & Fedorov 2003)

$$\xi \cosh(\xi\pi/2) \sin(2\varphi_k) = 2 \sinh(\xi(\pi/2 - \varphi_k)) , \quad (46)$$

where φ_k is now the only mass dependent parameter. The solution for $s_0 = \xi$ as function of the two mass ratios, m_2/m_1 and m_3/m_1 , is shown in figure 12.

The variation of ξ with the mass ratios cover all values from zero to infinity. Small values imply large distances between the Efimov states and for realistic finite scattering lengths there is only room for very few with smaller binding. For identical bosons the ratio of radii between two neighboring states is 22.7, that is to allow three states the scattering length must be about 10.000 times larger than the range of the potential.

On the other hand large values of ξ is also possible and many Efimov states can fit into the allowed interval. This is achieved when two masses are much larger than the third. The opposite situation with two light and one heavy mass is the least favorable to find Efimov states. Since at least two scattering lengths must be large it is much simpler to use two identical particles where any required tuning automatically is done simultaneously for both particles. However, this may also reduce the contributions to only these two subsystems where eq.(46) applies instead of eq.(42). If we maintain equal masses we find the somewhat less favorable value of $\xi = 0.499$ instead of $\xi = 1.00624$. However, if the mass of particle k is small compared to the masses of the other particles the value of ξ can be very large. The mass variation is much more efficient than increasing from two to three contributing subsystems.

The quantum statistics due to identical particles does not change anything for bosons. In contrast, none of the derivations are valid for three identical fermions where the antisymmetry requires either different s -states or at least one p -state. For two identical fermions precisely the same formulations apply since each spatial state can hold at least two fermions by use of different spin projections. The antisymmetry

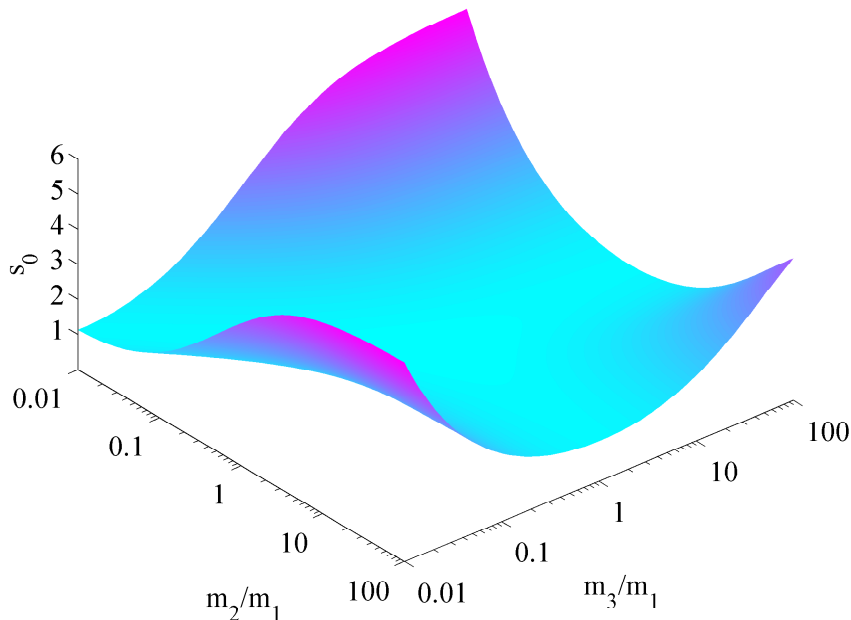


Figure 12. Surface plot of the scaling factor, $s_0 = \xi$, as function of the two mass ratios, m_2/m_1 and m_3/m_1 . The mass ratios are on a logarithmic scale.

is taken care of by the spin degree of freedom which effectively is absent for spin-independent interactions.

Unfortunately the jargon in present days cold atom physics can easily cause some confusion as we have discuss above. The single-particle states are hyperfine states of given angular momentum projection and a set of other quantum numbers related to the trap or momentum vector for a homogeneous system. The spin projection is then replaced by the hyperfine quantum numbers. Thus, since antisymmetry still is required, s -wave contact interactions are forbidden between particles in the same hyperfine state. Since two subsystems in s -waves are necessary with large scattering lengths we must have at least two different hyperfine states. Thus fermions in one of these states and the third particle (boson or fermion) in another state leave one p -wave interaction and two possible s -wave contact interactions. The total angular momentum is then at least 1 unit of \hbar . It is of course also possible to have identical fermions in three different hyperfine states. This allows all pairs to interact by s -wave contact interactions (Williams et al. 2009, Wenz et al. 2009, Nakajima et al. 2011).

The question then arises if Efimov states exist for finite three-body angular momentum $L > 0$. The answer is yes (Nielsen et al. 2001) but with conditions of sufficiently small mass, m_k , for the third s -wave interacting particle. The critical mass depends on L , which is the same as the orbital angular momentum of the two non- s wave interacting particles. For $L = 1$ the result was given as

$$m_k < 0.5(-m_i - m_j + \sqrt{(m_i + m_j)^2 + 0.60m_i m_j}). \quad (47)$$

Again only mass ratios enter the condition. This result is valid independent of the boson or fermion character of the particles. In particular, with all masses equal the requirement cannot be fulfilled since $1 > 0.5(-2 + \sqrt{4.6})$. Thus equal masses cannot

produce $L = 1$ Efimov states. Other studies have addressed the case of three identical fermions which require higher-partial wave interactions to accommodate the necessary antisymmetry (Suno et al. 2003, Macek & Sternberg 2006, Jona-Lasinio et al. 2008). We note that very recent studies indicate that p -wave interactions produce unphysical negative probabilities at the two-body level and thus also rule out an Efimov effect with p -wave interactions (Nishida 2012, Braaten et al. 2012).

As a curiosity we mention that the formulations of occurrence conditions can be investigated in any dimension d . The mathematical equations only leads to potentials of form eq.(40) and real values of ξ when $2.3 < d < 3.8$. Thus, $d = 3$ is the only integer dimension to exhibit the Efimov effect, and for that matter also the Thomas effect. However, recent investigations softened these conditions by allowing different participating particles to move in different dimensions, e.g. two particles confined to $d = 2$ and a third in $d = 3$ (see (Nishida & Tan 2011) for a recent review of such possibilities).

In a strict two dimensional setup we do not have the Efimov anomaly with infinitely many bound states around threshold but the spectrum of three-body states in the zero-range limit still has some rather peculiar features (Bruch & Tjon 1979, Nielsen et al. 1997, Nielsen et al. 1999, Volosniev et al. 2012a). In fact, for a system of three identical bosons, one finds exactly two bound three-body states, a ground state with energy $E_3 = 16.52E_2$ and an excited state with energy $E_3 = 1.27E_2$. Here $E_2 < 0$ is the energy of the two-body bound state of the zero-range potentials which always exists (Landau & Lifshitz 1981). Bosonic few-body states in two-dimensional setups with three (Adhikari et al. 1988, Adhikari et al. 1993, Brodsky et al. 2006, Kartavtsev & Malykh 2006) and four particles (Brodsky et al. 2006, Platter et al. 2004), as well as larger cluster have been studied (Hammer & Son 2004, Blume 2005, Lee 2006). In addition, the scattering (Brodsky et al. 2006) and recombination (Helfrich & Hammer 2011) has also been discussed. Recently, it explored how the number of bound states changes in system of two identical particles and a third distinct particle and for three distinct particles (Bellotti et al. 2011, Bellotti et al. 2012, Bellotti et al. 2013a).

6.2. Scaling properties and examples of Efimov physics

The almost complete absence of specific potential dependence of the derived results strongly suggests that all observables are connected by universal relations. Such model independent results are obviously valuable as predictions virtually without any input, apart from validity conditions, and as reference units to evaluate similarities and differences. A prominent and relevant example in the present context is early nucleon-nucleon scattering experiments where disparate potentials were able to reproduce the measured low-energy cross sections. The explanation was given by the effective range expansion theory where the phase shift δ was expanded as function of energy, i.e.

$$k \cot \delta(k) = -\frac{1}{a} + \frac{1}{2}k^2 R(k), \quad (48)$$

and $E = \hbar^2 k^2 / (2\mu)$. The scattering length, a , is a constant and R approaches a constant, the effective range, r_{e0} , for small k . Since a is a quantity depending on the entire potential similar to a weighted integral, the same low-energy cross section proportional to a^2 can be found from tremendously different potentials. Thus, all low-energy observables can be expressed by a without reference to specific potentials. It should be emphasized that the scattering length is periodic as function of potential

strength. The same a -dependence emerges independent of the number of deeper lying bound states.

A related result is the mean square radius of a weakly bound two-body state, i.e. $\langle r^2 \rangle = \hbar^2/(4\mu|E|)$, which only depends on the energy and the reduced mass μ . This radius-energy relation suggests a similar correlation for three-body systems. The mean square radius is now uniquely defined by $\langle \rho^2 \rangle = N \langle r^2 \rangle$ but now far from being a unique function of the three-body energy. First of all the quantities are not dimensionless but this is a problem already for the two-body system.

The first attempt towards universal curves is to use an appropriate length R related to the range of the potentials and consider $\langle (r/R)^2 \rangle = \hbar^2/(4\mu|E|R^2)$. Then all information about both radii and energies are maintained and the scale of the system does not enter. For short-range potentials a square well radius equivalent to the range of the true potential would be tempting. Since the spatial extension usually is measured by the root mean square value we could choose identical second moments of the potentials as criterion which for a gaussian of range b implies that $R = b\sqrt{5}/2$.

For three-body systems we still have to choose the scale ρ_0 (see below for some recent developments regarding this cut-off). One simple option would be to use eq.(39) with $\rho \rightarrow \rho_0$ and the two-body square well equivalent radii substituted on the right hand side. The curves of $\langle (\rho/\rho_0)^2 \rangle$ as function $\mu|E|\rho_0^2/\hbar^2$ is now closer to being universal. However, two different universal scaling functions appear (Jensen et al. 2004, Yamashita et al. 2011). One corresponds to the Efimov states with radii and energies related through eq.(41) either by varying ξ or for fixed ξ following the sequence of excited states. This is for large $|a|$. The other universal function corresponds to size and energy of Borromean states approaching the threshold for binding which occurs for moderate values of $|a|$.

For non-identical particles the individual two-body interactions can be varied independently to approach different thresholds for binding. Completely different behaviors, although still universal, are then possible for example transitions to two-body scaling behavior must appear in the limit towards a bound two-body subsystem.

Another established universal curve is the Phillips line, i.e. the three-body binding (triton) energy as function of the scattering length of the particle-dimer (nucleon-deuteron) system. This universality can be shown to originate from small energies of all involved subsystems in comparison to the nuclear potentials. The advantage of both radius and energy information can be traded for a proper universal curve. The ratio of two consecutive three-body binding energies ($|E_{n+1}|/|E_n|$) as function of relative two to three-body energies, $B_2/|E_n|$, was suggested in (Frederico et al. 1999). Measured points on such a curve are then signals of structure similar to the Efimov states.

The Efimov effect is concerned with the anomaly found for three particles when two-body subsystems are at the threshold of binding. The results are universal or model independent by depending only on the masses. This window of universality is only open when the scattering length, $|a|$, is large compared to the effective range of the interaction. It is then interesting to extend to other systems with a similar model independent description. The broader class of phenomena is naturally named Efimov physics which could be defined as physics where Universality and Scale Invariance apply. To be specific Universality then means that one global parameter determines all properties of the N -body system. Scale Invariance means that the same properties appear for any length scale whether it is in nuclei, atoms or molecules.

These concepts are easily misinterpreted to interchange meaning, i.e. scale invariance is taken to mean that the next state in a Efimov sequence of a given system has the same property as the previous state, and universality is taken to mean that different systems can be described with the same theory. We shall use our first definitions where universality means model independence and scale invariance means that the theory applies to any length and energy scale. The two ingredients begin to be similar when dimensionless quantities are used to express the physics observables. The scale dependence disappears and universal features are isolated.

The window of universality is for three particles between the two-body effective range and the scattering length. In terms of the hyperradius we have $r_e < \rho < a$. Viewed from the adiabatic hyper-radial potential the states are in the attractive region with positive hyper-radial kinetic energy. However, the size of the system is large and the two-body subsystems are quickly found far outside the range of their attraction. This means that classically forbidden regions are occupied with negative two-body kinetic energy. The origin of the model-independent features are then simply understood as properties determined outside the region of non-zero potential where the kinetic energy term decides the behavior. Due to quantum mechanics, the boundary conditions still link to the wavefunction behavior at small distance, but this is then the entire dependence describable by the model-independent scattering length parameter. Successful descriptions require spatially extended cluster systems which is difficult to achieve for self-bound systems with short-range interactions. Only s - and p -wave systems allow this. The other direction of more detailed information require short-distance properties which essentially excludes zero-range models even when effective range improvements are employed.

A number of systems are already found to exhibit universal features. The four-body energy (α -particle) is a unique function (Tjon line) of the three-body energy, i.e. the three and four-body energies are always found on the same curve (Tjon 1975). This result emerge from zero-range models which must be regularized to avoid Thomas collapse. It was shown in (Fedorov & Jensen 2001) that stabilization of the three-body system automatically ensures finite results for the N -body system. However, this does not immediately imply that all N -body systems are determined from two and three-body properties. This is still an open problem (Yamashita et al. 2010).

Universal behavior of excited four-boson states was recently found in both variational (von Stecher et al. 2009) and zero-range models (Hammer & Platter 2007). Each three-body state has two related four-body states at larger binding energy than this three-body state (Hanna & Bluhme 2006, von Stecher et al. 2009). They have too little energy to decay into this three-body state. In contrast, it was found in (Yamashita et al. 2006) that the four-body state depends on interaction details.

The concept of halo nuclei has been rudimentary extended to more than three particles. In general fully model independent nuclear N -body structures for $N > 3$ cannot be expected since all clusters are charged and either confined to small distances or repel each other by the Coulomb interaction. The line of arguments begins with assumptions of only s -waves and no correlations which prohibits halo existence (Riisager et al. 2000, Jensen et al. 2004). If correlations develop the N -body system tends to form substructures and effective reduction of the number of clusters. It is therefore interesting that (Yamashita et al. 2010) found that four and five identical bosons converge to a radius larger than the interaction range as the threshold of binding is approached. These weakly bound states have universal structures. More generally, it may be possible to use Efimov-type structures for $N = 3$ to build general

so-called higher-order Brunnian states (Baas et al. 2012).

Another class of universal Efimov-like structures was found in (Sørensen et al. 2002, Thøgersen et al. 2008a, von Stecher 2010) for N -body systems with the assumption of only two-body correlations in the variational wavefunction. This does not contradict the conclusion in (Amado & Noble 1971, Amado & Noble 1973) that the Efimov effect does not exist for $N > 3$. This result is more specifically stating that the threshold for binding the N -body system is not an accumulation point for infinitely many states.

For dilute systems two-body correlations are expected to be dominating. The sequence of excited states found between the interaction range and the scattering length obey the Efimov scaling equations in eq.(41). Whether these states (approximately) remain after extension of the Hilbert space to allow all correlations still needs to be tested. Where this conservation of identity is most likely to be preserved, for large scattering length or close to threshold of binding the N -body system, is unclear at the moment. Ground and lowest excited states may be outside the universal region and even higher excited states are the only hope for finding universal behavior. The scaling properties are expected to differ in these regions, as e.g. Borromean three-body states scale differently from Efimov states. In any case, Coulomb interactions between the particles strongly suppress the possibilities, see Section 5.

6.3. Measurable consequences in physics systems

In nuclei the clusters are all charged except for systems with neutrons surrounding a core. The Coulomb interaction is long-ranged and prevent the Efimov effect as it reaches to larger distances than the $1/\rho^2$ potential. In the pure form we are left with two neutrons and a core which again is unfavorable since the core necessarily is heavier than the neutrons. The well known case is ^{11}Li with approximately three scattering lengths each of about 20 fm which is about 8 times the core radius. The ξ value is 0.074 and the scale factor on energy and square radius is about $3 \cdot 10^{18}$. One Efimov state could then by chance be seen in the interval, but not two, and the scaling can thus not be tested.

Realistic two-body interactions for the two neutron- ^9Li system produce one bound state which moves down to about 1 MeV below threshold when the neutron- ^9Li interaction is tuned to have a bound state at zero energy. However, the many excited Efimov states can not be seen since already the first is located at an enormous distance outside the radius of the nucleus (Fedorov et al. 1994). This calculation assumes that ^9Li has angular momentum zero and therefore precisely the same interaction with both neutrons. For a non-zero ^9Li -spin the hyperfine splitting of the strong interaction prevents simultaneous large scattering lengths for both neutrons. Thus the Efimov conditions are therefore most easily met in nuclei for two neutrons and an even-even core-nucleus with zero spin.

It is still possible to see reminiscences of the Efimov effect in nuclear decays and possibly in nuclear scattering (Garrido et al. 2006). Assume for example that ^{11}Li is excited to a 1^- state above threshold for two-neutron emission. The momentum distributions of the decay products, two neutrons and ^9Li , can be measured simultaneously. Then characteristic peaks should appear in the probability for emission of both low and high energy neutrons. This corresponds to one neutron correlated with ^9Li at high energy and the other then emerges with very low

energy. The energy distribution for ${}^9\text{Li}$ has a peak at high energy corresponding to correlated emission of the two neutrons and a peak at intermediate energy originating from correlated emission of the neutron- ${}^9\text{Li}$ system. These structures are found experimentally (Hagino et al. 2009).

An example of an unexpected consequence is in dense plasma of α -particles and electrons (Jensen et al. 1995). The electron screening reduces the Coulomb repulsion between the α -particles, and in particular the long-range Coulomb tail is removed. This has first two interesting consequences, i.e. the energy of the ${}^8\text{Be}$ nucleus decreases towards zero and the Coulomb tail decreases between the α -particles. This in turn implies that the Efimov conditions are approached, and the corresponding three-body system, ${}^{12}\text{C}$, should have decreasing energies and if the screening is sufficiently strong more states should appear at the threshold. This is the triple α process proceeding via the Hoyle state. The rate could easily be dramatically changed for high plasma density and temperature.

An even more speculative example is the suggestion of recombination of three deuterons where two deuterons are bound in a molecule in a dense lattice (Engvild & Kowalski 2006). The third deuteron is injected and, catalysis-like, via three-body long-range interactions cause fusion of the molecular deuterons and expulsion of the injected deuteron. The energy gain is from formation of the α -particle.

The possibilities are enhanced by use of asymmetric systems with two heavy particles. Three-body combinations of ${}^3\text{He}$ -atoms and two alkali atoms could potentially increase the ξ -values substantially. As the scaling is exponential a number of Efimov states could appear with energy ratios of only 5 – 10. The mass ratio can be made much more extreme by using an electron as one of the particles and atoms or molecules for the other two (Jensen & Fedorov 2003). Then the energy and radius ratio of consecutive states could be very much more favorable by differing only a few percent.

Efimov scaling related to $1/r^2$ potentials appear obviously already for a charged particle in a sufficiently strong dipole field. However, coupling to rotational degrees of freedom would quickly destroy the simple properties. It was recently suggested that quantum dots and artificial atoms could prevent this rotational coupling and thus maintain the Efimov sequence (Schumayer et al. 2010).

Within the last five years a number of papers reported on experimental results obtained for cold atoms in traps and with Feshbach resonance techniques (Kraemer et al. 2006, Ottenstein et al. 2008, Zaccanti et al. 2009, Gross et al. 2009, Pollack, Dries & Hulet 2009, Barontini et al. 2009, Knoop et al. 2009, Huckans et al. 2009). The systems always consist of many particles and the Efimov states are only indirectly observed as enhanced (or depleted) probabilities for three-body decay of the trapped particles. The two-body effective interaction is varied through the magnetic field to pass values where the three-body system has zero energy. The decay into a deep dimer and a high energy third particle is enhanced since the relative and total energy of all three particles in the Efimov state is identical to their energies in the ultra cold trap. The coupling between these states is maximized and there is a transition through the Efimov state at threshold into deeper-lying dimer states accompanied by the third particle with the surplus energy to ensure energy conservation.

For very attractive two-body interactions that have positive scattering lengths ($a > 0$) and where a high-lying or shallow so-called Feshbach dimer state is present, a somewhat similar process also is enhanced. Two states have the same energy, that is the well-bound three-body Efimov state and a bound dimer with zero binding

of the third atom. From an atom-molecular cold gas the coupling between these states is largest and decay through this Efimov state into deeper-lying dimers is maximized. Periodic loss rate minima were predicted (Fedichev et al. 1996, Esry et al. 1999, Nielsen & Macek 1999, Nielsen et al. 2002) and recently also observed for two neighboring structures (Zaccanti et al. 2009). These variations should appear periodically with sizes scaled by the Efimov scaling factor of 22.7 for equal mass bosons. This three-body recombination process is discussed in details in (Esry & D’Incao 2007) and subsequently applied in analysis of the experiments. A number of these features are now confirmed (Pollack, Dries & Hulet 2009, Zaccanti et al. 2009, Gross et al. 2009), including the scale factor. We note that it is now also possible to study Efimov states in three-component ${}^6\text{Li}$ gases via radio-frequency association (Lompe et al. 2010, Nakajima et al. 2011).

The experimental study using ${}^{39}\text{K}$ presented in (Zaccanti et al. 2009) reported some deviations from universality which could potentially come from finite-range corrections beyond the universal theories that only take the scattering length into account. Some recent theoretical works have addressed the corrections coming from the finite range of inter-atomic potentials in the coordinate-space formalism (Thøgersen et al. 2008*b*, Thøgersen, Fedorov, Jensen, Esry & Wang 2009, Wang, D’Incao & Esry 2011, Sørensen et al. 2011) and using momentum-space effective field theory (Massignan & Stoof 2008, Platter et al. 2009, Ji et al. 2010, Naidon et al. 2012). In particular, the study of (Massignan & Stoof 2008) provide results that are close to the experimental data. On the nuclear physics side, finite-range corrections for three-nucleon systems have been considered by Efimov himself about two decades ago (Efimov 1991).

6.4. *New directions*

Investigations of different masses, dimensionality, and quantum statistics are also producing results both for two (Barontini et al. 2009) and three-component systems (Williams et al. 2009, Wenz et al. 2009, Nakajima et al. 2011). Now more than one three-body system can be tuned to fulfill the Efimov conditions. Two components can form light-light-heavy and light-heavy-heavy combinations with very different scaling properties as described above. For three different particles the pair interactions involve three different scattering lengths and a correspondingly more complicated analysis. To be in the universal window at least two scattering lengths must be large compared to the effective ranges of the interactions.

Extension to four-body universal states and corresponding recombination via four-body universal structures has been predicted (Hammer & Platter 2007, von Stecher et al. 2009) and now also experimentally observed for cold gasses (Pollack, Dries & Hulet 2009, Ferlaino et al. 2009). The general structures of Brunnian systems (no bound subsystems) can be anticipated to be universal provided the states are located outside the effective range. Such investigations are only barely conceived at the moment in cold gases. In nuclei such systems exist but are too spatially confined to be truly universal (Curtis et al. 2008, Muta et al. 2011). One of the latest experiments and corresponding theoretical work even seem to suggest that five-body features could be accessible in atomic gases (Zenesini et al. 2012).

A particularly surprising recent development has been the realization that the three-body parameter seems to be universal when expressed in units of the two-body interaction scale of the inter-atomic potential, which is the van der Waals

length, r_{vdW} . The three-body parameter was denoted ρ_0 in the coordinate-space hyperspherical approach discussed above but is also often quoted as a momentum-space cut-off (typically denoted Λ^* or similar). Since ρ_0 determines the lowest-lying Efimov state, the experimental findings can be written in terms of the threshold for the lowest Efimov state to appear out of the three-atom continuum on the $a < 0$ side of a Feshbach resonance. We denote this threshold a_- . The surprising result is that measurements on different atoms and using different Feshbach resonances yield $a_-/r_{\text{vdW}} \sim -9.1$ to within about 15% accuracy (Berninger et al. 2011, Wild et al. 2012, Knoop et al. 2012). This implies that there is some generic universality even in the three-body parameter which cannot be captured by simple zero-range models that need the ρ_0 supplied from elsewhere. A number of theoretical works have presented various models that explain the observations (Naidon et al. 2012, Chin 2011, Wang, D’Incao, Esry & Greene 2012, Schmidt et al. 2012, Wang, Wang, D’Incao & Greene 2012) and it seems clear that the two-body inter-atomic potential is the culprit since it has a large repulsion at short distance which will naturally provide a three-body cut-off (Sørensen et al. 2012*a*, Sørensen et al. 2012*b*). However, there is still a question of how the number of bound two-body states in the inter-atomic potential influences a_- (Wang, D’Incao, Esry & Greene 2012, Sørensen et al. 2012*a*).

In the case of nuclear physics, it seems clear that the dense environment and the complicated nuclear interaction should not allow such an easy relation. For the sake of argument, imagine that we find an Efimov state in some nuclear system with a corresponding a_-/r_0 , with r_0 the nuclear interaction range. If this number is of order -10 or so, then this implies that the nuclear system is universal since a_- is so much larger than r_0 . However, as we have discussed at length in the previous sections, this is very unlikely except for the case of pure neutron matter. Unfortunately, as pointed out above, the three neutron system is unbound.

Another interesting aspect in Efimov physics of recent times is the potential for Efimov states in the presence of long-range dipolar interactions. For fixed external polarization of the dipole moments (via applied magnetic or electric fields), it has been shown that the Efimov effect does occur for bosonic particles (Wang, D’Incao & Greene 2011*a*) while for fermionic atoms universal three-body states are possible (Wang, D’Incao & Greene 2011*b*). This is interesting in comparison to nuclear physics (and condensed-matter physics) since long-range interactions like Coulomb are generically present. One could thus hope that the analogy can be used to learn something about nuclei. These dipolar systems have also been studied in two-dimensional geometries (Wang et al. 2006, Wang 2007, Armstrong et al. 2010, Volosniev, Zinner, Fedorov, Jensen & Wunsch 2011, Zinner et al. 2012) and one-dimensional tubes (Klawunn et al. 2010, Wunsch et al. 2011, Zinner et al. 2011, Knap et al. 2012, Volosniev et al. 2013), where few-body bound states are even more prolific (Armstrong et al. 2012*d*, Volosniev et al. 2012*b*).

Efimov bound states also play a role in the recent exploration of the unitarity limit, where the so-called Tan relations can be used to deduce properties of bulk many-body systems from basic knowledge of few-body quantities (Tan 2008*a*, Tan 2008*b*, Tan 2008*c*, Braaten & Platter 2008, Combescot et al. 2009, Barth & Zwerger 2011, Pricoupenko 2011, Valiente et al. 2011, Langmack et al. 2012, Valiente 2012, Hofmann 2012, Valiente et al. 2012, Werner & Castin 2012*a*). It turns out that macroscopic observables such as the momentum distribution of a two-component Fermi system with $|a| \rightarrow \infty$ are universal and depend on only one parameter called the contact, C (Stewart et al. 2010, Kuhnle et al. 2010). However, in the case

of bosonic systems that allow Efimov three-body states, there are in fact both a parameter for two- (C_2) and three-body contributions (C_3) (Braaten et al. 2011, Castin & Werner 2011, Werner & Castin 2012*b*). Even the fact that Efimov physics does not occur in two dimensions can be observed by measuring the contact parameters (Bellotti et al. 2013*b*, Werner & Castin 2012*b*). As the contact parameters are expected to be universal, they should be the same for a nuclear system in the limit of large scattering length. Measuring the momentum distribution during nuclear break-up could perhaps be a way to test predictions from this universal theory of strong interaction and compare to the measurements in cold atomic gases. This could in turn teach us something about the strongly-coupled nuclear environment.

7. BCS-BEC in Nuclear Physics

The basic physics of the BCS-BEC crossover is contained in the Fermi gas of a homogeneous system of particles as described in Section 4. The parameters are the Fermi momentum k_F , or the density, and the s -wave scattering length a . In the ultracold gases one can fix the density n and vary the interaction parameter a through a Feshbach resonance. This variation takes the system from the BCS regime of unbound pairs, through the unitarity limit of $|a|^{-1} = 0$, and into the BEC regime of strongly bound pairs. The unitary regime can also be approached from either side by varying n for the Fermi gas since $n|a|^3$ (or $k_F|a|$) is the important parameter. This observation is the basis for attempts to find crossover effects in nuclear physics. Note, however, that it is not possible to cross unitarity by density variation and one will therefore be restricted to either BCS or BEC side of the crossover.

7.1. From infinite matter to neutron halo nuclei

As discussed earlier and listed in Tab. (1), the very large bare neutron-neutron scattering length implies that a large system of neutrons might reveal universal behavior corresponding to the limit $1/a = 0$. Such an example is a neutron star, essentially infinite neutron matter, which perhaps might be described as the universal point in a BCS-BEC crossover model.

Further investigations require an interaction but as we have discussed the bare nuclear force is only known phenomenologically, and the bare and effective in-medium nuclear interactions are different. This was evident in the discussion of polarization effects on the gap in Section 3. The details of the crossover strongly depends on the residual interaction beyond the mean-field approximation. Therefore to proceed we should separate mean-field and residual interactions. To illustrate, the BCS theory with the bare nuclear interaction produce a much smaller pairing gap in infinite nuclear matter than measured (Fetter & Walecka 1971, Dickhoff & Neck 2005). To improve one can introduce an effective and modified nuclear interaction with desired division between mean-field and residual interaction. However, this is then only applicable for a specific Hilbert space and a corresponding (BCS) approximation. The theoretical advantage of infinite nuclear matter is that the density and the corresponding interaction can be treated as a parameter. The crossover physics can then be studied as function of density.

We now turn to realistic finite nuclear systems with wave functions obtained from appropriate nuclear interactions. We immediately face several fundamental issues concerned with validity or transfer of the concepts to such systems. The interaction is

in principle fixed and at best results for the universal point can be obtained. Choice of interaction and separation into mean-field and residual parts could perhaps allow some freedom but then the chosen input conditions directly control the output. The finite systems further introduces conceptual problems of coordinates, the spurious center-of-mass motion of a self-bound system, and the definition of condensates in terms of density matrices as discussed in Section (5). We will focus on extracting the universal features related to the basic crossover concepts. Therefore we first need to address the separation of mean-field and residual interaction. The troubles of nuclear physics in this respect are no less pronounced in nuclear studies of predominantly neutron matter. Here structures (such as a bound state of two neutrons, see below) can arise purely out of particular choices of residual pairing interaction between the nucleons. Suitably adjusted zero-range interactions to describe the residual interaction between neutrons in finite nuclei have been used for many years (Skyrme 1956, Bertsch & Esbensen 1991). On the surface of it such interactions appear similar to the zero-range or short-range approximations of atomic physics. There is, however, problems with this analogy as we now explain.

The neutron-neutron interaction is often referred to as the pairing interaction which in nuclear physics is distinctly different from the full two-body interaction (Bertsch & Esbensen 1991). A commonly employed neutron-neutron pair residual interaction (Dobaczewski et al. 2001) has the form

$$V_{nn}(\mathbf{r}, \mathbf{R}) = V_0 \delta(\mathbf{r}) \left[1 - \eta \left(\frac{\rho(R)}{\rho_0} \right)^\alpha \right], \quad (49)$$

where $r = |\mathbf{r}_1 - \mathbf{r}_2|$ and $R = |\mathbf{r}_1 + \mathbf{r}_2|/2$ are the relative and center-of-mass coordinates of the neutrons and $\rho(R)$ the nuclear density at R with ρ_0 the typical nuclear saturation density (Bohr & Mottelson 1975). The parameters η and α determine the density-dependence of the interaction. Such density-dependent interactions are not used in atomic physics and any analogy must therefore be carefully examined. As one can see, for $0 < \eta < 1$ and $0 < \alpha < 1$, the pairing strength in Eq. (49) will be peaked on the surface of the nucleus, something we will return to below. Unfortunately it is not clear what values are consistent with experiments (Dobaczewski et al. 2001), and the residual interaction is therefore somewhat arbitrary.

Recent studies have made it clear that particularly the α parameter is crucial to get consistent, physically sound results (Dobaczewski et al. 2001, Rotival et al. 2009). The problem is that using $\eta = 1$ (strong pairing at the surface) and small $\alpha < 1$ can lead to crossover from BCS to BEC of neutron matter because the interaction unphysically binds the di-neutron system in the zero-density limit (Baldo et al. 1995). This leads, among other things, to prediction of neutron-rich halo nuclei that are much too large (Dobaczewski et al. 2001, Rotival et al. 2009). In particular, the pair density was found to have a constant profile out to large radii in Hartree-Fock-Bogoliubov calculations with $\alpha < 0.5$ (Rotival et al. 2009) due to the bound di-neutron. A recent study using the BCS gap equations (Matsuo 2006) recommends potentials with $\alpha < 1$ for use in nuclear calculations, which is in conflict with the observations that this binds the di-neutron system. In the latter study, the features of the neutron wave function were seen as signatures of BCS-BEC crossover behavior. However, the troublesome potential means that this conclusion is unlikely to be transferable to other nuclear or atomic systems.

The BCS-BEC crossover behavior seen in some nuclear studies using these parameters is then natural as the interaction favors it, but it might not be physical.

However, such density-dependent interaction can still be used to reliably calculate observables such as energies (Bertsch & Esbensen 1991), and also the pairing gap in nuclear matter (Baldo et al. 1995). Thus whereas average quantities like energies are accessible, the density-dependent pairing interactions like Eq. (49) can be unphysical in their predictions for the spatial structure of the neutron pair wave function.

7.2. Crossover in Finite Halo Nuclei

We now discuss recent studies of BCS-BEC crossover physics in finite nuclei. A bound state of two neutrons in a potential from an ordinary core-nucleus was recently introduced as an example of BCS-BEC crossover (Hagino et al. 2007, Horiuchi & Suzuki 2006*a*, Horiuchi & Suzuki 2006*b*). Thus a bosonic state of two neutrons is suggested to display both BCS and BEC behavior. This is truly the simplest scenario imaginable.

One of the most prominent examples of a nuclear three-body system is ^{11}Li ($^9\text{Li}+n+n$) where the two neutrons are distributed far outside the core-radius R_c . This is a Borromean halo system where none of the two-body subsystems are bound. Valence and core coordinates separate and the corresponding degrees of freedom decouple. The density variation then changes from normal nuclear density to an exponentially decreasing tail of the two neutrons. This interesting system was considered within BCS theory more than a decade ago (Barranco et al. 2001).

The physics of the halo nucleus ^{11}Li has been discussed in the context of the BEC and BCS concepts. The analogy is deduced from the behavior of the three-body wave function, $\Psi(\vec{r}, \vec{R})$, described in one set of Jacobi coordinates, where $\vec{r} = \vec{r}_1 - \vec{r}_2$ connects the neutrons and $\vec{R} = (\vec{r}_1 + \vec{r}_2)/2$ connect their center-of-mass to the core-nucleus. The s -wave part can then be projected out of Ψ and features of the remaining radial wave function $f_0(r, R)$ can be discussed in detail as function of the two coordinates (Hagino et al. 2007). The probability $|f_0|^2$ exhibits an oscillatory structure as function of r for fixed small values of R below about 1.5 fm. These oscillations disappear when R becomes larger than about 4 fm where only one peak remains. This is qualitatively the BCS-BEC crossover behavior as function of the strength of an attractive residual interaction, i.e. first the BCS oscillations and then the BEC bound state. The other potential signature of crossover is the root mean square radius of f_0 with respect to r , again as function of R . This average distance between the two neutrons goes through a minimum roughly when R is equal to the core-radius. This is a qualitative feature of crossover since the extension of a pair-wave function, as in Eq. (26), is decreasing from the BCS to the BEC-side because the attraction becomes stronger and finally binds (Eagles 1969, Leggett 1980, Leggett 2006).

We now discuss this interpretation of halo nuclei in terms of crossover physics to isolate the universality of the features of the physics involved and illustrate the influence of a particular model of the nuclear system under study and its interactions. The oscillatory behavior of the wave function and the minimum of the radius of the pair wave function must be generic, universal, and model-independent; unique signals only arising through the mechanism describing the BCS-BEC crossover. However, before discussing the question of universality, we caution that the suggested signatures involve non-observable quantities for the particular finite halo nuclei. It is therefore an indirect way to study crossover physics.

The oscillating probability as function of r is a structure appearing through correlations of different single-particle orbits in BCS theory (Leggett 2006). To assess

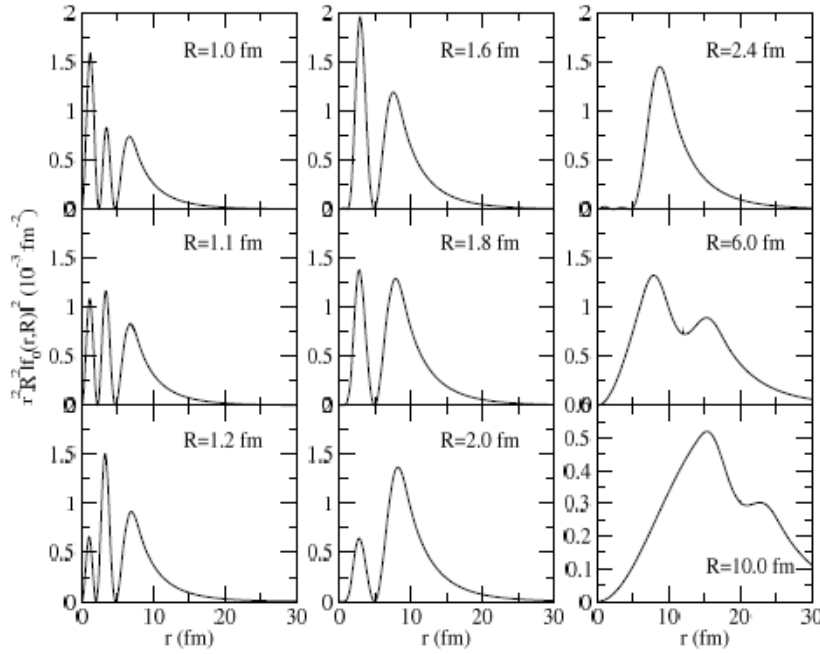


Figure 13. The probabilities as functions of r for different values of R for two non-interacting particles in the mean-field from a square well potential with depth 108 MeV and radius 3 fm. Both particles are in the second s -state each with energy -0.17 MeV. Taken from (Zinner & Jensen 2008b).

whether this is a universal feature in a finite nucleus, we take Ψ to be the uncorrelated product of two non-interacting single-particle neutron- ${}^9\text{Li}$ wave functions. We choose the second weakly bound s -wave in a square well potential and show in Fig. (13) the probabilities defined in (Hagino et al. 2007). The resemblance to the findings in (Hagino et al. 2007) is striking. However, the oscillations at small R are directly due to the nodes of the single-particle wave functions. They disappear when the lowest s -wave without nodes is used. As R increases these nodes are no longer geometrically compatible with at least one particle in the attractive part of the potential. Then the structure turns into one peak (Zinner & Jensen 2008b). Adding a short-range neutron-neutron attraction of moderate strength would maintain these features and keep the neutrons a little closer resulting in a slower increase of the peak position with R for large R .

We are led to conclude that the oscillatory behavior is not connected to many-body BCS-correlations, they are due to nodes of the single-particle neutron-core wave functions. Furthermore, the peak for large R is not a signal of a bound state or of condensation. This simple model reproduces the features which clearly demonstrates how careful one must be when assessing potential generic properties. It is always necessary to use more than one particular model of the system to check such behavior.

The second feature, a minimum in the root mean square neutron-neutron distance at a finite center-of-mass distance, is interpreted as evidence for change of BCS-correlations into BEC-structure with R . The minimum itself can be related to the

choice of interactions in (Hagino et al. 2007), which closely resembles Eq. (49) with $\eta \lesssim 1$ and $\alpha = 1$. The neutron-core interaction is attractive inside the core radius R_c and very small outside, and the neutron-neutron interaction is a δ -function in \vec{r} with an attractive strength which essentially is zero below R_c and full strength for larger R . When $R = 0$ the two neutrons can move independently inside the core, for $R = R_c$ the two neutrons can fully exploit their mutual attraction for $r = 0$, and for larger R they have to move apart to benefit from the more important neutron-core attraction. This produces the minimum in the rms value for $R \approx R_c$. We illustrate this in Fig. (14) by assuming a δ -shell potential at $R = R_c = 3$ fm. The key properties are that the neutron-neutron attraction increases with R while the neutron-core attraction vanishes outside the core.

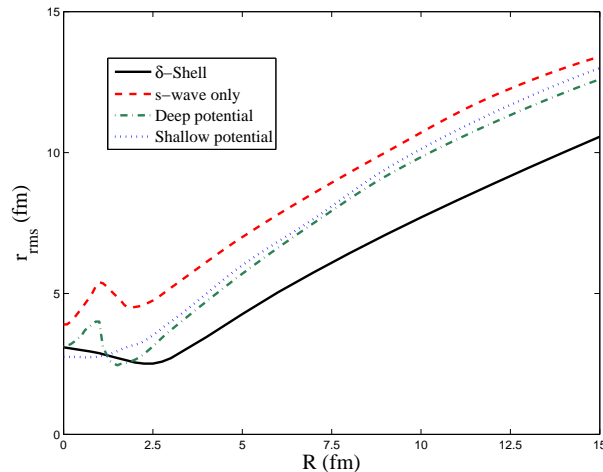


Figure 14. The root mean square distance between the two neutrons as function of their center-of-mass distance from the core. Deep (dot-dashed) and shallow (dotted) gaussian neutron-core potentials with one and with no bound states are used. We also show the results when only s -waves are retained for the deep potential (dashed), and for non-interacting neutrons in a delta-shell potential around the core (full).

Since ^{11}Li is very well studied in other successful three-body models, see e.g. (Garrido et al. 1999), we can compare results to test the universality requirement. We show in Fig. (14) neutron-neutron distances for a realistic bare neutron-neutron potential and different neutron-core potentials, i.e. a shallow and a deep gaussian without or with one bound state, respectively. These potentials are both able to reproduce the known three-body observables for ^{11}Li . They differ at short distances where the neutron is inside the core but this inner part is unimportant in descriptions of spatially extended halo nuclei. The behavior seen in Fig. (14) differ significantly from that of (Hagino et al. 2007). Either no minimum when the lowest s -state is populated or an oscillation with one maximum and one minimum when the second s -state is populated.

To see the effect of mixing partial waves we omitted p -waves, i.e. included only the s -waves in all Jacobi systems for the deep potential. The rms-curve remains similar but pushed to higher values. Finally we used a delta-shell neutron-core potential for two non-interacting neutrons. For a strongly attractive strength, where the neutrons

independently prefer to stay at R_c , the rms-curve should go from $2R_c$ through a small minimum at $R = R_c$ to a linearly increasing function at larger R . This only happens for very strong attraction otherwise the wave function is too smeared out although the same qualitative behavior remains. The conclusion is that generic pair correlations are not responsible for the rms minimum, which may appear for product wave functions and may be absent for correlated wave-mixed particles.

We have to conclude that features of BCS-BEC crossover in two-neutron halo nuclei are not generic signals and the behavior is not universal. The example demonstrates the troubles that one faces in finite systems when comparing to BCS and BEC concepts. It also demonstrates some of the inherent dangers with specific residual nuclear interactions when they are pushed beyond their designated boundaries.

8. Conclusions and perspective

The status in the fields of cold atomic gases and nuclear physics differ at the moment very much from each other. The cold atomic gases have well controlled, simple interactions and obey simultaneously simple dilute limit conditions. Nuclei are dense self-bound many-body systems with complicated phenomenological interactions but well-controlled advanced techniques. Concepts and techniques from these fields can support each other. Theoretical methods developed for nuclei are very suitable for investigations of moderate numbers of bosons and fermions and mixtures of non-identical particles. Concepts originating from condensed matter and nuclear physics, now investigated in cold atoms may reappear in nuclei, and experimental techniques will soon allow investigations of systems with striking similarity to finite nuclei, but with controlled variation of the interactions.

We have mainly focused on the simplest structures obtained in mean-field approximations. For bosons this implies that condensation could occur while for fermions pair correlations can lead to a superfluid state. In the fermionic case, the BCS-approximation is revealing after analogous degrees of freedom are identified. Pairs in time-reversed states in nuclei correspond to particles in two different internal (hyperfine) states but the same set of external confinement quantum numbers (usually parabolic traps). Relative s -waves are by far the dominating contributors to the interaction in the zero-range approximation. We consider how to relate BCS and BEC coherent quantum states from condensed matter and cold atomic gas physics to states in finite systems of few particles. The goal is to discuss universal features of these quantum states and phases and investigate whether they can be manifest in few-body systems with nuclei as the example. A particularly interesting venture at a time when trapping of small samples of only a few atoms have been realized experimentally (Serwane et al. 2011, Zürn et al. 2012, Bakr et al. 2010, Sherson et al. 2010, Weitenberg et al. 2011), implying that systems resembling few-body nuclei can be produced and studied in cold atomic gas experiments.

An important contrast is the fact that cold atomic gases are held together by an external field. For repulsive two-body interactions, an almost perfect BEC is possible (Anderson et al. 1995, Davis et al. 1995). The influence of correlations are small because the system is extremely dilute (Pethick & Smith 2008) (away from two-body scattering resonances, i.e. Feshbach resonances). For moderate attractive interactions and relatively few particles similar stable structures also exist (Ruprecht et al. 1995, Baym & Pethick 1996). However, attraction destabilizes these systems and collapse occurs into very dense and highly correlated structures (Bradley

et al. 1997, Roberts et al. 2001, Donley et al. 2001, Lahaye et al. 2008). Nuclear systems become similar to large samples of cold atoms only in the dilute limit when the density is about two orders less than that of nuclear saturation. Attempts to approach the limit of dilute nuclear states are found in the study of cluster states or weakly bound states close to particle or cluster thresholds. The BEC analog has been introduced as a few, or many, α -particles in a dilute state. However, the Coulomb repulsion would lead to immediate fragmentation or, if binding is achieved through the attractive nuclear interaction, the particles must be close-lying as for ordinary nuclei. This in turn implies that the diluteness criteria is violated and the BEC feature destroyed. Furthermore, detecting a condensate requires knowledge of the coherence in the system, for example through a two-particle correlation function. In the case of nuclear α -condensates this is impossible to measure and only standard one-body density information can be obtained. The notion of condensate in finite nuclei is therefore ill-defined and should be regarded as a crude approximation to the cluster structure of excited states in α -nuclei. Attempts to avoid the Coulomb interaction by using neutrons suffer from a similar deficiency, i.e. two neutrons can be weakly bound to a core and form a neutron halo, but adding more than a few extra nucleons would either make the system unstable due to the Pauli principle or lead to ordinary bound nuclear states. Many-body neutron halo states would fall apart or form clusters of two, three or more pieces. The external confining field is not present. Combinations allowing bosons as deuterons does not seem promising for the same reasons, i.e. the system becomes either unstable due to lack of attraction or the spatially extended deuteron structure is lost as soon as nuclear surface densities are reached.

A promising direction of cross-fertilization between nuclear physics and cold atomic gases has turned out to be the investigation of three-body bound states in the universal low-energy regime. The Efimov effect where an infinite number of three-body bound states appear near the threshold for two-body binding was initially predicted in the context of nuclear physics. With its recent experimental observation in cold atomic gases it has seen a great revival and tremendous activity in the area has ensued. Here we have discussed the universal predictions from the original hyperspherical point of view, and have suggested systems which have favourable parameters for observing the effect. The flexible tunability of experimental parameters in cold atomic gases can help elucidate the features of the Efimov effect, also beyond the universal predictions. This information could then be transferred to nuclear physics and aid in understanding why it is so difficult to see the Efimov effect in nuclear systems.

Understanding cold atomic Fermi gases are to a large extent based on pairing Hamiltonians, and the related BCS-type approximations. This is a much better approximation than for nuclei, but the theoretical models often employed in atomic physics are not always as accurate as the impressive experimental precision. In nuclear physics, improved models had to be developed, and these have now proven their capability in the description of many-fermion systems. Examples are large-scale shell-model methods, hyperspherical basis expansions, algebraic methods for pairing Hamiltonians, and density functional theory. They are based on first principle and go far beyond mean-field and pairing correlations. They are highly flexible in connection with choice of interactions and should thus be able to provide accurate results also for atomic gases. The methods are based on effective interactions adapted to reduced Hilbert spaces which is a tremendous advantage for the atomic N -body systems. These methods were first of all developed for handling identical fermions (nucleons), but also simpler bosonic systems can in most cases be treated with the same numerical

techniques. Strongly-coupled systems at unitarity and the BCS-BEC crossover region are thus obvious fields to explore. Also finite-range effects and other more complicated corrections are naturally handled by nuclear methods.

In summary, we have discussed the physics of BEC, BCS, and BCS-BEC crossover as studied in cold atomic gases from a nuclear physics perspective. We emphasized similarities, and differences through a detailed discussion of some relevant methods in wide use. We find that finite size effects in nuclear systems will most often destroy signatures of the coherent behavior that is routinely observed in cold atomic gases. No current models or measurements seem to support the interpretation of nuclear states as manifestations of BEC, BCS or crossover physics (with one potential exception being infinite neutron matter). At the moment it appears to be difficult to specify distinguishing measurable consequences or to design test experiments of the required generic features of universality, a basic first step in any successful transfer of these concepts to nuclei in particular and few-body systems in general. However, as cold atomic gas experiments with few particles become reality the situation is likely to change. On the other hand, here we have suggested some tempting cold atom systems to investigate with nuclear techniques in order to facilitate further exchange between the fields.

Acknowledgments. Numerous enlightening inputs from H. Fynbo are gratefully acknowledged. We thank M. Thøgersen, K. Riisager, D. V. Fedorov, N. Nygaard, H. Fogedby, K. Mølmer, and T. Neff for useful discussions. We thank E. Garrido for providing numerical results and N. Nygaard for providing data and invaluable help in making some of the figures.

Adhikari S K, Delfino A, Frederico T, & Tomio L 1993 *Phys. Rev. A* **47**, 1093.

Adhikari S K, Delfino A, Frederico T, Goldman I D & Tomio L 1988 *Phys. Rev. A* **37**, 3666.

Adornes A G & Kyotoku M 1992 *Z. Phys. A* **341**, 255–260.

Aleksandrov D V, Nikolskii E Y, Novatskii B G, Sakuta S B & Stepanov D N 2005 *JETP Lett.* **81**, 43–46.

Alhassid Y, Bertsch G F & Fang L 2008 *Phys. Rev. Lett.* **100**, 230401.

Ali S & Bodmer A R 1966 *Nucl. Phys.* **80**, 99.

Allen J F & Misener A D 1938 *Nature* **141**, 75.

Amado R D & Noble J V 1971 *Phys. Lett. B* **35**, 25.

Amado R D & Noble J V 1973 *Phys. Rev. D* **7**, 2517.

Amorim A E A, Frederico T & Tomio L 1997 *Phys. Rev. C* **56**, R2378.

Anderson M H, Ensher J R, Matthews M R, Wieman C E & Cornell E A 1995 *Science* **269**, 198.

Anderson P W 1959 *J. Phys. Chem. Solids* **11**, 26.

Armstrong J R, Zinner N T, Fedorov D V & Jensen A S 2010 *Euro. Phys. Lett.* **91**, 16001.

Armstrong J R, Zinner N T, Fedorov D V & Jensen A S 2011 *J. Phys. B: At. Mol. Opt. Phys.* **44**, 055303.

Armstrong J R, Zinner N T, Fedorov D V & Jensen A S 2012a *Physica Scripta* **T151**, 014061.

Armstrong J R, Zinner N T, Fedorov D V & Jensen A S 2012b *Phys. Rev. E* **85**, 021117.

Armstrong J R, Zinner N T, Fedorov D V & Jensen A S 2012c *Phys. Rev. E* **86**, 021115.

Armstrong J R, Zinner N T, Fedorov D V & Jensen A S 2012d *Eur. Phys. J. D* **66**, 85.

Ashcroft N W & Mermin N D 1976 *Solid State Physics* Brooks Cole, 1st Ed.

Astrakharchik G E, Boronat J, Casulleras J & Giorgini S 2004 *Phys. Rev. Lett.* **93**, 200404.

Baas N A, Fedorov D V, Jensen A S, Riisager K, Volosniev A G & Zinner N T 2012 *arXiv:1205.0746*

Bachor H A & Ralph T C 2004 *A Guide to Experiments in Quantum Optics* Wiley-VCH, Weinheim.

Bakr W S, Peng A, Tai M E, Simon J, Gillen J I, Fölling S, Pollet L & Greiner M 2010 *Science* **329**, 547–550.

Baldo M, Lombardo U & Schuck P 1995 *Phys. Rev. C* **52**, 975.

Bardeen J, Cooper L N & Schrieffer J R 1957 *Phys. Rev.* **108**, 1175.

Barnea N 2008 *Phys. Rev. A* **78**, 053629.

- Barontini G, Weber C, Rabatti F, Catani J, Thalhammer G, Inguscio M & Minardi F 2009 *Phys. Rev. Lett.* **103**, 043201.
- Barranco F, Bortignon P F, Broglia R A, Colò G & Vigezzi E 2001 *Eur. Phys. Jour. A* **11**, 385.
- Barrett B R 1980 *Phys. Scr.* **21**, 266.
- Barth M & Zwerger W 2011 *Ann. Phys. (Berlin)* **326**, 2544–2565.
- Baym G 1969 *Lectures on Quantum Mechanics* W.A. Benjamin, Inc., New York.
- Baym G 1998 *Act. Phys. Pol. B* **29**, 1839–1884.
- Baym G & Pethick C J 1996 *Phys. Rev. Lett.* **76**, 6.
- Bellotti F F, Frederico T, Yamashita M T, Fedorov D V, Jensen A S & Zinner N T 2011 *J. Phys. B: At. Mol. Opt. Phys.* **44**, 205302.
- Bellotti F F, Frederico T, Yamashita M T, Fedorov D V, Jensen A S & Zinner N T 2012 *Phys. Rev. A* **85**, 025601.
- Bellotti F F, Frederico T, Yamashita M T, Fedorov D V, Jensen A S & Zinner N T 2013 *J. Phys. B: At. Mol. Opt. Phys.* **46**, 055301.
- Bellotti F F, Frederico T, Yamashita M T, Fedorov D V, Jensen A S & Zinner N T 2013b *Phys. Rev. A* **87**, 013610.
- Berninger M, Zenesini A, Huang B, Harm W, Nägerl H C, Ferlaino F, Grimm R, Julienne P S & Hutson J M 2011 *Phys. Rev. Lett.* **107**, 120401.
- Bertsch G F 1998 in ‘Conference talk’.
- Bertsch G F & Esbensen H 1991 *Annals of Phys.* **209**, 327.
- Bevelacqua J J 1980 *Nucl. Phys. A* **341**, 414–420.
- Bloch I, Dalibard J & Zwerger W 2008 *Rev. Mod. Phys.* **80**, 881.
- Bloch I, Hänsch T W & Esslinger T 2000 *Nature* **403**, 166.
- Blume D 2005 *Phys. Rev. B* **72**, 094510.
- Blume D & Daily K M 2009 *Phys. Rev. A* **80**, 053626.
- Blume D & Daily K M 2010 *Phys. Rev. Lett.* **105**, 170403.
- Blume D & Greene C H 2001 *Phys. Rev. A* **63**, 063601.
- Blume D, von Stecher J & Greene G H 2007 *Phys. Rev. Lett.* **99**, 233201.
- Bogner S K, Furnstahl R J & Schwenk A 2010 *Prog. Part. Nucl. Phys.* **65**, 94–147.
- Bohn J L, Esry B D & Greene C H 1998 *Phys. Rev. A* **58**, 584.
- Bohr A & Mottelson B R 1975 *Nuclear Structure, Vol. I and II* Benjamin, Reading Massachusetts.
- Bohr A, Mottelson B R & Pines D 1958 *Phys. Rev.* **110**, 936.
- Braaten E, Hagen P, Hammer H W & Platter L 2012 *Phys. Rev. A* **86**, 012711.
- Braaten E, Kang D & Platter L 2011 *Phys. Rev. Lett.* **106**, 153005.
- Braaten E & Platter L 2008 *Phys. Rev. Lett.* **100**, 205301.
- Bradley C C, Sackett C A & Hulet R G 1997 *Phys. Rev. Lett.* **78**, 985.
- Brandow B 1967 *Rev. Mod. Phys.* **39**, 771.
- Brink D M 1966 in C Bloch, ed., ‘Proceedings of the International School of Physics “Enrico Fermi”’, Course 36, Varenna, 1965’ Academic Press.
- Brodsky I V, Kagan M Y, Klaptsov A V, Combescot R & Leyronas X 2006 *Phys. Rev. A* **73**, 032724.
- Brosens F, Devreese J T & Lemmens L F 1997a *Phys. Rev. E* **55**, 227.
- Brosens F, Devreese J T & Lemmens L F 1997b *Phys. Rev. E* **55**, 6795.
- Brosens F, Devreese J T & Lemmens L F 1997c *Phys. Rev. A* **55**, 2453.
- Brosens F, Devreese J T & Lemmens L F 1998a *Phys. Rev. E* **57**, 3871.
- Brosens F, Devreese J T & Lemmens L F 1998b *Phys. Rev. E* **58**, 1634.
- Bruch L W & Tjon J A 1979 *Phys. Rev. A* **19**, 425.
- Bruun G M & Baym G 2006 *Phys. Rev. A* **74**, 033623.
- Bulgac A 2007 *Phys. Rev. A* **76**, 040502(R).
- Busch T, Englert B G, Rzazewski K & Wilkens M 1997 *Found. Phys.* **28**, 549.
- Carlson J, Chang S Y, Pandharipande V R & Schmidt K E 2003 *Phys. Rev. Lett.* **91**, 050401.
- Casalbuoni R & Nardulli G 2004 *Rev. Mod. Phys.* **76**, 263.
- Castin Y & Werner F 2011 *Phys. Rev. A* **83**, 063614.
- Chang S Y & Bertsch G F 2007 *Phys. Rev. A* **76**, 021603(R).
- Chang S Y, Pandharipande V R, Carlson J & Schmidt K E 2004 *Phys. Rev. A* **70**, 043602.
- Chen J M C, Clark J W, Dav R D & Khodel V V 1993 *Nuclear Physics A* **555**, 59–89.
- Chen Q, He Y, Chien C C & Levin K 2009 *Rep. Prog. Phys.* **72**, 122501.
- Chen Q, Stajic J, Tan S & Levin K 2005a *Phys. Rep.* **412**, 1.
- Chen Q, Stajic J, Tan S & Levin K 2005b *Phys. Rep.* **412**, 1–88.
- Chernykh M, Feldmeier H, Neff T, von Neumann-Cosel P & Richter A 2007 *Phys. Rev. Lett.* **98**, 032501.
- Chin C 2011 *arXiv:1111.1484*.

- Chin C, Grimm R, Julienne P & Tiesinga E 2010 *Rev. Mod. Phys.* **82**, 1225.
- Combescot R, Alzetto F & Leyronas X 2009 *Phys. Rev. A* **79**, 053640.
- Cook C W 1957 *Phys. Rev.* **107**, 508.
- Cooper L N 1956 *Phys. Rev.* **104**, 1189.
- Curtis N, Achouri N L, Ashwood N I, Bohlen H G, Catford W N, Clarke N M, Freer M, Haigh P J, Laurent B, Orr N A, Patterson N P, Soic N, Thomas J S & Ziman V 2008 *Phys. Rev. C* **77**, 021301.
- Daily K M & Blume D 2010 *Phys. Rev. A* **81**, 053615.
- Daley A J, Boyd M M, Ye J & Zoller P 2008 *Phys. Rev. Lett.* **101**, 170504.
- Davis K B, Mewes M O, Andrews M R, van Druten N J, Durfee D S, Kurn D M & Ketterle W 1995 *Phys. Rev. Lett.* **75**, 3969.
- de Diego R, Garrido E, Fedorov D V & Jensen A S 2007 *Nucl. Phys. A* **786**, 71–89.
- de Gennes P G 1999 *Superconductivity of Metals and Alloys* Westview Press; 2nd Ed.
- De S, Dammalapati U, Jungmann K, & Willmann L 2009 *Phys. Rev. A* **79**, 041402(R).
- Dean D J & Hjorth-Jensen M 2003 *Rev. Mod. Phys.* **75**, 607.
- Deltuva A & Lazauskas R 2010 *Phys. Rev. A* **82**, 012705.
- Descouvemont P 2002 *Nucl. Phys. A* **709**, 275.
- Dickhoff W H & Neck D V 2005 *Many-Body Theory Exposed!* World Scientific Publishing Co.
- Dietrich K, Mang H J & Pradel J H 1964 *Phys. Rev.* **135**, B22.
- Dobaczewski J & Nazarewicz W 2012 *arXiv:1206.2600* .
- Dobaczewski J, Nazarewicz W & Reinhard P G 2001 *Nucl. Phys. A* **693**, 361.
- Donley E A, Claussen N R, Cornish S L, Roberts J L, Cornell E A & Wieman C E 2001 *Nature* **412**, 295.
- Dreizler R M & Gross E K U 1995 *Density Functional Theory* Plenum Press, New York.
- duBois J L & Glyde H R 2001 *Phys. Rev. A* **63**, 023602.
- Dukelsky J, Pittel S & Sierra G 2004 *Rev. Mod. Phys.* **76**, 643.
- Eagles D M 1969 *Phys. Rev.* **186**, 456.
- Ebran J P, Khan E, Nikšić T & Vretenar D 2012a *Nature* **487**, 341–344.
- Ebran J P, Khan E, Nikšić T & Vretenar D 2012b *arXiv:1207.7277* .
- Efimov V N 1970 *Phys. Lett. B* **33**, 563.
- Efimov V N 1971 *Sov. J. Nucl. Phys.* **12**, 589.
- Efimov V N 1991 *Phys. Rev. C* **44**, 2303–2310.
- Engelbrecht J R, Randeria M & Sá de Melo C A R 1997 *Phys. Rev. B* **55**, 15153.
- Engvild K C & Kowalski L 2006 in C. M. N Science, ed., ‘10th International Conference on Cold Fusion, Date: AUG 24-29, 2003 Cambridge MA’ pp. 825–829.
- Epelbaum E, Hammer H W & Meissner U G 2009 *Rev. Mod. Phys.* **81**, 17731825.
- Esry B D & D’Incao J P 2007 *J. Phys.: Conf. Ser.* **88**, 012040.
- Esry B D, Greene C H & Jr. J P B 1999 *Phys. Rev. Lett.* **83**, 1751.
- Fairman S & Meyerhof W E 1973 *Nucl. Phys. A* **206**, 1.
- Fattori M, D’Errico C, Roati G, Zaccanti M, Jona-Lasinio M, Modugno M, Inguscio M, & Modugno G 2008 *Phys. Rev. Lett.* **100**, 080405.
- Fattori M, Roati G, Deissler B, D’Errico C, Zaccanti M, Jona-Lasinio M, Santos L, Inguscio M & Modugno G 2008 *Phys. Rev. Lett.* **101**, 190405.
- Fedichev P O, Reynolds M W & Shlyapnikov G V 1996 *Phys. Rev. Lett.* **77**, 2921.
- Fedorov D V & Jensen A S 2001 *Jour. Phys. A* **34**, 6003–6012.
- Fedorov D V, Jensen A S & Riisager K 1994 *Phys. Rev. Lett.* **71**, 2817.
- Ferlaino F, Knoop S, Berninger M, Harm W, D’Incao J P, Nägerl H C, & Grimm R 2009 *Phys. Rev. Lett.* **102**, 140401.
- Fetter A L & Walecka J D 1971 *Quantum Theory of Many-Particle Systems* McGraw-Hill San Francisco.
- Fölling S, Gerbier F, Widera A, Mandel O, Gericke T & Bloch I 2005 *Nature* **434**, 481–484.
- Frederico T, Tomio L, Delfino A & Amorim A 1999 *Phys. Rev. A* **60**, R9.
- Freer M 2007 *Rep. Prog. Phys.* **70**, 2149–2210.
- Fukuhara T, Sugawa S, Sugimoto M, Taie S & Takahashi Y 2009 *Phys. Rev. A* **79**, 041604(R).
- Funaki Y, Girod M, Horiuchi H, Röpke G, Schuck P, Tohsaki A & Yamada T 2010 *J. Phys. G: Nucl. Part. Phys.* **37**, 064012.
- Funaki Y, Horiuchi H, Tohsaki A, Schuck P & Röpke G 2002 *Prog. Theor. Phys.* **108**, 297.
- Funaki Y, Horiuchi H, von Oertzen W, Röpke G, Schuck P, Tohsaki A & Yamada T 2009 *Phys. Rev. C* **80**, 064326.
- Funaki Y, Tohsaki A, Horiuchi H, Schuck P & Röpke G 2003 *Phys. Rev. C* **67**, 051306(R).
- Funaki Y, Yamada T, Horiuchi H, Röpke G, Schuck P & Tohsaki A 2008 *Phys. Rev. Lett.* **101**, 082502.

- Gaebler J P, Stewart J T, Drake T E, Jin D S, Perali A, Pieri P & Strinati G C 2010 *Nature Phys.* **6**, 569–573.
- Gajda M 2006 *Phys. Rev. A* **73**, 023603.
- Gao B 1998 *Phys. Rev. A* **58**, 4222–4225.
- Garrido E, Fedorov D V & Jensen A S 1999 *Nucl. Phys. A* **650**, 247.
- Garrido E, Fedorov D V & Jensen A S 2006 *Phys. Rev. Lett.* **96**, 112501.
- Gezerlis A & Carlson J 2010 *Phys. Rev. C* **81**, 025803.
- Giorgini S, Boronat J & Casulleras J 1999 *Phys. Rev. A* **60**, 5129.
- Giorgini S, Pitaevskii L P & Stringari S 2008 *Rev. Mod. Phys.* **80**, 1215.
- Gorkov L P & Melik-Barkhudarov T K 1961 *Zh. Eksp. Teor. Fiz.* **40**, 1452.
- Gorshkov A V, Hermele M, Gurarie V, Xu C, Julienne P S, Ye J, Zoller P, Demler E, Lukin M D & Rey A M 2010 *Nature Physics* **6**, 289 – 295.
- Gorshkov A V, Rey A M, Daley A J, Boyd M M, Ye J, Zoller P & Lukin M D 2009 *Phys. Rev. Lett.* **102**, 110503.
- Gross C, Zibold T, Nicklas E, Esteve J & Oberthaler M K 2010 *Nature* **464**, 1165.
- Gross E P 1961 *Nuovo Cimento* **20**, 454.
- Gross N, Kokkelmans Z S S & Khaykovich L 2009 *Phys. Rev. Lett.* **103**, 163202.
- Grynberg G & Robilliard C 1999 *Phys. Rep.* **355**, 335.
- Hagino K, Sagawa H, Carbonell J & Schuck P 2007 *Phys. Rev. Lett.* **99**, 022506.
- Hagino K, Sagawa H, Nakamura T & Shimoura S 2009 *Phys. Rev. C* **80**, 031301.
- Haken H & Wolf H C 1995 *Molecular Physics and Elements of Quantum Chemistry: Introduction to Experiments and Theory* Springer-Verlag Telos.
- Hammer H W & Platter L 2007 *Eur. Phys. Jour. A* **32**, 113.
- Hammer H W & Son D T 2004 *Phys. Rev. Lett.* **93**, 250408.
- Hanbury-Brown R & Twiss R Q 1956 *Nature* **177**, 27–29.
- Hanna G J & Bluhme D 2006 *Phys. Rev. A* **74**, 063604.
- Harvey M & Jensen A S 1972 *Nucl. Phys. A* **179**, 33.
- Heiselberg H, Pethick C J, Smith H & Viverit L 2000 *Phys. Rev. Lett.* **85**, 2418–2421.
- Helfrich K & Hammer H W 2011 *Phys. Rev. A* **83**, 052703.
- Hemmdan A, Glöckle W & Kamada H 2002 *Phys. Rev. C* **66**, 054001.
- Henny M, Oberholzer S, Strunk C, Heinzel T, Ensslin K, Holland M & Schenberger C 1999 *Science* **284**, 296–298.
- Hodgman S, Dall R, Manning A, Baldwin K & Truscott A G 2012 *Science* **331**, 1046–1049.
- Hofmann J 2012 *Phys. Rev. Lett.* **108**, 185303.
- Horiuchi H 1970 *Prog. Theor. Phys.* **43**, 375.
- Horiuchi W & Suzuki Y 2006a *Phys. Rev. C* **74**, 034311.
- Horiuchi W & Suzuki Y 2006b *Phys. Rev. C* **73**, 037304.
- Hoyle F 1954 *ApJ Suppl. Ser.* **1**, 121.
- Hu H, Liu X J, Drummond P D & Dong H 2010 *Phys. Rev. Lett.* **104**, 240407.
- Huang K 1987 *Statistical Mechanics* 2nd ed. Wiley, New York.
- Huckans J H, Williams J R, Hazlett E L, Stites R W & O’Hara K M 2009 *Phys. Rev. Lett.* **102**, 165302.
- Iannuzzi M, Orecchini A, Sacchetti F, Facchi P & Pascazio S 2006 *Phys. Rev. Lett.* **96**, 080402.
- Ikeda K, Takigawa N & Horiuchi H 1968 *Prog. Theor. Phys. Supp. Extra Number* p. 464.
- Janko B, Maly J & Levin K 1997 *Phys. Rev. B* **56**, R11407–R11410.
- Jensen A S & Fedorov D V 2003 *Europhys. Lett.* **62**, 336–342.
- Jensen A S, Fedorov D V, Langanke K & Müller H M 1995 in Simon & Sorlin, eds, ‘ENAM 95, Int. Conf. on exotic nuclei and atomic masses’ Edition Frontieres p. 677.
- Jensen A S, Garrido E & Fedorov D V 1997 *Few-Body Syst.* **22**, 193–236.
- Jensen A S & Hansen P G 1984 *Nucl. Phys. A* **431**, 393.
- Jensen A S, Riisager K, Fedorov D V & Garrido E 2004 *Rev. Mod. Phys.* **76**, 215.
- Ji C, Phillips D R & Platter L 2010 *Euro. Phys. Lett.* **92**, 13003.
- Jona-Lasinio M, Pricoupenko L & Castin Y 2008 *Phys. Rev. A* **77**, 043611.
- Jonsell S 2004 *J. Phys. B: At. Mol. Opt. Phys.* **37**, S245.
- Kagan Y, Muryshev A E & Shlyapnikov G V 1998 *Phys. Rev. Lett.* **81**, 933.
- Kanada-En’yo Y 1998 *Phys. Rev. Lett.* **81**, 5291.
- Kapitza P L 1938 *Nature* **141**, 913.
- Kartavtsev O I & Malykh A V 2006 *Phys. Rev. A* **74**, 042506.
- Ketterle W & Zwierlein M W 2008 in M Inguscio, W Ketterle & C Salomon, eds, ‘Ultracold Fermi Gases, Proceedings of the International School of Physics “Enrico Fermi”, Course CLXIV, Varenna, 20 - 30 June 2006’ IOS Press, Amsterdam.
- Kiesel H, Renz A & Hasselbach F 2002 *Nature* **418**, 392–394.

- Kinoshita T, Wenger T & Weiss D S 2004 *Science* **305**, 1125.
- Klawunn M, Duhme J & Santos L 2010 *Phys. Rev. A* **81**, 013604.
- Knap M, Berg E, Ganahl M & Demler E 2012 *Phys. Rev. B* **86**, 064501.
- Knoop S, Borbely J S, Vassen W & Kokkelmans S J J M F 2012 *Phys. Rev. A* **86**, 062705.
- Knoop S, Ferlaino F, Mark M, Berninger M, Schöbel H, Nägerl H C & Grimm R 2009 *Nature Physics* **5**, 227.
- Köhler T, Góral K & Julienne P S 2006 *Rev. Mod. Phys.* **78**, 1311.
- Kohn W & Sham L J 1965 *Phys. Rev.* **140**, A1133.
- Koonin S, Dean D J & Langanke K 1997 *Phys. Rep.* **278**, 1.
- Kraemer T, Mark M, Waldburger P, Danzl J G, Chin C, Engeser B, Lange A D, Pilch K, Jaakkola A, Nägerl H C & Grimm R 2006 *Nature* **440**, 315.
- Kuhnlé E D, Hu H, Liu X J, Dyke P, Mark M, Drummond P D, Hannaford P & Vale C J 2010 *Phys. Rev. Lett.* **105**, 153005.
- Lahaye T, Metz J, Fröhlich B, Koch T, Meister M, Griesmaier A, Pfau T, Saito H, Kawaguchi Y & Ueda M 2008 *Phys. Rev. Lett.* **101**, 080401.
- Landau L D 1941 *J. Phys. USSR* **5**, 71.
- Landau L D & Lifshitz E M 1958 *Statistical Physics* Pergamon, Oxford.
- Landau L D & Lifshitz E M 1981 *Quantum Mechanics* Butterworth-Heinemann; 3rd Edition.
- Langmack C, Barth M, Zwirger W & Braaten E 2012 *Phys. Rev. Lett.* **108**, 060402.
- Lattimer J M & Prakash M 2004 *Science* **304**, 536.
- Lazauskas R & Carbonell J 2005 *Phys. Rev. C* **71**, 044004.
- Lee D 2006 *Phys. Rev. A* **73**, 063204.
- Leggett A J 1980 in J Ehlers, K Hepp, R Kippenhahn, H. A Weidenmüller & J Zittartz, eds, 'Modern Trends in the Theory of Condensed Matter' Springer-Verlag p. 13.
- Leggett A J 1999 *Rev. Mod. Phys.* **71**, S318.
- Leggett A J 2006 *Quantum Fluids* Oxford University Press.
- Lemmens L F, Brosens F & Devreese J T 1999 *Phys. Rev. A* **59**, 3112.
- Lieb E H, Seiringer R, Solovej J P & Yngvason J 2002 *Current Developments in Mathematics, 2001*, pp. 131-178 International Press, Cambridge.
- Lompe T, Ottenstein T B, Serwane F, Wenz A N, Zürn G & Jochim S 2010 *Science* **330**, 904.
- London F 1938 *Nature* **141**, 643.
- Macek J H & Sternberg J 2006 *Phys. Rev. Lett.* **97**, 023201.
- Magierski P, Wlazłowski G & Bulgac A 2011 *Phys. Rev. Lett.* **107**, 145304.
- Magierski P, Wlazłowski G, Bulgac A & Drut J E 2009 *Phys. Rev. Lett.* **103**, 210403.
- Marqués F M, Labiche M, Orr N A, Anglique J C, Axelsson L, Benoit B & *et al.* 2002 *Phys. Rev. C* **65**, 044006.
- Massignan P & Stoof H T C 2008 *Phys. Rev. A* **78**, 030701(R).
- Matsumura H & Suzuki Y 2004 *Nucl. Phys. A* **739**, 238.
- Matsuo M 2006 *Phys. Rev. C* **73**, 044309.
- Mottelson B R 1999 *Nucl. Phys. A* **649**, 45c.
- Mueller E J, Ho T L, Ueda M & Baym G 2006 *Phys. Rev. A* **74**, 033612.
- Muta K, Furumoto T, Ichikawa T & Itagaki N 2011 *Phys. Rev. C* **84**, 034305.
- Myers W D & Swiatecki W J 1969 *Ann. Phys.* **55**, 395-505.
- Naidon P, Hiyama E & Ueda M 2012 *Phys. Rev. A* **86**, 012502.
- Nakajima S, Horikoshi M, Mukaiyama T, Naidon P & Ueda M 2010 *Phys. Rev. Lett.* **105**, 023201.
- Nakajima S, Horikoshi M, Mukaiyama T, Naidon P & Ueda M 2011 *Phys. Rev. Lett.* **106**, 143201.
- Naraschewski M & Glauber R J 2001 *Phys. Rev. A* **59**, 4596-4607.
- Neff T & Feldmeier H 2004 *Nucl. Phys. A* **738**, 357.
- Negele J W 1982 *Rev. Mod. Phys.* **54**, 913.
- Negele J W & Vautherin D 1972 *Phys. Rev. C* **5**, 1472.
- Negele J W & Vautherin D 1975 *Phys. Rev. C* **11**, 1031.
- Nielsen E, Fedorov D V & Jensen A S 1997 *Phys. Rev. A* **56**, 3287.
- Nielsen E, Fedorov D V & Jensen A S 1999 *Few-Body Syst.* **27**, 15.
- Nielsen E, Fedorov D V, Jensen A S & Garrido E 2001 *Phys. Rep.* **347**, 373-459.
- Nielsen E & Macek J H 1999 *Phys. Rev. Lett.* **83**, 1566.
- Nielsen E, Suno H & Esry B D 2002 *Phys. Rev. A* **66**, 012705.
- Nishida Y 2012 *Phys. Rev. A* **86**, 012710.
- Nishida Y & Tan S 2011 *Few-Body Syst.* **51**, 191.
- Oliver W D, Kim J, Liu R C & Yamamoto Y 1999 *Science* **284**, 299-301.
- Ottenstein T B, Lompe T, Kohonen M, Wenz A N & Jochim S 2008 *Phys. Rev. Lett.* **101**, 203202.
- Özen C & Zinner N 2009 *arXiv:0902.4725* .

- Pan F & Draayer J P 1999 *Ann. Phys.* **271**, 120–140.
- Papenbrock T & Bertsch G F 1999 *Phys. Rev. C* **59**, 2052.
- Paredes B, Widera A, Murg V, Mandel O, Fölling S, Cirac I, Shlyapnikov G V, Hänsch T W & Bloch I 2004 *Nature* **429**, 277.
- Penrose O 1951 *Philos. Mag.* **42**, 1373.
- Penrose O & Onsager L 1956 *Phys. Rev.* **104**, 576.
- Perali A, Palestini F, Pieri P, Strinati G C, Stewart J T, Gaebler J P, Drake T E & Jin D S 2011 *Phys. Rev. Lett.* **106**, 060402.
- Perali A, Pieri P, Strinati G C & Castellani C 2002 *Phys. Rev. B* **66**, 024510.
- Pethick C J & Pitaevskii L P 2000 *Phys. Rev. A* **62**, 033609.
- Pethick C J & Smith H 2008 *Bose-Einstein Condensation in dilute Gases* Cambridge University Press, 2nd Ed.
- Petrov D S 2004 *Phys. Rev. Lett.* **93**, 143201.
- Pieper S C 2003 *Phys. Rev. Lett.* **90**, 252501.
- Pitaevskii L P 1961 *Zh. Eksp. Teor. Fiz.* **40**, 646.
- Pitaevskii L P & Lifshitz E M 1980 *Statistical Physics* Butterworth-Heinemann.
- Pitaevskii L P & Stringari S 2003 *Bose-Einstein Condensation* Clarendon Press, Oxford.
- Platter L, Hammer H W & Meissner U G 2004 *Few-body Syst.* **35**, 169.
- Platter L, Ji C & Phillips D R 2009 *Phys. Rev. A* **79**, 022702.
- Pollack S E, Dries D & Hulet R G 2009 *Science* **326**, 1683.
- Pollack S E, Dries D, Junker M, Chen Y P, Corcovilos T A & Hulet R G 2009 *Phys. Rev. Lett.* **102**, 090402.
- Poves A & Zuker A P 1981 *Phys. Rep.* **70**, 235.
- Pricoupenko L 2011 *Phys. Rev. A* **83**, 062711.
- Randeria M 1998 in G Iadonisi, J. R Schrieffer & M. L Chiofalo, eds, ‘Proc. Internat. School Phys. ‘Enrico Fermi’, Course 136’ IOS Press pp. 53–57.
- Randeria M 2010 *Nature Phys.* **6**, 561–562.
- Reimann S M & Manninen M 2002 *Rev. Mod. Phys.* **74**, 1283.
- Richardson R W 1963 *Phys. Lett. B* **3**, 277.
- Riisager K, Fedorov D & Jensen A S 2000 *Europhys. Lett.* **49**, 547.
- Ring P & Schuck P 1980 *The Nuclear Many-Body Problem* Springer-Verlag, Berlin.
- Roati G, Zaccanti M, D’Errico C, Catani J, Modugno M, Simoni A, Inguscio M & Modugno G 2007 *Phys. Rev. Lett.* **99**, 010403.
- Roberts J L, Claussen N R, Cornish S L, Donley E A, Cornell E A & Wieman C E 2001 *Phys. Rev. Lett.* **86**, 4211.
- Rom T, Best T, van Oosten D, Schneider U, Fölling S, Paredes B & Bloch I 2006 *Nature* **444**, 733–736.
- Rontani M, Armstrong J R, Yu Y, Åberg S & Reimann S M 2009 *Phys. Rev. Lett.* **102**, 060401.
- Rotival V, Bennaceur K & Duguet T 2009 *Phys. Rev. C* **79**, 054309.
- Ruprecht P A, Holland M J, Burnett K & Edwards M 1995 *Phys. Rev. A* **51**, 4704.
- Schellekens M, Hoppeler R, Perrin A, Gomes J V, Boiron D, Aspect A & Westbrook C I 2005 *Science* **310**, 648 – 651.
- Schmidt R, Rath S P & Zwerger W 2012 *Eur. Phys. J. B* **85**, 386.
- Schulze H J, Cugnon J, Lejeune A, Baldo M & Lombardo U 1996 *Physics Letters B* **375**, 1–8.
- Schumayer D, van Zyl B P, Bhaduri R K & Hutchinson D A W 2010 *Europhys. Lett.* **89**, 13001.
- Schwenk A & Pethick C J 2005 *Phys. Rev. Lett.* **95**, 160401.
- Serwane F, Zürn G, Lompe T, Ottenstein T B, Wenz A N & Jochim S 2011 *Science* **332**, 336–338.
- Sherson J F, Weitenberg C, Endres M, Chaneau M, Bloch I & Kuhr S 2010 *Nature* **467**, 68.
- Siemens P J & Jensen A S 1987 *Element of Nuclei* Addison-Wesley.
- Simon B 1976 *Ann. Phys.* **97**, 279.
- Skyrme T H R 1956 *Phil. Mag.* **1**, 1043.
- Sørensen O, Fedorov D V & Jensen A S 2002 *Phys. Rev. Lett.* **89**, 173002.
- Sørensen O, Fedorov D V & Jensen A S 2004 *Phys. Rev. A* **70**, 013610.
- Sørensen P K, Fedorov D V & Jensen A S 2011 *arXiv:1112.4962* .
- Sørensen P K, Fedorov D V, Jensen A S & Zinner N T 2012a *Phys. Rev. A* **86**, 052516.
- Sørensen P K, Fedorov D V, Jensen A S & Zinner N T 2012b *arXiv:1212.1398* .
- Stetcu I, Barrett B R, can Kolck U & Vary J P 2007 *Phys. Rev. A* **76**, 063613.
- Stewart J T, Gaebler J P, Drake T E & Jin D S 2010 *Phys. Rev. Lett.* **104**, 235301.
- Stewart J T, Gaebler J P & Jin D S 2008 *Nature* **454**, 744–747.
- Stoof H T C, Dickerscheid D B M & Gubbels K 2009 *Ultracold Quantum Fields* Springer, 1st Ed.
- Suno H, Esry B & Greene C H 2003 *Phys. Rev. Lett.* **90**, 053202.
- Suzuki K 1982 *Prog. Theor. Phys.* **68**, 1999.

- Suzuki K & Lee S Y 1980 *Prog. Theor. Phys.* **64**, 2091.
 Suzuki Y & Takahashi M 2002 *Phys. Rev. C* **65**, 064318.
 Tan S 2008a *Ann. Phys.* **323**, 2952.
 Tan S 2008b *Ann. Phys.* **323**, 2971.
 Tan S 2008c *Ann. Phys.* **323**, 2987.
 Tempere J, Brosens F, Lemmens L F & Devreese J T 1998 *Phys. Rev. A* **58**, 3180.
 Tempere J, Brosens F, Lemmens L F & Devreese J T 2000 *Phys. Rev. A* **61**, 043605.
 Thoennessen M 2004 *Rep. Prog. Phys.* **67**, 1187–1232.
 Thøgersen M, Fedorov D V & Jensen A S 2007 *Eur. Phys. Lett.* **79**, 40002.
 Thøgersen M, Fedorov D V & Jensen A S 2008a *Eur. Phys. Lett.* **83**, 30012.
 Thøgersen M, Fedorov D V & Jensen A S 2008b *Phys. Rev. A* **78**, 020501(R).
 Thøgersen M, Fedorov D V, Jensen A S, Esry B D & Wang Y 2009 *Phys. Rev. A* **80**, 013608.
 Thøgersen M, Zinner N T & Jensen A S 2009 *Phys. Rev. A* **80**, 043625.
 Thomas L H 1935 *Phys. Rev.* **47**, 903.
 Tjon J A 1975 *Phys. Lett. B* **56**, 217.
 Tohsaki A, Horiuchi H, Schuck P & Röpke G 2001 *Phys. Rev. Lett.* **87**, 192501.
 Tohsaki A, Horiuchi H, Schuck P & Röpke G 2004 *Nucl. Phys. A* **738**, 259.
 Uegaki E, Okabe S, Abe Y & Tanaka H 1977 *Prog. Theor. Phys.* **57**, 1262.
 Valiente M 2012 *Phys. Rev. A* **85**, 014701.
 Valiente M, Zinner N T & Mølmer K 2011 *Phys. Rev. A* **84**, 063626.
 Valiente M, Zinner N T & Mølmer K 2012 *Phys. Rev. A* **86**, 043616.
 Vollhardt D & Wölfle P 1990 *The Superfluid Phases of Helium 3* Taylor and Francis, London.
 Volosniev A G, Armstrong J R, Fedorov D V, Jensen A S, Valiente M & Zinner N T 2013 *arXiv:1301.2159* .
 Volosniev A G, Fedorov D V, Jensen A S & Zinner N T 2011 *Phys. Rev. Lett.* **106**, 250401.
 Volosniev A G, Fedorov D V, Jensen A S & Zinner N T 2012a *arXiv:1211.3923* .
 Volosniev A G, Fedorov D V, Jensen A S & Zinner N T 2012b *Phys. Rev. A* **85**, 023609.
 Volosniev A G, Zinner N T, Fedorov D V, Jensen A S & Wunsch B 2011 *J. Phys. B: At. Mol. Opt. Phys.* **44**, 125301.
 von Stecher J 2010 *J. Phys. B: At. Mol. Opt. Phys.* **43**, 101002.
 von Stecher J, D’Incao J P & Greene C H 2009 *Nature Physics* **5**, 417.
 von Stecher J & Greene C H 2007 *Phys. Rev. Lett.* **99**, 090402.
 von Stecher J, Greene C H & Blume D 2008 *Phys. Rev. A* **77**, 043619.
 Wambach J, Ainsworth T L & Pines D 1993 *Nuclear Physics A* **555**, 128–150.
 Wang D W 2007 *Phys. Rev. Lett.* **98**, 060403.
 Wang D W, Lukin M D & Demler E 2006 *Phys. Rev. Lett.* **97**, 180413.
 Wang J, D’Incao J P, Esry B D & Greene C H 2012 *Phys. Rev. Lett.* **108**, 263001.
 Wang Y, D’Incao J P & Esry B D 2011 *Phys. Rev. A* **83**, 042710.
 Wang Y, D’Incao J P & Greene C H 2011a *Phys. Rev. Lett.* **106**, 233201.
 Wang Y, D’Incao J P & Greene C H 2011b *Phys. Rev. Lett.* **107**, 233201.
 Wang Y, Wang J, D’Incao J P & Greene C H 2012 *Phys. Rev. Lett.* **109**, 243201.
 Wefelmeier W 1937 *Naturwiss.* **25**, 525.
 Weiner J, Bagnato V S, Zilio S & Julienne P S 1999 *Rev. Mod. Phys.* **71**, 1.
 Weitenberg C, Endres M, Sherson J F, Chaneau M, Schauß P, Fukuhara T, Bloch I & Kuhr S 2011 *Nature* **471**, 319–324.
 Wenz A N, Lompe T, Ottenstein T B, Serwane F, Zürn G & Jochim S 2009 *Phys. Rev. A* **80**, 040702(R).
 Werner F & Castin Y 2006a *Phys. Rev. Lett.* **97**, 150401.
 Werner F & Castin Y 2006b *Phys. Rev. A* **74**, 053603.
 Werner F & Castin Y 2012a *Phys. Rev. A* **86**, 013626.
 Werner F & Castin Y 2012b *Phys. Rev. A* **86**, 053633.
 Wheeler J A 1937 *Phys. Rev.* **52**, 1083.
 Wigner E P 1937 *Phys. Rev.* **51**, 106.
 Wild R J, Makotyn P, Pino J M, Cornell E A & Jin D S 2012 *Phys. Rev. Lett.* **108**, 145305.
 Williams J R, Hazlett E L, Huckans J H, Stites R W, Zhang Y & OHara K M 2009 *Phys. Rev. Lett.* **103**, 130404.
 Wunsch B, Zinner N T, Mekhov I B, Huang S J, Wang D W & Demler E 2011 *Phys. Rev. Lett.* **107**, 073201.
 Xu C 2010 *Phys. Rev. B* **81**, 144431.
 Yamada T, Funaki Y, Horiuchi H, Röpke G, Schuck P & Tohsaki A 2008 *Phys. Rev. A* **78**, 035603.
 Yamada T, Funaki Y, Horiuchi H, Röpke G, Schuck P & Tohsaki A 2009 *Phys. Rev. C* **79**, 0543.

- Yamashita M T, Fedorov D V & Jensen A S 2010 *Phys. Rev. A* **81**, 063607.
Yamashita M T, Fedorov D V & Jensen A S 2011 *Few-Body Syst.* **51**, 135.
Yamashita M T, Tomio L, Delfino A & Frederico T 2006 *Europhys. Lett.* **75**, 555.
Yan J 2003 *J. Stat. Phys.* **113**, 623.
Yanase Y & Yamada K 1999 *J. Phys. Soc. Jpn.* **68**, 2999–3015.
Yang C N 1962 *Rev. Mod. Phys.* **34**, 694.
Yasuda M & Shimizu F 1996 *Phys. Rev. Lett.* **77**, 30903093.
Zaccanti M, Deissler B, D’Errico C, Fattori M, Jona-Lasinio M, Müller S, Roati G, Inguscio M & Modugno G 2009 *Nature Physics* **5**, 586.
Zaluska-Kotur M A, Gajda M, Orłowski A & Mostowski J 2000 *Phys. Rev. A* **61**, 033613.
Zenesini A, Huang B, Berninger M, Besler S, Nägerl H C, Ferlaino F, Grimm R, Greene C H & von Stecher J 2012 *arXiv:1205.1921* .
Zinner N T 2009 *arXiv:0909.1314* .
Zinner N T 2011 *arXiv:1112.6358* .
Zinner N T 2012 *J. Phys. A: Math. Theor.* **45**, 205302.
Zinner N T, Armstrong J R, Volosniev A G, Fedorov D V & Jensen A S 2012 *Few-body Syst.* **53**, 369–385.
Zinner N T & Jensen A S 2008a *Phys. Rev. C* **78**, 041306(R).
Zinner N T & Jensen A S 2008b *Phys. Rev. Lett.* **101**, 179201.
Zinner N T, Mølmer K, Özen C, Dean D J & Langanke K 2009 *Phys. Rev. A* **80**, 013613.
Zinner N T & Thøgersen M 2009 *Phys. Rev. A* **80**, 023607.
Zinner N T, Wunsch B, Mekhov I B, Huang S J, Wang D W & Demler E 2011 *Phys. Rev. A* **84**, 063606.
Zürn G, Serwane F, Lompe T, Wenz A N, Ries M G, Bohn J E & Jochim S 2012 *Phys. Rev. Lett.* **108**, 075303.